GRAVITY MODELING FOR PRECISE

TERRESTRIAL INERTIAL NAVIGATION

DISSERTATION PROSPECTUS .

Presented to the Faculty of the School of Engineering

of the Air Force Institute of Technology

Air University

in Partial Fulfillment of the Requirements

for Admission to Candidacy for the

Degree of Doctor of Philosophy
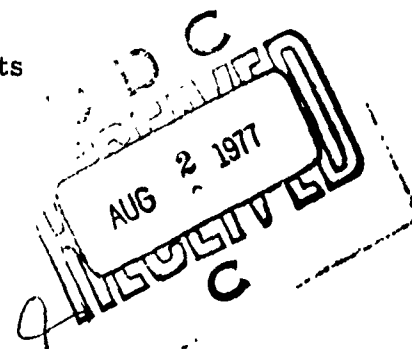
by

Robert M. Edwards/ B.S., S.M.

Major   USAF

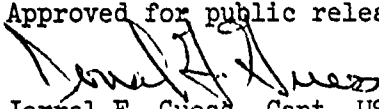June 1977

Approved for public release; distribution unlimited

SECURITY CLASSIFICATION OF THIS PAGE *(When Data Entered)*

REPORT DOCUMENTATION PAGE		READ INSTRUCTIONS BEFORE COMPLETING FORM
1. REPORT NUMBER	2. GOVT ACCESSION NO.	3. RECIPIENT'S CATALOG NUMBER
4. TITLE *(and Subtitle)* GRAVITY MODELING FOR PRECISE TERRESTRIAL INERTIAL NAVIGATION		5. TYPE OF REPORT & PERIOD COVERED PhD Dissertation Prospectus
		6. PERFORMING ORG. REPORT NUMBER
7. AUTHOR(s) Robert M. Edwards Major USAF		8. CONTRACT OR GRANT NUMBER(s)
9. PERFORMING ORGANIZATION NAME AND ADDRESS Air Force Institute of Technology (AFIT-EN)√ Wright Patterson AFB, Ohio 45433		10. PROGRAM ELEMENT, PROJECT, TASK AREA & WORK UNIT NUMBERS
11. CONTROLLING OFFICE NAME AND ADDRESS		12. REPORT DATE June 1977
		13. NUMBER OF PAGES 158
14. MONITORING AGENCY NAME & ADDRESS*(If different from Controlling Office)*		15. SECURITY CLASS. *(of this report)* Unclassified
		15a. DECLASSIFICATION/DOWNGRADING SCHEDULE

16. DISTRIBUTION STATEMENT *(of this Report)*

Approved for public release; distribution unlimited.

17. DISTRIBUTION STATEMENT *(of the abstract entered in Block 20, If different from Report)*

Approved for public release; IAW AFR 190-17

Jerral F. Guess, Capt, USAF

18. SUPPLEMENTARY NOTES

19. KEY WORDS *(Continue on reverse side if necessary and identify by block number)*

Gravity	Geopotential Modeling	G&G	ALCM
Gravitation	Vertical Deflections	Upward Continuation	ASALM
Geopotential	Gravity Anomaly	Navigation	FFT
Gravity Modeling	Gradiometer	Inertial Navigation	
Gravitational Modeling	Geodesy	Cruise Missile	

20. ABSTRACT *(Continue on reverse side if necessary and identify by block number)*

A historical perspective of gravity modeling for terrestrial navigation is presented. The traditional ellipsoidal model is explained, and the consequent errors are discussed. The propagation of these errors into navigation estimation errors is presented. A brief survey of advanced modeling methods and the pertinent theory is presented.

The system design problem of selecting an advanced gravity model is presented

DD FORM 1473 EDITION OF 1 NOV 65 IS OBSOLETE
1 JAN 73

SECURITY CLASSIFICATION OF THIS PAGE *(When Data Entered)*

as a scenario to motivate the proposed research. To address this problem, a new theoretical analysis technique is developed. This technique includes the effects of navigation error propagation, the statistics of the anomalous field (the residual after ellipsoidal or other reference field modeling), the statistics of gravity survey errors, and the advanced gravity modeling. These effects are combined to yield a measure of system performance cost as reflected in the navigation error state covariance due to gravity modeling errors acting alone.

This report contains references to 82 items in the open literature pertinent to this subject area.

Foreword

A dissertation prospectus is primarily a research proposal and is not normally published or released outside the academic institution involved. This prospectus contains an unusual amount of background material, and the state of the research is advanced for such a document. This prospectus is being published to make this background material and the analytical methods immediately available.

The problem of gravity modeling for terrestrial inertial navigation is discussed at length. This historical and technical perspective provides a survey of this area not available in the literature. Since this discussion will not be repeated in its entirety in the dissertation, publication of this prospectus will provide this material to other interested researchers.

The analytical development in the proposed approach (Part III) includes results which apply to more general model evaluations than the subject research. These methods can be applied to current studies of geodetic effects on navigation accuracy. Publishing these results will make them immediately available.

i

Contents

iii

Figures

Terms, Symbols and Notation

<div align="right">
Reference
Page(s)
</div>

Terms and Acronyms

ACF	$\underline{A}$uto $\underline{C}$orrelation $\underline{F}$unction	121
arcsecond	A second of arc = $1^o/60$	13
CCF	$\underline{C}$ross $\underline{C}$orrelation $\underline{F}$unction	122
CEP	$\underline{C}$ircular $\underline{e}$rror $\underline{p}$robable	127
ECE	$\underline{E}$arth-$\underline{c}$entered, $\underline{E}$arth-$\underline{f}$ixed orthogonal coordinate reference frame	6
ECI	$\underline{E}$arth-$\underline{c}$entered $\underline{i}$nertial coordinate reference frame	6
e-frame	ECE	6
EU	$\underline{E}$ötvös $\underline{u}$nit, 10^{-9} sec^{-2}	38
ft	feet	22
FFT	$\underline{F}$ast $\underline{F}$ourier $\underline{T}$ransform	33
FFT^{-1}	Inverse FFT	100
horizontal channel	INS estimates or errors projected onto either of two orthogonal coordinate directions in the local-level plane	12
hr	hour	20
ICBM	$\underline{I}$nter$\underline{c}$ontinental $\underline{B}$allistic $\underline{Mi}$ssile	14
i-frame	ECI	6
INS	$\underline{I}$nertial $\underline{N}$avigation $\underline{S}$ystem	2

Notation for Reference to Literature

(Ref n:i-j) should be read as "pages i through j of reference number n."
The list of references appears after the appendices.

Symbols

---

*$\underline{G}_m$ up to page 57 is synonymous with $\underline{G}_{ref}$. On page 57, $\underline{G}_m$ is redefined to include additional modeling $\delta\underline{g}_m$.

Mathematical Notation

Abstract

A historical perspective of gravity modeling for terrestrial navigation is presented. The traditional ellipsoidal model is explained, and the consequent errors are discussed. The propagation of these errors into navigation estimation errors is presented. A brief survey of advanced modeling methods and the pertinent theory is presented.

The system design problem of selecting an advanced gravity model is presented as a scenario to motivate the proposed research. To address this problem, a new theoretical analysis technique is developed. This technique includes the effects of navigation error propagation, the statistics of the anomalous field (the residual after ellipsoidal or other reference field modeling), the statistics of gravity survey errors, and the advanced gravity modeling. These effects are combined to yield a measure of system performance cost as reflected in the navigation error state covariance due to gravity modeling errors acting alone.

This report contains 82 references to the open literature in this subject area.

I. Purpose

This prospectus defines my dissertation research topic and provides a basis for comments or approval.   To this end, it:

    a. Places the proposed work in perspective;

    b. Specifies the research question to be addressed;

    c. Specifies the proposed approach and, where necessary, points out areas which will not be addressed;

    d. Specifies the method for confirming the final result;

    e. Outlines the Final Report;

    f. Describes the applicability of this research to the mission of the Air Force Avionics Laboratory; and

    g. Discusses the aspects of this research perceived to be original.

II. Background

The proposed study concerns changes to the current methods of accounting for gravitational acceleration in inertial navigation; a brief discussion of the state-of-the-art is in order. The gravity model[*] is a closed-form mathematical expression, or algorithm, which together with a set of predetermined parameters, or data, define a vector valued function which approximates the Earth's gravitational acceleration throughout some three-dimensioned region of operation. Such a model is an integral part of an inertial navigation system (INS). Technological advances in INS instrument designs and new mission requirements call for a reappraisal of gravity modeling errors. Improvements to the model must be based on available gravity data; on our knowledge of gravitational theory; and on our knowledge of the time spectral response of the navigation filter. Of course, this study must branch from the past and current gravity modeling research. We begin with an assessment of where gravity modeling evolution has led to date.

---

[*]The term "gravity model" can be m sleading. The term "gravitation" will always refer to the mass attraction ($\underline{G}$) effect alone, whereas "gravity" will <u>usually</u> refer to the combined effect of mass attraction and Earth's rotation ($\underline{g}$).

A. The Role of the Gravity Model in an INS

A gravity model is a fundamental component of any precision INS. We shall restrict our attention to "precision" navigation.[*] An inertial navigation system senses inertial translational acceleration and rotational velocity, tracks attitude by integrating the rotational velocity, and calculates translational position and velocity as integrals of acceleration from the Newton's Second Law equation: Force equals mass times acceleration. The mathematical form of the translational solution algorithm depends on both the coordinate frame in which the sensors are mounted, instrument or platform frame, and the coordinate frame in which the computations are carried out; computational frame (Ref 1). Usually, the rotational velocity is sensed by a set of gyroscopes. For the translational acceleration, sensors called accelerometers are used. The accelerometers use a test mass suspended, in some manner, within the instrument case as an acceleration detector. Thus, the accelerometer only senses the differential acceleration between the test mass and the instrument case which is mounted through a suspension system to the body of the vehicle. This differential acceleration is called specific force, $\underline{f}$, and results from forces which act directly on the vehicle such as thrust or aerodynamic lift. Gravitational attraction acts simultaneously on the test mass and the

_____

[*]Examples of systems not included are those which do not inertially instrument the vertical channel (Ref 1:109) and systems with modeling assumptions which would mask any improvement in the gravity model (e.g. Ref 2:133).

3

vehicle. hence it cannot be sensed by the accelerometers (Ref 3:230-231, and Ref 1:2). The total inertial acceleration is the sum of the sensed specific force and the unsensed gravitational acceleration. Since gravitational attraction is not sensed directly, an INS must contain a gravity model to complete the information needed for the translational navigation task.

B. Traditional Modeling Approaches

The nature of past INS gravity models for airborne use (Ref 4: pp. 1-4, 6) has been driven by two predominant factors. First, computer memory space and computation time represent a precious system resource. Other mission requirements are frequently asynchronous to, and higher priority than, the navigation function: for example the attitude control function. The second factor is the existence of inertial instrument errors. The sensed specific force and the computed gravity are, symbolically at least, summed before entering the first level of integration. Thus, there is little incentive for creating a gravity model which is much better than the accelerometer uncertainty level. These factors have led to the use of simple models which are based on an intuitive, but effective, idealization. In this section we shall discuss the historical basis for this ideal or normal gravity model, we shall evaluate the effectiveness of this ideal field as an approximation to the true field, and we shall discuss the practical approximations to this ideal model which are actually used.

4

The fundamental shape of the Earth is well-described by an ellipsoid (an ellipse of revolution about its minor axis through the poles). This notion was conceived by Newton (Ref 8). It is based on the concept of water, the seas, not flowing on an equipotential surface, mean sea-level for example. This lack of flow also indicates the force, gravity in this case, is perpendicular to the surface (hence the term "normal field"). It is interesting to note that the shape of a homogeneous fluid rotating at Earth rate would be an ellipsoid with eccentricity very near that of the reference ellipsoids used in geodetic surveys and systems (Ref 9). The term "ellipsoid gravity model" refers to a model based on the gravity vector being perpendicular to the surface-approximating ellipsoid.

This ellipsoidal model requires only three parameters, but it is impressive in terms of the small residual error between model gravity and true gravity. This error never exceeds 400 mgal (1 mgal = 10^{-5}m/ sec^2, approximately 1 μg)--an error of approximately one part per 2500. Kayton (Ref 5:Vol II p 289) suggests that the ellipsoidal model is adequate for systems with accelerometer uncertainty levels greater than 20 mgal. This results from the premise that we view accelerometer and gravity model errors in a static sense. A more precise measure would consider the time spectral properties of these different system error sources. We must understand more about the application of the ellipsoidal model before this point can be pursued.

The ellipsoidal model is cumbersome to program since it calls

for terms not necessary for any other navigation function. The result

is approximations of the approximation. That is, computationally

efficient simplifications are used in place of the complete ellipsoidal

formulae. The simplifications are developed around readily available

navigation quantities, and this set varies with specific navigation

algorithm. Two examples are the local-level computational frame and

the inertial computational frame. An INS which computes in a local-

level (Ref 1:109) coordinate frame tends to have latitude and altitude

available. Hence, approximations are made based on these inputs

(Ref 4:1-11, 1-16, 1-23, and 1-28). For Earth-centered inertial[*] (als

known as geocentric inertial, ECI, or i-frame) or in Earth-centered

Earth-relative[*] (Geocentric relative, ECE, or e-frame), the "gravita-

tional" field resulting from an ellipsoid "gravity" model is computed

directly from the Cartesian components of the position vector. For

this case, the formula used is based on a truncated series expansion of

the ellipsoidal potential. This spherical harmonic model requires the

definition of a number of coefficients called J-terms. These J-terms

are based on satellite and ground survey gravity data. This approach

is well-documented (see Ref 1:49-53; Ref 5:309-313; Ref 6:195-225;

Ref 9:Appendix; Ref 10:App.B; Ref 11:App.E; Ref 12:35-43; Ref 13:36-

42; Ref 14:20-35; Ref 15:139-142; and Ref 16:419-423). We shall return

---

[*]Typically these frames are centered at the Earth's center of
mass (Ref 5:Vol I, pp 6-9 and Vol II, pp 288-289); the i-frame is non-
rotating with respect to the distant stars.

to this particular model later, but for now, consider the results of these approximations to the ellipsoid gravity model.

The standard for comparison of modeling simplifications is the WGS 72 ellipsoid (Ref 17). The local-level models vary as much as 20 mgal from this reference. This result is due to the altitude correction simplifications. The spherical harmonic model can be more precise; it reproduces the ellipsoidal model to within 0.1 mgal in one example (Ref 4:1-5).

Direct comparison of these simplified ellipsoid models with true gravity have not been made. Geodetic gravity surveys measure gravity on the Earth's surface and extrapolate to a reference ellipsoid. This measure of gravity at the ellipsoid surface can be compared directly to the ellipsoid gravity model value (Refs 9, 14, and 17). A good ellipsoid can result in global maximum error of approximately 400 mgal. The ellipsoid can also be varied to produce a better local fit in some region of interest. The nature of these errors in modeling is important and merits further discussion.

C. The Nature of Modeling Errors

The Earth's gravity field varies with position and with time. The time variations can be subdivided into categories:

  a. The Earth's rotation with respect to inertial space,

  b. Celestial bodies (primarily the Sun and Moon), and

  c. Earth's mass redistributions (primarily tides).

The effects due to b. and c. are on the order of tenths of a milli-gal (Ref 18:76-77). The effects due to a. are on the order of hundreds (not hundredths) of milli-gals. Although modeling the effects due to b. and c. would be relatively simple, this effort would be pointless without a major resolution of the a. effects. So, we shall restrict our attention to the Earth rotation effect which is simpler from an Earth-relative observer's point of view. Since we are ignoring the tidal and celestial body effects, an Earth-relative observer would see a static gravity field at each point. The true (time-average, Earth-relative) gravity field is then a vector function of an Earth-relative position vector (e-frame for convenience). Symbolically, we are stating that

$$\underline{G}^e(\underline{r}, t) \approx \underline{G}^e(\underline{r}^e) \tag{1}$$

The model we seek is a closed-form mathematical relationship either $\underline{G}_m(\underline{r}^e)$ to approximate gravitation $\underline{G}(\underline{r}^e)$ or $\underline{g}_m(\underline{r}^e)$ to approximate gravity $\underline{g}(\underline{r}^e)$.

Going back to our inertial observer, we may mathematically express what he will see in terms of the above function definitions.

$$\underline{G}^i(\underline{r}^e) = C_e^i \, \underline{G}^e(\underline{r}^e) = C_e^i \underline{G}^e(C_i^e \, \underline{r}^i) \tag{2}$$

where C_e^i is the e-frame to i-frame coordinate transformation matrix; C_i^e is its inverse. Elements of C_e^i are trignometric functions of the product of time and Earth rotation rate, $\omega_{ie} t$ (Ref 1:36 for example). So, for a fixed $\underline{r}^i$, the gravity field is periodic at Earth rate. Then,

8

$\underline{G}^i(\cdot)$ is an explicit function of time through C_i^e and an implicit function of time through $\underline{r}^e(t)$. With our assumptions, we consider $\underline{G}^e(\cdot)$ to be only an implicit function of time via $\underline{r}^e(t)$.

We may now formally define the gravitation, or gravity, modeling errors by

$$\delta\underline{g}(\underline{r}^e) = \underline{g}_m(\underline{r}^e) - \underline{g}(\underline{r}^e). \qquad (3)$$

Since, $$\underline{g} = \underline{G} - \underline{\omega}_{ie} \times (\underline{\omega}_{ie} \times \underline{r}), \qquad (4)$$

we also have

$$\delta\underline{g}(\underline{r}^e) = \underline{G}_m(\underline{r}^e) - \underline{\omega}_{ie} \times \underline{\omega}_{ie} \times \underline{r} - [\underline{G}(\underline{r}^e) - \underline{\omega}_{ie} \times \underline{\omega}_{ie} \times \underline{r}].$$

Hence, $$\delta\underline{g}(\underline{r}^e) = \underline{G}_m(\underline{r}^e) - \underline{G}(\underline{r}^e). \qquad (5)$$

The gravitational and the gravity modeling errors are the same. This process is depicted in flow-chart form in Figure 1.

D. Propagation of Errors in an INS

The resulting error vector, $\delta\underline{g}$, is an explicit time function in the i-frame and an implicit function of time in the e-frame. Since $\underline{G}_m^e(\cdot)$ models the Earth-relative time-average gravitational field, $\underline{G}^e(\cdot)$, we must view $\delta\underline{g}^e(\cdot)$ as the time average gravitational error for each argument $\underline{r}^e$. Having defined this error, we now turn our attention to the effect it has on navigation performance. We need to understand how these errors enter the navigation algorithm, what in mathematical

9

Earth's True Gravity

$$\underline{g}(\underline{r}, t)$$

Time average in
Earth relative frame

$\underline{g}(\underline{r}^e)$, representative Earth
gravity

$$\underline{\omega}_{ie} X(\underline{\omega}_{ie} X\underline{r})$$

$\delta\underline{g}(\underline{r}^e)$
gravity
modeling
error

$\underline{g}_m(\underline{r}^e)$
model
gravity

$\underline{G}(\underline{r}^e)$
representative
gravitation

$$\underline{\omega}_{ie} X\underline{\omega}_{ie} X\underline{r}$$

$$\underline{G}_m(\underline{r}^e)$$

Earth's Gravitation Model
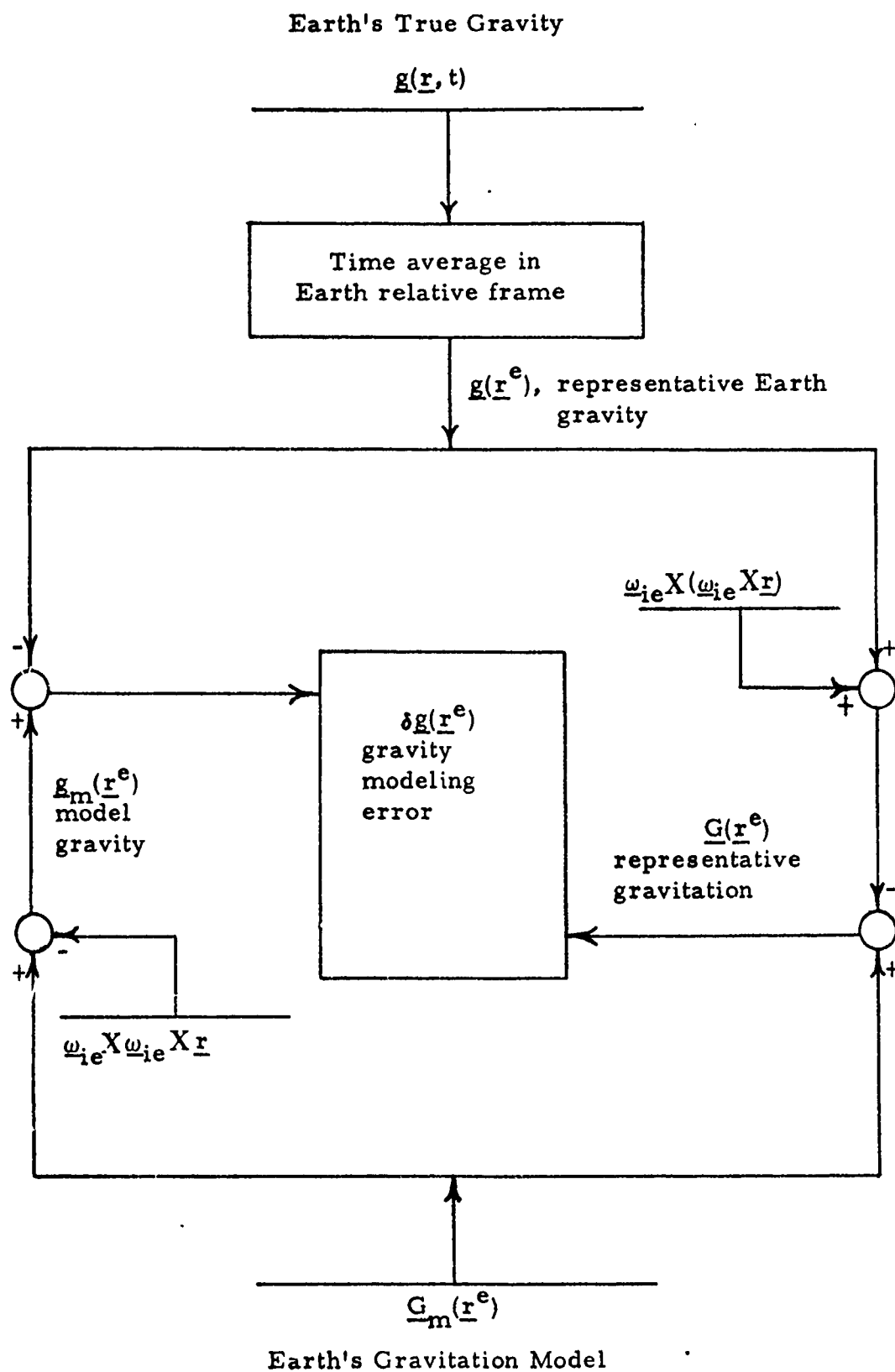
Figure 1. The Gravity Modeling Error

10

terms the algorithm does to these errors, and the nature and extent of corruption of navigation estimates.

The INS solves for position and velocity by a double integration of an estimate of acceleration. This estimate is formed by summing the specific force sensed by accelerometers with the model-computed gravitational acceleration. We must clearly distinguish between the modeling error, $\delta \underline{g}$, and the INS propagation error which results from an error in the INS position estimate. This propagation error can be formally defined as the gravitation at the estimated position, $\underline{G}(\hat{r})$, less the gravitation at the true position, $\underline{G}(r)$. With this distinction between the different types of gravitational modeling errors, we may proceed with an INS error analysis.

We are interested in INS estimates, so we need to define position and velocity error quantities. Let

$$\delta \underline{r}(t) = \hat{\underline{r}}(t) - \underline{r}(t) \tag{6}$$

and

$$\delta \underline{\dot{r}}(t) = \hat{\underline{\dot{r}}}(t) - \underline{\dot{r}}(t) . \tag{7}$$

The exact form of the relationships between $\delta \underline{g}$, $\delta \underline{r}$, and $\delta \underline{\dot{r}}$ depends on the specific navigation mechanization and computational approach. Such matters as independently-sensed velocity feedback and vertical channel altimeter aiding introduce analysis complexities that would obscure the fundamental point we are pursuing at this time. These issues must be dealt with, but we shall table them for now. We can see

11

the basic interrelationship by considering a first-order perturbation of the navigation differential equation

$$\ddot{\underline{r}} = \underline{f} + \underline{G}(\underline{r}^e),\tag{8}$$

where $\underline{f}$ is the true specific force.

The specific form of (8) depends on the computational coordinate frame. Reference 1 presents a full description of this topic and introduces the notation used herein. References 2 and 19 are extensions, corrections and clarifications of this work. Many error sources must be included to perform a complete navigation error analysis. We are restricting our scope to gravity modeling errors and their propagation (e. g. $\delta\underline{f} = \underline{0}$). The first-order differential equation from (8) becomes

$$\delta\ddot{\underline{r}} = \delta\underline{g}(\underline{r}^e) + \Gamma(\underline{r}^e)\,\delta\underline{r}\tag{9}$$

where $\Gamma(\underline{r}^e)$ is the gravitation tensor $\partial\underline{G}(\underline{r}^e)/\partial\underline{r}$ (see Appendix A).

This equation describes the propagation of both types of gravity errors: gravity modeling errors given by $\delta\underline{g}(\underline{r}^e)$ and the error in calculating gravity with an error in the position estimate. Since we assume no velocity or altitude aiding, we may obtain $\delta\underline{r}$ by a double integration of (9). Appendix B shows the inherent instability of the "vertical channel" of (9). In practice altimeter aiding is used to stabilize this channel and this will complicate the analysis. It will suit our purposes to consider only the horizontal channels for a simple example of error propagation. Again, Appendix B develops the

12

homogeneous portion of (9) for one horizontal coordinate. Adding the modeling error back in yields

$$\delta\ddot{x} = \delta g_x - \omega_s^2 \, \delta x \qquad (10)$$

where ω_s is the Schuler rate given by $\sqrt{g/r}$.

This undamped, second-order error differential equation has well-known characteristics. Sinusoidal steady-state analysis shows a high sensitivity to time-frequencies near this Schuler rate. The steady-state analysis fails for inputs of δg_x at the Schuler rate since the particular solution to (10) is unbounded. This case can be analyzed in the time domain and can give some insight into the problems that gravity modeling errors might cause.[*] Reference 20 provides data on the variation of gravity, or gravitation, from a reference ellipsoidal field along a transcontinental path across the 35° latitude line of the United States. The horizontal component is recorded as the angle true gravity is deflected from the ellipsoidal gravity in East-West, prime, and North-South, meridian, directions. The root-mean-square value for each direction is near five arcseconds (Ref 21), which translates to approximately 25 mgal. Suppose the δg_x driving term in (10) is sinusoidal in its argument for horizontal motions. Let d be the spatial period so

---

[*]This example is contrived to show the worst accuracy degradation, however it provides a simple closed-form demonstration of some basic concepts.

13

$$\delta g_x(\underline{r}^e) = \delta g_x(x) = 25 \sin\left(\frac{2\pi}{d}x\right) \text{ mgal.} \tag{11}$$

Now suppose the vehicle travels at constant velocity such that

$v_x = \omega_s d/2\pi$. Express x as: $x = v_x t + 0 = (\omega_s d/2\pi)t$. Then

$$\delta g_x = 25 \sin(\omega_s t) \text{ mgal.} \tag{12}$$

Identify $\delta \dot{x}$ as δv_x and assume zero initial conditions on (10).

We can solve the particular problem now by LaPlace transforms and

find $\delta v_x(t) = (25 \text{ mgal}) \, t \sin(\omega_s t)$. \hfill (13)

Note that the amplitude of the sinusoid grows linearly with

time--an unbounded response. Take for example the air launch of an

ICBM as a way of gauging our concern with (13). We know (Ref 16:305)

that at ICBM ranges a one foot-per-second velocity error can cause a

one nautical mile miss. At this rate, we would only have two minutes

of cruise time before (13) would indicate error divergence with the

potential for a 0.1 n.mi. miss from gravitational modeling effects alone.

The point of this much-contrived example is that there are conceivable

applications where present gravity models are inadequate. Also, it

should be clear that the extent to which our estimates are corrupted by

this gravity noise depends on the spatial frequency of the gravity model-

ing errors, on the time frequency response of the INS, and on the

mission velocity which translates the spatial gravity modeling error

function into the time domain.

E. Magnitude of Resulting INS Errors

With this background, let us consider more complete studies of

gravity modeling effects on INS estimates. The open literature contains two distinct types of studies on navigation accuracy with gravity modeling errors: statistical and deterministic. The statistical studies (Refs 21, 22 and 23) are covariance analyses or Monte Carlo analyses based on a statistical model of the gravity modeling disturbance. The deterministic studies (Refs 24 and 25) are simulation analyses which include detailed local gravity models for the region of interest. The statistical studies provide parametrically the expected accuracy degradation, whereas the deterministic studies give specific case data which include error time histories.

1. <u>Statistical Analyses</u>. Historically the statistical studies appear first. The gravity modeling error is itself statistically modeled. The disturbance vector, δg, is not necessarily modeled directly; in Reference 21, the deflection angles, ξ and η, are modeled as the outputs of spatial linear systems driven by white gaussian noise (Ref 26). Statistical model details vary, and a great deal of research has been devoted to defining a statistical model which is consistent with both observed gravity data and with gravitational field theory. The statistical model issues are discussed in Appendix C; our concern here is the effect of gravity modeling errors on navigation accuracy.

The Levine and Gelb paper (Ref 21) is the classic in the statistical studies category. Their approach is a steady-state-covariance analysis (Ref 27) which requires the total problem to be cast in the

form of a linear, time-invariant stochastic differential equation. The statistical model for the gravity error is based on an exponential auto-correlation function, for example

$$\phi_{\xi\xi}(x) = \sigma_\xi^2 \, e^{- \frac{|x|}{d_\xi}} \tag{14}$$

where ξ is the meridian vertical deflection,

x is the shift distance,

σ_ξ^2 is the variance of ξ, and

d_ξ is the correlation distance.

With (14), σ_ξ^2 and d_ξ completely specify the statistical model. Gravity disturbance components are assumed uncorrelated, so ξ and η (the prime deflection) are uncorrelated. This assumption statistically uncouples the horizontal channels. The INS model, also, dynamically uncouples these channels. Rate feedback from a non-inertial sensor is assumed and the error propagation is governed by (10) with the addition of the rate feedback term:

$$\delta\ddot{x} = -K \, \delta\dot{x} - \omega_s^2 \, \delta x - \delta g_x \tag{15}$$

where K is the feedback gain for the non-inertial velocity damping. Recall that the disturbance term is a function of Earth-relative position. To implement (15) we must convert the disturbance term to the time domain. This is accomplished through two steps: model (14) as a first-order, linear, time-invariant stochastic differential equation in

16

the argument x and use velocity to convert x, hence (14), to the time domain. First,

$$\frac{d\xi(x)}{dx} = - \frac{1}{d_\xi} \xi(x) + q_\xi(x) \qquad (16)$$

where $q_\xi(x)$ is a zero-mean, white, gaussian noise process with auto-correlation function of $\frac{2\sigma_\xi^2}{d_\xi} \delta(x)$. $\delta(x)$ is the Dirac delta function which satisfies

$$\left\{ \begin{array}{ll} \delta(x) = 0 & \text{for all } x \neq 0 \\ \displaystyle\int_{-\epsilon}^{\epsilon} \delta(x)\, dx = 1 & \text{for all } \epsilon > 0. \end{array} \right\} \qquad (17)$$

The entire analysis is performed in a quasi-static sense with a constant velocity assumed then varied parametrically. Then,

$$dx = v_x\, dt, \qquad (18)$$

and

$$\delta[x(t)] = \delta(v_x t) = \frac{1}{v_x} \delta(t). \qquad (19)$$

So,

$$\dot{\xi}(t) = - \frac{v_x}{d_\xi} \xi(t) + q_\xi'(t) \qquad (20)$$

where $q_\xi'(t)$ is zero-mean white gaussian noise with autocorrelation of $2\sigma_\xi^2 \left(\frac{v_x}{d}\right) \delta(t)$. Because deflection angles are small we assume

$$\delta g_x = \xi g. \qquad (21)$$

17

With (21), equations (15) and (20) form the required stochastic time differential relationship for the steady-state covariance analysis. In retrospect, it is interesting to compare the transition from spatial, (11), to time, (12), domain in the simple closed-form example above to the transition in this stochastic analysis from (16) to (20).

With this system of differential equations driven by white gaussian noise, the steady state covariance of navigation position and velocity errors can be found using LaPlace transform techniques on the system covariance matrix equation. The structure of the Levine and Gelb analysis is easier to summarize than the results. Velocity, correlation distance, and INS damping, K, are varied parametrically. The independent variations of v_x and d_ξ are unnecessary since in the final results they always appear in the ratio

$$\beta_\xi = v_x/d_\xi \qquad (22)$$

This result is important in its own right; this implies that the same rms navigation error results from an increase in velocity as in a decrease in correlation distance. In the limit, increased velocity or decreased correlation distance cause the gravity disturbance to approach white noise (which is precisely what zero correlation distance would mean in the spatial domain) with the exponential function approaching the delta function and correlation time $(1/\beta_\xi)$ approaching zero. In the limit in this direction, both position and velocity rms errors approach zero.

18

For the other extreme, consider either velocity decreasing or correlation distance increasing (β_ξ approaching 0). Then, the disturbance looks more like a constant. Since we have a non-inertial, and for now presumably perfect, velocity sensor, the steady-state velocity error goes to zero. The position error approaches the constant value that reflects the position offset, incurred while nulling the velocity, required to exactly cancel the gravity disturbance. From (15), this offset can be seen as the gravity disturbance divided by the square of the Schuler rate.

While the position rms error is maximum for this near-constant disturbance, the velocity rms error behaves quite differently. As discussed, the velocity rms error approaches zero for the cases of β_ξ approaching either zero or infinity. This result is predicated on σ_ξ^2 staying finite and some further analysis is really required if we want to let $\delta g_x(t)$ approach white noise. The velocity rms error per unit of standard deviation has a maximum when β_ξ equals the Schuler rate ω_s. The δg_x spectral characteristics are best aligned with the navigation filter under these velocity/correlation distance conditions. Hence, in studying gravity error propagation, we need to pay attention to this type alignment since the error sensitivity is highest there. In particular, if we decompose the gravity disturbance into a Fourier series from the spatial domain, we get a sum of sinusoidal terms similar to (11). The velocity interpolation can then be used, as in (12), to convert to the time domain. Then, we can identify those frequencies which will cause

19

the greatest navigation rms errors.

Other observations can be made on the various interplays between the statistical model and the INS dynamics; however these results are somewhat intangible. What we need is a perspective on how realistic gravity disturbances compare with other navigation error sources. The traditional way of presenting these data is an error budget which, for a specified set of hardware and a specified mission, allocates the expected error into compartments labeled by the various recognized error contributors. This more satisfying approach was taken by Nash, D'Appolito, and Roy in Reference 23.

For a given polar flight profile, a gravity-error-alone analysis shows, over the first phase of the mission, a 0.03 n.m. position error per hour of flight per arcsecond rms deflection of the vertical. Next, an integrated system based on a 0.5 n.m./hr. INS hardware. Doppler radar velocity aiding and Loran position aiding were included in the integrated system analysis. A severe gravity disturbance model was used with a 20 arcsecond rms deflection and 20 n.m. correlation distance. In the final analysis, the errors due to vertical deflections were substantial. Approximately seventy-five percent (75%) of the radial velocity error, thirty percent (30%) of the radial position error, and fifteen percent of the heading error were attributed to the vertical deflections. Even if the input deflections were reduced to a more globally representative rms level, say seven arcseconds, the resulting navigation errors would constitute a significant and irreducible error

20

term with the traditional gravity model. More significantly, the vertical deflection induced errors would be on the same level as the gyro and accelerometer induced errors. A significant improvement in the inertial sensors, say to a 0.1 n.m./hr system, would not correspondingly improve integrated system accuracy since the gravity modeling error would remain.

2. Deterministic Analyses. From both parametric and specific mission studies, the statistical approaches have shown the nature and extent of navigation errors induced by gravity modeling errors. The deterministic approach allows a means of comparing these statistical results with a gravity field which is very nearly a duplication of the actual field in some area of the world. Also, by forming a truth model to simulate the actual field we can simulate a navigation mission and produce error time histories. These data complement the average, or expected, data from statistical analyses.

Chatfield, Bennett, and Chen presented such an analysis in Reference 24. For a specific flight path in the western United States, they constructed an extensive point-mass anamolous gravity model from available measured gravity data. We shall discuss this modeling technique later; for now, it is sufficient to note that this point-mass model together with the reference ellipsoid model form a much closer approximation of the true field in a deep volume of space surrounding the flight path. The comparison of model gravity with the surface gravity

21

data shows residuals within a mgal directly over the grid midpoints.

With this near-perfect model, simulated aircraft test runs were made assuming both aided and unaided INS. The point mass truth model was used to generate true position and velocity. The simulated INS used only the ellipsoidal model. Differences between the two gravity calculations were as high as 50 mgals during the simulated missions. The differences in position and velocity between INS estimates and the truth model output represent the INS estimation errors. These errors are indicative of what one could expect in an actual flight.

The unaided INS errors reached peaks of near 2000 ft in position, 2 ft/sec in velocity, and 15 arcseconds in heading. The aided INS case assumed position checkpoints periodically spaced along the flight path and assumed doppler radar velocity measure. Since only gravity anomaly errors were simulated, these aids were noise-free and substantially improved performance. The position errors were suppressed below 400 ft, while velocity error stayed under 1 ft/sec. The heading angle, while smaller than in the unaided case most of the time, did reach a peak value near 20 arcseconds. A cursory comparison of the error time histories shows for the unaided case that the statistical methods of Levine and Gelb (Ref 21) would have accurately characterized the rms errors. The time histories of errors, of course, would not be available from a purely statistical approach.

Reference 25 contains results from a continuation of the Reference 24 studies. These results are interesting because they point out

22

a problem associated with gravity modeling beyond the INS estimate errors. In a flight test of an INS, one goal is to assess INS accuracy and to also determine the accuracy of individual components and sub-systems. The usual approach is to structure the analysis along filter-ing theory lines. Component error sources are modeled and integrated with the INS error dynamics model to form a system model. Check-point and other tracking data give a measure of the INS error at various points during the mission. Post flight data processing typically employs regression analyses to find the component error model parameters which best fit the observed data in the sense that the error residuals are minimized in some way. These error parameters can only be identified by the spectral properties of their resulting INS errors. When gravity model errors are not included in the above analysis, the gravity model-ing induced errors spill over spectrally into this component parameter identification process thus corrupting the results. This problem has been ignored heretofore since INS component errors were large in com-parison. This study (Ref 25) was conducted for Holloman AFB INS test-ing and is evidence that the day has arrived when we can no longer ignore this factor. Plans for testing state-of-the-art inertial systems are beginning to include the requirement for detailed local gravity data for use in the regression analyses.

F. Impetus for Improvements

We have seen the nature of gravity modeling errors and the

23

magnitude of INS errors they cause. It is easy to understand why a detailed new model might be used in a flight test environment where data purity is important. One could question the need for model refinements since the errors induced are not unacceptable for most navigation applications. The impetus comes from the potential military application-- where the impetus for inertial navigation originated. In the delivery of weapons, any error diminishes weapon system's effectiveness, so these gravity induced errors cannot be ignored. The self-contained nature of inertial navigation virtually assures a continued dependence even with advanced radiometric navigation systems available. The evolution of strategic force concepts provides the prime motivation for the increased emphasis on refining the traditional gravity modeling techniques.

The United States' lead in quality of ICBMs is expected to decline (Ref 26) in the next decade. One proposed response to a growing counterforce threat is to mobilize the currently silo-based ICBMs (Refs 27 and 28). Leaving the static silo environment for a dynamic, air launch, or intermittently dynamic, revetment launch, environment will certainly decrease the expected accuracy of this force (Ref 29). One cause for this loss, is the fact that silo-based missiles are targeted with the aid of extensive point-mass models for the launch region (Ref 30). While this loss could eventually be recovered by modeling all the possible mobile launch regions, we still have to deal with the problem of initial conditions for the missile navigation algorithm.

The silo-based missile INS can be initialized with the known position and with an (expected) zero Earth-relative velocity prior to launch activities. In any dynamic launch, these data must be provided by navigation. Our earlier example of the nature of INS error propagation indicated that in that contrived case only minutes would elapse before gravity modeling errors would blunt the weapon system's effectiveness. The deterministic study (Ref 24) of the last section indicates that for that case, even with many external aids, the velocity errors can grow to the one-foot-per-second level. At ICBM ranges this error has the potential to cause a 1 n mi miss (Ref 16:305). From Reference 26, this type of accuracy virtually eliminates such a weapon system from use against targets hardened to nuclear attack.

The ICBM concern is not the only one. Proposed air-launched cruise missiles (Ref 31) will encounter similar problems. The potential degradation may be greater due to the longer navigating flight time of the missile. Also, one must consider the counterforce mission these cruise missiles are postulated to perform.

From these uniquely military applications, we can see a need to refine gravity modeling. The nature of the refinements must be predicated on the real-time and on-board need for the data. The dynamic nature of future missions is likely to preclude the extensive ground-based pre-mission targeting which compensates for these gravity effects today. So, whatever new methods evolve, they must be computationally efficient: yielding the greatest accuracy improvement

25

for the investment of on-board computer storage space and execution time.

G. Improvement Approaches

There are many current and past activities that either directly or indirectly suggest approaches to this problem. The "software" approaches fall into several categories. The statistical approach simply employs filter theory to form an estimate of the gravity disturbance. The point-mass model is an example of finite-element approaches which, in essence, build mass distribution perturbation models. Another software approach simply employs fundamental potential integral relationships. These integrals are approximated using observed gravity data. Then transform techniques can be employed to decrease the computational burden. Aside from these approaches, new inertial instruments are being developed for gravity mapping (Ref 32). As McKinley has noted (Ref 29), it is ironical that the instrument (gradiometer) developed for the mapping application can simultaneously make the mapping unnecessary. We need to delve into all these areas before addressing a plan of attack on the model refinement problem.

1. Statistical

Statistical methods can be employed pre-mission (a priori) or during the mission (real-time). Pre-mission data preparation might include forming a mission-dependent ellipsoid model to lower the rms

26

anomalous gravity for that specific mission trajectory or area. Another à priori approach is to define the navigation mission in great detail, simulate the trajectory with an accurate gravity model, and off-set the initial conditions of the navigation filter to compensate for the expected errors. Such à priori methods are open-loop in that the actual trajectory may vary considerably from the planned one due to environmental effects or other modeling errors. Changing the INS algorithm to reject the short spatial wavelength gravity noise is unacceptable because we would also reject any measured acceleration which fell into the same time spectrum. The real-time role for statistics has little more potential.

In real-time, we can use statistical methods to predict the near-term influence of anomalous gravity on navigation estimates. To implement such a scheme, we need external navigation fixes which allow us to observe the navigation errors periodically. With anomalous gravity modeled as a Gauss-Markov process (see Appendix C) in our Kalman filter, the estimated states associated with this model will allow us to statistically predict our near-term anomalous gravity effects. This approach has been considered for INS flight tests (Ref 25) as a means of removing the effects of gravity noise from INS component performance estimates.

These statistical methods have limited scope because they do not take advantage of all available gravity data except in an average sense from the empirical autocorrelation function (see Appendix C).

27

The following methods, in one form or another, use the gravity data.

2. Finite Element Methods

The term "finite element" to some connotes a recursive approximation based on a tri-diagonal Grammian matrix. We use the term to denote all gravitation or geopotential modeling which are based either on a finite partition of the geoid surface for integration approximation, on a finite number of mass distribution elements, or on a finite set of local approximating (interpolating) functions. Of all the methods we shall discuss, only the point-mass method has ever been used for INS aiding--and this aiding was pre-mission, not in-flight (Ref 30). So, these methods are discussed because they have the capability to form improved INS gravity models. All of these models have been proposed to support the basic task of Physical Geodesy: defining the geoid (Refs 8 and 34).

Since we already have Legendre polynomial spherical harmonic functions as a spanning set of functions, one might ask why we do not fill out the coefficients to the degree and order necessary. The truncated spherical harmonic series forms a finite element model by the above definition, so we shall treat it as such and discuss its merits as an improvement candidate. Since this model is global in scope, it requires global data for complete coefficient identification.[*] The Earth

---

[*]Local models can, however, be created by using restricted-area data.

is large and we must have information in our model of relatively short spatial wavelength. Shannon's sampling theorem tells us to collect data on a grid finer than the shortest wavelength that we wish to represent--such a survey is not economically or politically feasible. With extensive new data from GRAVSAT/GEOPAUSE, Koch (Ref 35) points out the potential for rather severe aliasing at the order-and-degree 12 truncation level. The message is clear, if you want to significantly improve the gravity model, you should concentrate your model and your survey in the local area of operation.

As mentioned, the subject methods are all suggested for subtasks in defining the geoid. The most basic methods come directly from potential theory: the surface integrals of anomalous potential (equivalent to undulation) or gravity anomaly. These integrals map the anomalous potential or gravity anomaly over some closed surface onto the gravity disturbance vector at any point outside the closed surface (see Section H below). These integrals are approximated by partitioning this reference surface into a finite number of elemental areas and forming the sum of the products of the approximated integrand and the respective elemental area. The global nature of this task can be ameliorated by a variable grid spacing: a fine grid in the immediate vicinity of the evaluation nested in a sequence of grids of ever-increasing coarseness (Ref 14:120). The number of elements for a coarse global $5^\circ X5^\circ$ partition is over 2500, so the number of parameters for such a model could easily reach 10,000. The number of multiply and add operations would be on

that order also for _each_ gravity evaluation.

Morrison (Ref 36) suggests another integral approach based on integrating over a geoidal surface density model. In the geopotential application he suggests partitioning the geoid surface into 1640 equal-area elements. Although more flexibility can be formulated, the computationally efficient form is to assume constant density layers within each block. In this form, the model seems no different for our application than the point mass model.

The point mass model is the prime candidate from the mass distribution modeling area. Other mass distribution models appear in geophysical prospecting (Refs 18 and 37), but they offer no special advantage for our purpose. The mass distribution techniques allow a direct gravity calculation using Newtonian gravity formula, in turn, on each mass element. We can model the anomalous field as closely as we wish by increasing the number of elements and decreasing the grid spacing (Ref 38). Such a modeling technique has global (Ref 39) as well as local (Refs 24 and 30) possibilities.

The MINUTEMAN Launch Region Gravity Model is an application of point mass modeling to aid INS performance. As mentioned previously, this model was not stored in and executed by the airborne computer; the effect of anomalous gravity was compensated for in pre-mission targeting calculations using a larger ground-based computer. The point mass grid spacing, similar to our integral approximation, is based in a nested sequence of grids of ever-increasing coarseness.

30

The finest grid is, naturally, in the area immediately surrounding the silo. The point masses are submerged below the reference surface a depth equal to the grid spacing to enhance parameter identification convergence (Ref 40:5-6). This method has built-in upward continuation in the Newton gravitation inverse-square equation. The problems associated with parameter identification and the computational burden of the inverse-square calculation for a large number (2520 for MINUTEMAN) of point masses must be considered when evaluating this modeling technique. A method which eliminates these costly global calculations might prove more useful.

The local functional expansions might fill this expectation. Paraphrasing Junkins (Ref 41), we may build a global (or less) family of locally valid functional expansions rather than one globally valid series expansion. These techniques are closely associated with interpolation techniques--indeed it can be argued that that is all they really are. Junkins (Ref 41, 42 and 43) builds a general technique of partitioning the shell of space out to some radius above the geoid into prisms. Then, gravity is modeled by a functional expansion within each prism. Special interpolation techniques are discussed should some order of continuity be desired from block to block. The functional form is discussed in general, but Chebychev polynomials are stressed. Other potential modeling functions could come from bicubic spline functions (Ref 44), multiquadric equations (Ref 45), binary sampling functions (Ref 46), or Walsh functions (Ref 46). Some extension, say from bicubic to tricubic

31

. splines, and some additional development is required to put any of these latter functions in a form compatible with airborne use.

3. Transformed Integrals

The concept of applying integral transform techniques to gravity data processing is not a new one. Geophysical interpretation by "wave-number" filtering techniques have been used by the petroleum industry since about 1955 (Ref 18:158). An example application is solving the inverse gravity problem (mass distribution from gravity measurements) to surmise the shape and location of ore deposits (Ref 18: 179-185). This process requires a downward continuation of measured gravity; we are concerned with an upward continuation of this same type data.

Transform techniques have only recently been considered for gravity survey purposes. Heiskanen and Moritz make no mention of this possibility in Physical Geodesy (Ref 14) published in 1967 and the standard reference in the field. In 1974, Davis, et al (Ref 47) used Fourier transform analyses in comparing relative errors for several algorithms used in computing vertical deflections. Then, Davis (Ref 48) used one- and two-dimensional Fourier transform error analyses as a basis for designing geophysical surveys. In 1975, Long (Ref 49:44-45) suggested applying Fast Fourier Transform (FFT) techniques to solutions of Stokes and Vening-Meinesz integrals. More recently (1976), Thomas and Heller (Ref 50:Chapters 3 and 4) proposed a comprehensive

32

gravity data processing system based on frequency domain techniques.

These works and suggestions have dwelled on surface gravity calculations. The obvious extension is to apply these methods to airborne gravity calculations. Prado (Refs 51 and 52) has developed this strategy using Hilbert transforms to convert the spatial convolution integral equations (upward continuation and Vening-Meinesz) into spatial frequency domain multiplications. Closed-form expressions are presented for the flat-Earth case; the spherical-Earth case remains an area of active research. Reference 52 also provides an analytical approach for specifying the density and extent of the survey required. Presumably, the transformed data from a gridded survey would be stored in-flight, so gravity model parameter storage requirements can also be assessed.

A definite consideration is the existence of specific hardware to perform the "butterfly" operation (Ref 53:296-297) that is the heart of the FFT. One can conceive of an anomalous gravity computer as a separate functional module. Such a unit would accept navigation position estimates from the airborne computer as input; would perform the necessary transform inverse and interpolation; and would provide anomalous gravity as the output. Such a unit would allow this technique to be incorporated in present systems with modest interface and computational burden on existing airborne computers.

4. Gradiometry

We cannot overlook the one development which treats the gravity error not as a modeling problem but as a measurement problem. The gradiometer research and development addresses the real-time measurement of the gravity tensor, $\Gamma(\underline{r}^e)$, which will allow computation of anomalous gravity in a manner which permits real-time compensation for its effect on navigation estimates. Although gradiometers date back to the late nineteenth century experiments of Baron Von Eötvös, research has been concentrated in the last decade. The motivation for this research is the desire to mobilize the gravity survey.

Gravimeters used in static gravity measurements are accelerometers which, in that role, measure the acceleration required to keep a test mass stationary with respect to an Earth-bound observer. If we use a gravimeter in the dynamic environment of a mobile survey, say airborne, we must compensate for base motions. From the Principle of Equivalence (Ref 1:2), we cannot measure gravitation directly; so, the gravimeter has the same gravitation observation as the accelerometers in an INS. The combination of an INS and a gradiometer can provide the basis for a statistical estimate of gravitation (Refs 54 and 55), but these procedures are not compatible with real-time compensation. Moritz (Ref 56) demonstrated that the spatial derivative of gravitation can be measured, in principle, in a dynamic environment. Conceptually, we could calculate gravity from this measurement through a spatial integration if we know our path through space and we

34

are given an initial condition for gravity at our original coordinates. Thus, a gravity survey could be conducted. In reality, we would need real-time position information which could come from an INS. So, the optimal combination of gradiometer and INS evolves naturally. Since the INS needs gravitation, either model or measured, as an input, we can improve overall system performance by using the results of the gradiometer measurements. To avoid the open-loop propagation of gradiometer errors, the reference field can be used to make gradiometer biases observable (Ref 57 or Ref 58). We need a mathematical formulation for computing anomalous gravity from gradiometer measurements and from the reference field properties.

The first step in this formulation is to recall the definition

$$\delta \underline{g}(\underline{r}^e) = \underline{G}_m(\underline{r}^e) - \underline{G}(\underline{r}^e). \tag{5}$$

Now consider the time derivative of $\delta \underline{g}$ from an e-frame observer's point of view. Operating on (5) we get

$$\left[\frac{d\delta\underline{g}(\underline{r}^e)}{dt}\right]_e = \left[\frac{d\underline{G}_m(\underline{r}^e)}{d\underline{r}^e}\right]\underline{v}_e - \left[\frac{d\underline{G}(\underline{r}^e)}{d\underline{r}^e}\right]\underline{v}_e$$

$$= \left[\Gamma_m(\underline{r}^e) - \Gamma(\underline{r}^e)\right]\underline{v}_e , \tag{23}$$

where the subscript e denotes the time derivative with respect to an e-frame observer. Extending (23) to other coordinate frames follows from a straightforward application of vector calculus. We have $\Gamma_m(\cdot)$,

35

where the subscript here refers to the model not the frame, from our low-order reference model. We are proposing to measure $\Gamma(\cdot)$ with gradiometers. We can form an estimate of $d\delta g/dt_e$ with the additional position and velocity from our navigation filter:

$$\left[\widehat{d\delta g(\underline{r}^e)}/dt\right]_e = \left[\Gamma_m(\underline{\hat{r}}^e) - \tilde{\Gamma}(\underline{r}^e)\right]\underline{v}_e \qquad (24)$$

Given initial conditions, we can estimate δg by integrating (24). Given this $\widehat{\delta g}$, we can estimate total gravitation by inverting (5):

$$\widehat{\underline{G}(\underline{r}^e)} = \underline{G}_m(\underline{\hat{r}}^e) + \widehat{\delta g}. \qquad (25)$$

This demonstrates the possibility of using gravity gradient measurements to calculate total gravitation; again, we must put such a calculation into a total navigation algorithm which will identify and account for gradiometer bias for practical use of the new information (Refs 57 and 58).

We have discussed the use of these gravity gradient measures without discussing how such measures could be made. The Principle of Equivalence eliminates the accelerometer, or gravimeter, as a gravitation sensor. However two accelerometers in the same dynamic environment, with input axes parallel and separated by a small distance can be used to sense differential acceleration. Since the dynamics are essentially the same for such an accelerometer pair mounted on a space-stable inertial platform, any differential acceleration can be attributed to variations in gravitation. We do not require an inertial platform; if

36

the accelerometer pair is allowed to rotate with respect to inertial space we must sense this rotation and compensate for its affect when processing the accelerometer measurements, however. A simple way of seeing the nature of the measurement, is to view the two accelerometers as the simple test masses they embody. One gradiometer design by The Charles Stark Draper Laboratory is based on this simple mass dipole[*] concept. If we treat these test masses as point masse, separated by a lever arm, the difference in gravitation between the pair will create a torque requirement based on maintaining a constant relative orientation of the axis passing through the mass elements. This torque has two degrees of freedom in that a two dimensional vector space of torques is required to counteract any possible torque generated by gravity variations. Decomposing this torque into coordinates perpendicular to the dipole axis and dividing each component by the product of elemental mass and mass separation distance squared yields a discrete approximation of two components of the gravity tensor (see Figure 2 for an example).

With this method for computing the measured gravity tensor components, let us investigate the number of gradiometers required to completely specify the full tensor. In Appendix A we show that the nine elements of the gravity tensor are related through LaPlace's equation and continuity such that only five of the components are independent. Then three of our two-degree-of-freedom gradiometers can provide

---

[*]Dipole is used here for two positive mass units which is at variance with the electromagnetic use of this term.

37
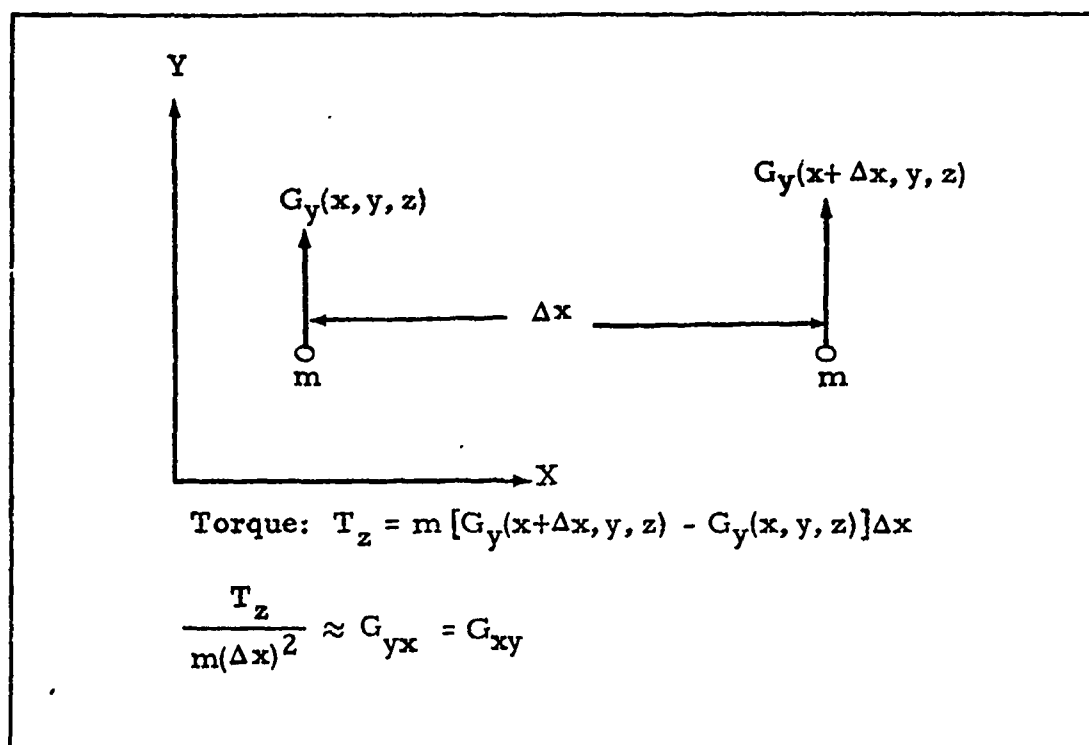
Fig. 2. Example Gradiometer Output

measurements which span this five dimensional space--similar to two

two-degree-of freedom gyroscopes spanning the three dimensional

angular rotation space for an INS.

With the implementation concepts outlined, we return to the

question of gradiometer errors. We have indicated, in general terms,

how the reference field can be used as an aid to eliminate gradiometer

bias effects from our estimates. The gradiometer error models are in

a formative stage. Some parametric studies have been completed (Refs

57 through 61) which give an indication of how much relief we can expect

from these instruments. The goal for these residual errors is on the

order of 0.1 Eötvös units (1 Eötvös unit = 1 EU = $10^{-9}\sec^{-2}$). This

goal is based on gravity survey, not navigation, requirements. These

38

studies indicate that substantial navigation improvements are attained with instrument errors an order of magnitude higher.

With such devices in prototype testing, one might question the need for improving the traditional gravity modeling techniques. The fact is that operational gradiometers are no near-term certainty. The additional weight, space and power required to suspend this gradiometer triad, in a manner which allows us to isolate from or compensate for inertial effects of rotation, will limit gradiometer use to relative large systems. So gradiometers are not a panacea for our gravity modeling problems. They may, however, provide the only economical method for collecting the gravity survey data which will support the model improvements we may propose.

H. Basic Theory

Each of these candidate gravity modeling improvements consists of a process for producing a local gravity estimate using available gravity measurements. The gravity data is collected where and how economical measurements can be made; we require gravity estimates throughout the region of possible INS operation. This practical problem must be approached by appealing to Newtonian gravitational theory. This theory has developed over the centuries, but only a small subset applies to our problem. While some theoretical aspects have arisen in previous discussions, our attention was directed elsewhere and the theoretical aspects were incompletely covered. The following account recapitulates

39

and amplifies those areas directly applicable to the proposed research.

In Newtonian gravitational theory, the fundamental information is encoded in the mass distribution. We conceive an Earth mass distribution function expressed as a density (mass per unit volume) function of the radius vector: $\rho(\underline{r})$.[*] This information is transmitted in the form of gravitational force by the relationship

$$\underline{G}(\underline{r}) = \iiint_E \frac{K \rho(\underline{r}')}{|r' - \underline{r}|^3} (\underline{r}' - \underline{r}) \, dv \tag{26}$$
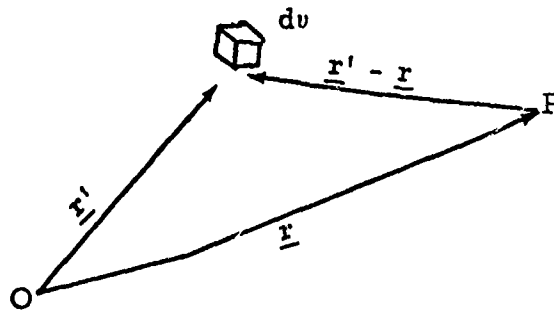
where the triple integral is over the set E which encompasses all Earth mass, K is the Newtonian gravitational constant, $\underline{r}'$ is the Earth-relative radius vector to the incremental volume element symbolically called dv, and $\underline{r}$ is the radius vector to the point P where gravitational force evaluation is made. The gravitational potential function, $V(\cdot)$, summarizes this information as a scalar by

$$V(\underline{r}) = \iiint_E \frac{K \rho(\underline{r}')}{|\underline{r}' - \underline{r}|} \, dv \tag{27}$$

---

[*]We drop the superscript e since these equations do not involve time derivatives and are generally valid for any choice of coordinate frame.

These fundamental gravitational quantities are related by

$$\underline{G}(\underline{r}) = dV(\underline{r})/d\underline{r} \qquad (28)$$

We may derive (26) by formally applying (28) to (27).

These equations are necessary theoretical concepts, but a direct approximation of either (26) or (27) requires a measure of density throughout the Earth's volume which is impractical if not impossible. Fortunately, the information necessary to reproduce the external gravity field is completely summarized in the form of either potential or normal gravitational force, G_n, over a closed surface* S which encloses the set E. There are some drawbacks to this simplification; however we now have a problem that is merely impractical, not impossible. That is, we can collect sufficient Earth surface gravity data to produce useful representation of the Earth's gravitational field.

We can measure gravity directly on the Earth's surface with accelerometers, called gravimeters, which are held fixed with respect to the rotating Earth. These measurements can be processed ("reduced" in the parlance of Physical Geodesy) to produce a representative free-air gravity on the geoid such that Earth mass above the geoid is accounted for and can be neglected (Ref 14:Chapter 3 and 242). The gravitational

---

*Potential theory includes much broader classes of closed surfaces, but this depth will suffice for our purposes. The simply-closed surface is analogous to the Jordan curve from complex variable theory. It is a two-dimensional, connected and closed manifold of finite area and enclosing a finite, non-zero volume (open set) in Euclidian three space.

41

potential can also be measured. This indirect measurement treats the sea-surfaces as (on the average) equipotential surfaces and uses satellite-to-sea altimetry as a measure, albeit noisy, of the geoidal height or undulation, N, above the reference surface. For example, if the satellite altimeter measure is $\tilde{h}$ and if we estimate the altitude using both satellite ephemeris and our Earth surface model to be $\hat{h}$, we may define a measure of geoidal height by

$$\tilde{N} = \tilde{h} - \hat{h}. \tag{30}$$

We get anomalous potential T by a simple first order calculation

$$\tilde{T} = \hat{\gamma}\,\tilde{N} \tag{31}$$

where $\hat{\gamma}$ is the reference gravity value on the reference surface directly below the sea surface point representative of the footprint illuminated in the measurement. Gravitational potential V varies from the reference value by this anomalous amount T, so we can form a measure of V by

$$\tilde{V} = \tilde{T} + \hat{V}_{ref} = \hat{\gamma}\,(\tilde{h} - \hat{h}) + \hat{V}_{ref}. \tag{32}$$

Other methods exist for measuring gravity anomalous behavior. Most are based on variational techniques; for example, attributing satellite orbit perturbations to unmodeled gravitational effects (Ref 14:341-357).

We are concerned here with demonstrating the possibility of such measurements, not an exhaustive recounting of the methods. Now,

having demonstrated the possibility of measuring either gravity or potential over the surface of the Earth, we can direct our attention to Newtonian potential theory. This theory justifies these data sets as sufficient to predict gravitation throughout space above the Earth's surface.

We start with the fact that V from (27) satisfies Poisson's Equation

$$\Delta V = - 4\pi K\rho \tag{33}$$

where Δ is the LaPlacian operator.[*] In regions outside the Earth's mass (ignoring the atmosphere and extraterrestrial bodies for now) ρ is zero so V satisfies LaPlace's Equation

$$\Delta V = 0. \tag{34}$$

Equation (34) is an elliptic partial differential equation which leads to Fredholm type integral equations (Ref 62:230). Solutions to (34) are called harmonic functions and, in general, form an infinite dimensional algebraic vector space. The general solution can be expressed as a linear combination of some basis set of functions with component coefficients to be determined by constraints placed on the solution by the particular problem. By selecting coefficients which meet the boundary conditions of our surface gravity measurements, for example, we

---

[*]In Cartesian coordinates $\Delta = \dfrac{\partial^2}{\partial x^2} + \dfrac{\partial^2}{\partial y^2} + \dfrac{\partial^2}{\partial z^2}$.

43

produce a solution which both satisfies (34) and reproduces the observed data. The only questions of such a solution are existence, uniqueness, and continuous dependence on the data.

The continuity question is easily answered since the data is inside the Fredholm integral. As long as the data is reasonably well behaved (and we have it completely), the derivatives are assured. The solution exists according to Dirichlet Principle and is uniquely defined by boundary conditions of potential or normal gravity by Stoke's Theorem (Ref 14:16-17). When the potential is the boundary condition, we call this the Dirichlet Problem; when the normal gravity is the boundary condition we call this the Neumann Problem.

Thus, knowledge of V or G_n over an enclosing surface is sufficient information to recreate the gravitational field of the Earth's mass distribution. While this condensed information can recreate the gravitational field, it does not uniquely characterize the mass distribution which created it. This non-uniqueness for the inverse problem-- determining mass distribution from potential on a surface--is the bane of geophysical prospecting and Physical Geodesy where the mass distribution is inherently valuable information. This issue is important to us since some modeling techniques (e.g. point mass models) are based on mass distribution representation.

Geophysical, or geological, prospecting has been the prime motivation for development of the inverse solution techniques. The problem is not only ambiguous; it can be ill-posed as well (Ref 40) since

44

·we will never have data at every point on an enclosing surface. These difficulties have not prevented the use of inverse techniques (Refs 18 and 37) since human interpretation can be used to filter out obvious trends. Also, the recognition that most calculations can be posed as multi-dimensional digital filtering problems has resulted in the more successful techniques (Ref 18:157-185).

While we must be aware of the possible ill-posed nature of identifying model parameters, we must keep in mind that our final objective is to model the gravitational force, not the underlying mass distribution. Lee (Ref 63) expresses the appropriate point of view for this situation: objective-oriented identification. Interpreting this concept in terms of the model identification tasks we shall face: We must judge our parameter identification not by how well the Earth's mass distribution is represented but by how well measured gravity data is recreated and how consistent this process is with respect to gravitational theory extant. Since we are modeling for an INS, we should judge the final model performance weighted by the spectral response of the navigation filter. That is, we shall search for models that are most accurate in the passband of the INS algorithm with special emphasis on behavior near the Schuler frequency.

Returning now to our discussion of (34), we may formally solve for the potential at any point outside S, the enclosing surface, by identifying the coefficients for the previously mentioned basis functions. In gravitational theory, the most common set of basis functions are the

45

spherical harmonics. We generate these solutions by first expressing (34) in spherical coordinates:

$$\Delta V = \frac{\partial^2 V}{\partial r^2} + \frac{2}{r} \frac{\partial V}{\partial r} + \frac{1}{r^2} \frac{\partial^2 V}{\partial \phi^2} - \frac{\tan \phi}{r^2} \frac{\partial V}{\partial \phi} + \frac{1}{r^2 \cos^2 \phi} \frac{\partial^2 V}{\partial \lambda^2} = 0$$

(34a)

where r is the radius, ϕ is geocentric latitude, and λ is longitude (either inertial or Earth-relative longitude applies in this case). By separation of variables, the solution $V(r, \phi, \lambda)$ is formed. The familiar spherical harmonics are the outcome of this development. Heiskanen and Moritz (Ref 14:18-35) give a lucid description of this method. The general solution can be written as

$$V(r, \phi, \lambda) = \sum_{n=0}^{\infty} \left\{ \frac{1}{r^{n+1}} \sum_{m=0}^{\infty} \left\{ \left[a_{n,m} \cos(m\lambda) + b_{n,m} \sin(m\lambda) \right] P_{n,m} (\cos \phi) \right\} \right\}$$

(35)

where $P_{n,m}$ is the Legendre function of degree n and order m, and where $a_{n,m}$ and $b_{n,m}$ are the associated undetermined coefficients. As previously mentioned (page 28), determination of these coefficients in a global sense is an inefficient means of producing a detailed, localized gravity model.

Another approach to solving (34) subject to boundary conditions on V or G_n over S is to form the associated integral equation. This approach is simpler when the enclosing surface is a spherical shell.

46

Our surface measurements can be reduced to the geoid which is well-approximated by a Bjerhammer sphere. This approximation introduces errors (Ref 14:241-242) on the order of Earth flattening (1/298.26, Ref 17:16) which is troublesome if we deal with full-valued V and G_n. This problem is ameliorated if we subtract the reference field contribution from the reduced data. The remaining anomalous quantities can be treated as first-order errors and since the flattening is of the same order, the resulting products can be neglected as second order terms. This method is analogous to INS modeling techniques (Ref 1), and thus, this approximation of the geoid by a sphere is consistent with our other analytical tools.

This approach leads to the Poisson Integral characteristic of the upward continuation of a harmonic function:

$$T(r, \phi, \lambda) = \frac{R(r^2 - R^2)}{4\pi} \int_{x=0}^{2\pi} \int_{\phi'=-\frac{\pi}{2}}^{\frac{\pi}{2}} \frac{T(R, \phi', \lambda')}{|\underline{R}' - \underline{r}'|^3} \cos \phi' d\phi' d\lambda' \quad (36)$$

where R is Bjerhammar sphere radius; $\underline{R}'$ is the radius vector to the sphere surface incremental area defined by geocentric latitude ϕ' and longitude λ'; and $\underline{r}$ is radius vector to point defined by r, ϕ, and λ (Ref 14:37). Hereinafter the set $\{r, \phi, \lambda\}$ and $\underline{r}$ will be used interchangeably; also, the integral over the unit sphere will be abbreviated to $\int_\sigma (\ ) d\sigma$ where σ represents unit sphere surface (the limits of integration in (36)) and $d\sigma$ represents $\cos \phi' d\phi' d\lambda'$.

This equation assumes we have as input data the function $T(\underline{R}')$ over the surface of the reference sphere. Another form for expressing $T(\underline{R}')$ in integral form comes from the relationship of T to the gravity anomaly Δg (Ref 14:89):

$$\Delta g = - \partial T/\partial r - 2T/r . \tag{37}$$

This relationship, applied to (36), leads to Stoke's Formula:

$$T(\underline{r}) = \frac{R}{4\pi} \int_\sigma \Delta g(\underline{R}') \, S(r,\psi) \, d\sigma \tag{38}$$

where ψ is the central angle between $\underline{r}$ and $\underline{R}'$ and where $S(r,\psi)$ is Stoke's function given by (Ref 14:233)

$$S(r,\psi) = \frac{2R}{|\underline{R}'-\underline{r}|} + \frac{R}{r} - \frac{3R|\underline{R}'-\underline{r}|}{r^2} - \frac{R^2}{r^2} \cos \psi$$

$$\left[5 + 3 \ln \left(\frac{r-R \cos \psi + |\underline{R} - \underline{r}|}{2r}\right)\right] \tag{39}$$

Equation (38) requires input data of gravity anomaly over the sphere. The set (36) and (38) then provide two direct methods of computing $T(\underline{r})$ from measured data. Since we ultimately want the gravity disturbance vector function, $\delta \underline{g}(\underline{r})$, we can use

$$\delta \underline{g}(\underline{r}) = dT/d\underline{r} . \tag{40}$$

For spherical coordinates, this becomes

48

$$\delta g_r = \partial T / \partial r, \qquad (40a)$$

$$\delta g_\phi = \frac{1}{r} \, \partial T / \partial \phi, \qquad (40b)$$

and

$$\delta g_\lambda = \frac{1}{r \cos \phi} \, \partial T / \partial \lambda. \qquad (40c)$$

We can now apply (40) to (36) and (38), in turn, to yield integral relationships between the input data (T or Δg, respectively) and the desired final result $\delta \underline{g}$. In applying (40) it is convenient to express ψ in terms of the latitudes and longitudes or the defining vectors $\underline{R}'$ and $\underline{r}$:

$$\psi = \cos^{-1} \left[\sin \phi \, \sin \phi' + \cos \phi \, \cos \phi' \, \cos (\lambda' - \lambda) \right]. \qquad (41)$$

Now since $|\underline{R}' - \underline{r}| = |R^2 + r^2 - 2rR \cos \psi|^{1/2}$ $\qquad (42)$

by the Law of Cosines, we have

$$|\underline{R}' - \underline{r}| = \left\{ R^2 + r^2 - 2rR \left[\sin \phi \sin \phi' + \cos \phi \cos \phi' \cos (\lambda' - \lambda) \right] \right\}^{1/2}.$$

$$(43)$$

With (43) the necessary partial derivatives are straightforward, and we get from (36):

$$\delta g_r = \frac{R}{4\pi} \int_\sigma M(r, \psi) T(\underline{R}') \, d\sigma \qquad (44a)$$

where

$$M(r, \psi) = \frac{5R^2 r - r^3 - Rr^2 \cos \psi - 3R^3 \cos \psi)}{|\underline{R}' - \underline{r}|^5} \quad , \text{(Ref 14:37)}$$

$$(44b)$$

49

$$\delta g_\phi = \frac{3R^2(r^2 - R^2)}{4\pi} \int_\sigma \frac{T(\underline{R}')\ [\cos\phi\sin\phi' - \sin\phi\cos\phi'\cos(\lambda' - \lambda)]\ d\sigma}{|\underline{R}' - \underline{r}|^5}$$

$$(44c)$$

$$\delta g_\lambda = \frac{3R^2(r^2 - R^2)}{4\pi} \int_\sigma \frac{T(\underline{R}')\ \cos\phi'\sin(\lambda' - \lambda)}{|\underline{R}' - \underline{r}|^5}\ d\sigma\ .$$

$$(44d)$$

Now, in applying (40) to (38) it is convenient to define an azimuth α of

the line segment, or arc, from $\underline{r}$ to $\underline{R}'$ (see Figure 3).

$$\tan\alpha = \frac{\cos\phi'\sin(\lambda' - \lambda)}{\cos\phi\sin\phi' - \sin\phi\cos\phi'\cos(\lambda' - \lambda)}$$

$$(45)$$

And note that $\partial\psi/\partial\phi = -\cos\alpha$

$$(46a)$$

and $\qquad\qquad \partial\psi/\partial\lambda = -\cos\phi\sin\alpha.$

$$(46b)$$

Then, (38) becomes

$$\delta g_r = \frac{R}{4\pi} \int_\sigma \triangle g(\underline{R}')\ \frac{\partial S(r,\psi)}{\partial r}\ d\sigma,$$

$$(47a)$$

$$\delta g_\phi = -\frac{R}{4\pi} \int_\sigma \triangle g(\underline{R}')\ \frac{\partial S(r,\psi)}{\partial\psi}\ \cos\alpha\ d\sigma,$$

$$(47b)$$

$$\delta g_\lambda = -\frac{R}{4\pi} \int_\sigma \triangle g(\underline{R}')\ \frac{\partial S(r,\psi)}{\partial\psi}\ \sin\alpha\ d\sigma$$

$$(47c)$$

where

$$\frac{\partial S(r,\psi)}{\partial r} = -\frac{R(r^2 - R^2)}{r|\underline{R}' - \underline{r}|^3} - \frac{4R}{r|\underline{R}' - \underline{r}|} - \frac{R}{r^2} + \frac{6R|\underline{R}' - \underline{r}|}{r^3}$$

$$+ \frac{R^2}{r^3}\ \cos\psi\left[13 + 6\ln\left(\frac{r - R\cos\psi + |\underline{R}' - \underline{r}|}{2r}\right)\right]$$

$$(47d)$$

50

North Pole

σ, surface of unit sphere

$\frac{\pi}{2} - \phi'$

λ

$\frac{\pi}{2} - \phi$

α

$d\sigma$

ψ

$r, \underline{r}$

$R', \underline{R}'$

Earth Center
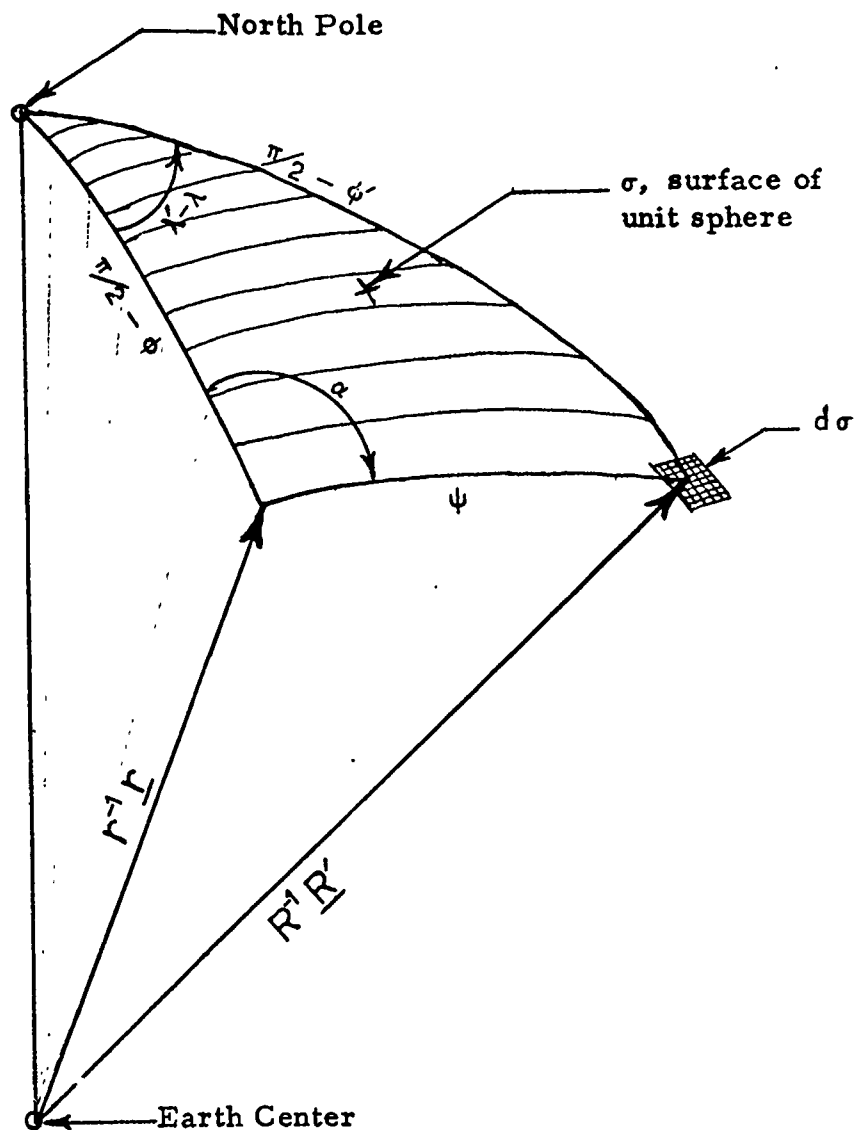
Figure 3. Geometry on the Unit Sphere (Ref 14:113)

and

$$\frac{\partial S(r, \psi)}{\partial \psi} = \sin \psi \left\{ - \frac{2R^2 r}{|\underline{R}' - \underline{r}|^3} - \frac{6R^2}{r|\underline{R}' - \underline{r}|} + \frac{8R^2}{r^2} \right.$$

$$\left. + \frac{3R^2}{r^2} \left[\frac{r - R\cos\psi - |\underline{R}' - \underline{r}|}{|\underline{R}' - \underline{r}|\sin^2\psi} + \ln \left(\frac{r - R\cos\psi + |\underline{R}' - \underline{r}|}{2r} \right) \right] \right\}$$

(47e)

Equations (45), (46) and (47) are adaptations of the development

51

presented in Reference 14 on page 234.

Equations (44) and (47) present the direct methods for computing
the disturbance vector from either type of input data: T or Δg. Since
this disturbance vector represents the error in our model or reference
gravity formula, we may compensate the reference model by adding this
computed disturbance acceleration to the reference gravitation accelera-
tion vector. Hence, our algorithm for approximating either (44) or (47)
provides one alternative gravitational modeling improvement as we
discussed in the last section.

Another method for calculating the disturbance vector uses the
technique of replacing the disturbing masses by an equivalent surface
mass layer (see Theorem of Chasles (Ref 14:13). Once this surface mass
distribution function has been defined from the input data, we simply
apply (26) taking advantage of the fact that the volume integral can now
be replaced by a surface one. This "coating method" requires both types
of input data (T or N and Δg) to compute the surface density function
(Ref 14:236-238). The resulting formulae are simpler than those for the
direct methods. This factor might offset the costs of additional meas-
urements, and calculation in forming the surface density function.

These three methods (Poisson Integral, Stoke's Integral and
coating) have approximately the same accuracy (Ref 14:243). To imple-
ment one of these integral methods, we must face the issue of a discrete
approximation method. One can see for the coating method that the most
important data is that near $\psi = 0$. This idea carries over to the other

52

direct methods but with less intuitive appeal than the surface distribution case. Hirvonen and Moritz (Ref 64) considered this factor in a comparison study on the direct Stoke's (47) and the coating methods. The idea is to investigate the effect of ignoring distant data in approximating these integrals. They statistically predict the root-mean-square (rms) residual gravity for each component of the disturbance vector when the integration set σ is approximated by the points within a central angle ψ_o of $\underline{r}$. The statistical error estimation made use of the anomaly covariance function (see Appendix C) as a basis for statistically characterizing the effects of the distant zones.

To interpret the results of this study, we should point out that each component of the disturbance vector on the Earth's surface is an approximately 35 mgal rms process (Ref 50). This figure corresponds to a $\psi_o = 0$ when the compensating integral covers no area. For a $\psi_0 = 9^o$, the estimated rms residual is down to 8 mgal and 6 mgal for the direct and coating methods, respectively. So, covering 0.6% of the Earth's surface decreases our expected rms gravity disturbance to, on the order of, 20% of the uncompensated level. We require a central angle coverage of 90°, or one-half the Earth's surface, to lower the estimated rms disturbance to 10% of the uncompensated value demonstrating a severe Law of Diminishing Return for increasing ψ_0.

We conclude that we will require a gravity survey over a vast area to support any of these integral approaches. We can diminish the computational burden by variable grid spacing of the area necessary for

53

adequate compensation accuracy. This variable spacing policy was mentioned earlier and is the basis of point mass modeling techniques. We can use the integral kernels and our knowledge of expected flight path to select a grid schedule of approximately equal statistical influence. That is, the error introduced by the finest grid spacing terms should be on the same order as that expected from the coarsest grid spaces. Such a technique, it must be noted, will place flight path restrictions on the mission if we intend to salvage the accuracy for which we are building the compensation.

The problem of approximating these integrals, as noted in the previous section, might be handled with integral transform methods. The computational structure of the Fast-Fourier Transform makes it attractive. The data could conceivably be transformed pre-mission leaving only the interpolative inverse transform as real-time computational burden. Some research is required to adapt these FFT methods to the variable grid spacing that we must consider.

These, then, are some of the basic theoretical concepts and concerns relating to our gravity modeling task. We are at a point where concrete plans can be made for future research. The subject of gravity modeling, as we have seen, is broad and reaches into the fields of Physical Geodesy and Inertial Navigation. Some thought must be given to a proper division of responsibilities in the overall research of this subject.

·J. The Geodesy Connection

To get the total view of this process, it is instructive to consider a signal flow graph of the "information" stemming frcm the mass distribution and terminating in the navigation estimates. With some poetic license, Figure 4 presents such a view. This figure graphically displays the chronological processing of gravitational information with emphasis on the new tasks associated with the augmentation of the reference field model. We shall discuss the nature of these tasks which compensate the reference field. We shall, also, describe how the design error budget provides criteria for model performance and, in general terms, how the model selection process should logically be conducted. These concepts are important because the proposed research will be conducted along lines compatible with model selection even though it will not include a complete trade-off study for every conceivable model compensation method. Finally, as mentioned previously, we shall discuss the logical assignment of these new tasks to the fields of Physical Geodesy and Inertial Navigation.

Before we cover these interface concerns, we need to reestablish what the term "model" means. As shown in Figure 4, the complete gravitational model consists of two parts: (1) The reference gravitational field based on a surface-approximating ellipsoid and (2) the compensation model which calculates local variations. The standard names and notation become troublesome at this time since the disturbance vector, δg, which has been treated as a perturbation quantity, is now

55
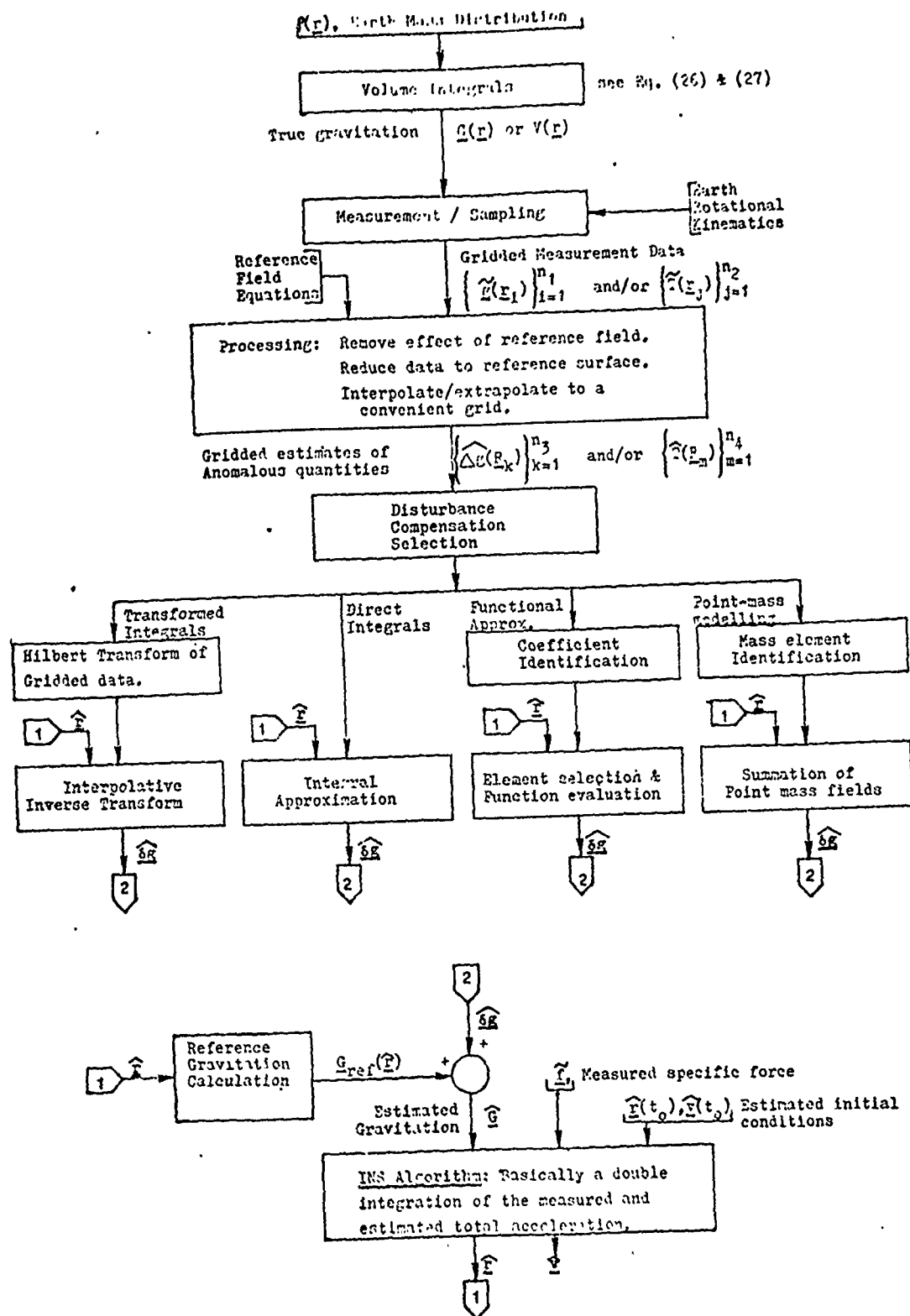
Figure 4. Gravitational Information Flow Graph

being approximated. We need an unambiguous name and symbol for the new residual gravitational modeling error. We shall continue to call the variation from the reference field $\delta\underline{g}$. The ellipsoidal field in earlier discussions was synonymous with the model. Since our new model will include this ellipsoidal one as an element, we shall refer to it as the _reference_ _field_, symbolized by $\underline{G}_{ref}(\cdot)$. We shall refer to the _compensation_ _model_ as such and use the symbol $\delta\underline{g}_m(\cdot)$. The remaining _residual_ _disturbance_ will be symbolically $\underline{\delta}(\cdot)$. With these new definitions (5) on page 9 should be rewritten as

$$\delta\underline{g}(\underline{r}^e) = \underline{G}_{ref}(\underline{r}^e) - \underline{G}(\underline{r}^e). \tag{5a}$$

Our complete model is now

$$\underline{G}_m(\underline{r}^e) = \underline{G}_{ref}(\underline{r}^e) - \delta\underline{g}_m(\underline{r}^e). \tag{48}$$

The traditional modeling methods can be viewed as a degenerate form of (48) with $\delta\underline{g}_m$ defined as a constant zero vector function. The residual disturbance vector is then defined by

$$\underline{\delta}(\underline{r}^e) = \underline{G}_m(\underline{r}^e) - \underline{G}(\underline{r}^e) = -\left[\delta\underline{g}_m(\underline{r}^e) - \delta\underline{g}(\underline{r}^e)\right]. \tag{49}$$

In Figure 4, $\widehat{\delta\underline{g}}$ refers to $\delta\underline{g}_m(\hat{\underline{r}})$ and $\widehat{\underline{G}}$ refers to $\underline{G}_m(\hat{\underline{r}})$. With the notation issue resolved, we can discuss how this new modeling process will be accomplished.

Again returning to Figure 4, we will require an extensive local

57

gravity survey to provide the short spatial wavelength information necessary for model improvement. This survey data, taken over a grid convenient for measurement, must be reduced to the reference surface and interpolated to form a data set on the grid which we shall establish for model parameter identification. This interpolation will undoubtedly be necessary since the parameter identification algorithm must work for arbitrary survey grid structure. The parameter identification and functional evaluation blocks are shown for four example compensation methods. We can see the variety of forms these tasks might take. The parameter identification varies considerably from possibly using the interpolated gridded data directly as a parameter set to the search procedures already developed for point mass modeling (Ref 30). After the modeling method has been selected and the parameters have been identified, the model is completely defined. The next step, functional evaluation must occur in the navigation computer for real time compensation since the position estimate is required. Once this gravitational disturbance estimate is combined with the estimated reference field, the INS algorithm is unchanged. Figure 4 provides examples of how such compensation might be accomplished. Clever computational schemes might eliminate some of the blocks but the equivalent of the four tasks must be accomplished: survey, process to computational grid, identify parameters and functionally evaluate.

The new tasks fall into categories based on the discipline primarily responsible for the theoretical development and implementation of the

task. The gravity survey and subsequent data processing are in the province of Physical Geodesy. The real-time functional evaluation is obviously in the field of Inertial Navigation. The remaining tasks of model selection and parameter identification are at the intersection of these fields of interest. The functional evaluation accuracy is so dependent on parameter identification criteria that these tasks rightfully belong together. The model selection has a pervasive effect on the nature of tasks performed in either area. The choice of compensation method will rest on a trade-off which is difficult to describe in generality. A specific design setting provides the constraints and goals to structure such a trade-off without lapsing into abstruse generalities.

Let us construct such a design scenario to understand how the compensation selection process might logically be conducted. The navigation subsystem will typically be given an accuracy criteria based on some overall system performance requirement. This crit ria is based on an expected environment and is usually statistical in nature (e. g. rms position, velocity, and attitude levels throughout the mission). Suppose we have been handed such an error budget. Furthermore, suppose we have performed some analyses along the lines suggested by Levine and Gelb (Ref 21) which indicates that the ellipsoidal reference field is unacceptable as a total model. Such a scenario might be a strategic bomber mission which precludes electro-magnetic emissions for detectability and which assumes other navigation aids will not be available. We conclude then that we must provide some compensation to the reference

59

field to decrease the effects of gravity disturbances. The INS error budget must be decomposed to budgets for the elements of the INS (e. g. accelerometers, gyroscopes, gravitation model, and algorithm numerical quantization). With this parceling out of the error budget, the gravitational model will have a specific accuracy goal to meet. The next step is to select a compensation scheme which meets this derived criteria and which is least burdensome in some overall sense.

"Least burdensome" is subjective since many diverse costs must be considered. The spectral content of the gravity disturbance, if known or approximated, will allow us to specify a minimum spatial frequency to accomplish the accuracy goal. By the Shannon sampling theorem this implies a minimum density for the gravity survey. The extent of the survey will depend on the convergence properties of the compensation method. As we have seen, the coating method tends to converge faster (in a spherical cap size sense) than the direct Stoke's integral method. The coating method requires two types of input data, however, so survey extent is not a full account of survey cost.

The data processing task, also, depends heavily on the compensation model choice. The integral techniques and the point mass model need data over a two-dimensional surface. The functional approximation methods, however, need a three dimensional array of information for the three-dimensional function parameters (e.g. Ref 43). This processing of raw survey data and model parameter identification will likely occur pre-mission with relatively large computational facilities

used. So, the costs may be less onerous in this area if the method is particularly efficient in the functional evaluation phase.

On the implementation of a real-time computation, the constraints and costs are primarily associated with the airborne computer memory storage and computational cycle time. The fine gravity model for Reference 24, for example, requires over 10,000 point masses. Each point mass requires four parameters; so, over 40,000 memory locations might be required for parameter storage alone. Furthermore, the functional evaluation requires the summation of the Newtonian gravitational acceleration from each point mass. The impact of such massive computational and storage requirements can be put in perspective when you consider that operational flight computer memories, today, have less than 40,000 words for data and program storage. Prototype computing systems with mega-word capability are available. So, future systems may have the flexibility to consider these more complete compensation models.

The crux of all these costs is the compensation method. It is clear from the costs associated with the survey and the real-time evaluation that some comprehensive, coordinated model selection study must be performed for each different mission and system. While the proposed research does not cover the total model selection issue, it is important to realize these issues to keep the proposed work in context. The structure of the study and the motivation for many assumptions and procedures will be founded on these considerations. That is, we shall

61

assume that the least costly method to reach a prescribed mission navigation accuracy is the driving force behind what we do.

The proposed research will concentrate on the Inertial Navigation aspects of the problem. We shall assume that the Physical Geodesy connection exists and will provide the required gravitational data on a computationally convenient grid. Thus, we shall concentrate on minimizing the real-time INS costs. Again, the proposed research should be viewed in the context of providing information to answer the larger issue of model compensation selection.

III. Research Topic

The background of INS gravitational modeling shows the growing need to develop and demonstrate techniques to compensate the traditional (usually ellipsoidal) INS gravitational model. The research proposed in the following sections addresses the system design problem of selecting a compensation modeling concept and of selecting the level of model complexity (i.e. number of parameters) consistent with design constraints. The problem is placed in this context by addressing the design trade-off between the system performance cost and the system resource cost associated with the gravitational model. The specific objective is to provide the analytical means to evaluate model performance at the system level so that one can choose both the model concept and the degree of model complexity. We shall discuss below the general setting for the overall analysis required to select a gravitation model. The problem is partitioned in such a manner that the fundamental analysis required is to determine INS performance for a finite set of design missions. All higher level problems can be approached given this basic analysis capability. An example is suggested to demonstrate the analysis method since many of the analysis steps depend on the modeling concept.

63

A. Study Context

An abstract study of gravitational modeling errors seems a barren exercise to one aware of the strictures of an operational, real-time environment. The choice of a gravitational model is made in a system design context. The gravitational model is one component of the INS which, in turn, is an element of some larger system designed to perform some mission. The gravitational model is not intrinsically interesting from this total system perspective. We are interested in the effect modeling errors have on system performance and the impact of the model on such system resources as computer memory. A conflict exists between our desire for increased performance and for efficient use of resources. An increase in model complexity can yield improved system performance, but it implies additional computer usage. This conflict generates a system design trade-off which requires evaluation of both model performance costs and model resource costs to answer questions such as:

1. Given X amount of computer memory (or computation time) which model concept at what degree of complexity yields the best system performance? and

2. Given Y system performance criteria (say rms position accuracy) which model requires the least computer resources? The context of this study will be to provide the analytical methods to answer such design trade-off questions. This approach should make the resulting methods immediately applicable and the motivation

64

more comprehensible.

We shall concentrate attention on the performance cost evaluation, but we will need a measure of system resource cost as a foil in the trade-off exercise. The modeling concepts we shall consider have the quality that, barring other errors, they can represent true gravitation to any desired level of residual by increasing the number of model parameters (e.g. more point masses). Model complexity shall be used synonymously with number of parameters. The computational overhead for each model concept is the algorithm storage requirement. For a given model concept this requirement should not be strongly influenced by the number of parameters to be processed. We shall neglect this algorithm storage cost in our analysis since we shall concentrate on one modeling concept as an example. Of course, this cost must be considered in any comparison between different modeling concepts (e.g. point mass versus Stoke's Integral).

The other side of this system design trade-off is the system performance cost. We consider those applications where a system "miss" is directly associated with navigation accuracy. The system miss is assumed to be in the form of a miss vector which has components we wish to drive to zero (e.g. downrange and crossrange miss for a ballistic weapon delivery). We assume a system cost function is associated with this miss vector. This cost function maps the miss vector space into the real numbers and provides a means of ordering miss vectors as either more or less costly in comparison

65

with other system misses. Our system design must account for a wide range of operational environments for a given mission. So, we want to decrease the expected value of this system performance cost over the range of missions and environments. The nature of this cost function and the nature of the statistical expectation are important in formulating our analysis method.

From a system perspective, we desire a measure of the system performance cost which reflects the evaluation of system cost function for every conceivable mission and environment--a weighted sum or integral. The weighting should include not only the probability of a given mission but the relative importance of that mission with respect to other missions, as well. Such abstract analysis is not performed in system design studies because the resources to conduct such studies are limited. The integral over all missions is approximated by a discrete summation. The <u>mission space</u> is subdivided into <u>mission regions</u> each of which is represented by one <u>design mission</u>.

The ICBM provides an easily understood example of this mission partition concept. For a given target range and azimuth the ICBM usually has two solutions to the two point boundary value problem: burn-out state vector to hit a specific target. This generates a discrete (binary in this case) partition of the mission space into low and high trajectories. The range and azimuth offer a two-fold continuum for mission partitions. A design mission might, for example, be specified as the high trajectory for range X and azimuth Y. This

design mission would represent in our system studies all high

trajectory missions over a set of ranges within $X \pm \Delta X$ and over a

set of azimuths within $Y \pm \Delta Y$. A collection of such design missions

can be analyzed and the results combined with appropriate weighting

to approximate the integral over the mission space.

The mission space for a strategic bomber, for example, is

much more complex due to the system's flexibility. This diversity

would be reflected in a higher number of design missions--not a

change in the analysis method. So, we can focus our attention on pro-

viding the analysis methods to characterize the gravitational model

system performance on a restrictive mission type. A mission taxon-

omy can be based on geometry and the geography. The geometrical

qualities one might use are, for example, range, altitude and azimuth

relative to downrange. If mission velocity is not prescribed by these

geometrical considerations, the mission partition must include these

variations. The mission type is, also, characterized by such geo-

graphic considerations as the area of mission origins and the azimuth

of the downrange groundtrack. Both geometric and geographic terms

affect the system level performance of the gravitational model.

The design mission can be used to characterize the effects of

anomalous gravitation for a region of mission space. The variations

of gravitation within the geographic bounds of the mission region is

the underlying random process. The INS error dynamics are also

influenced by the geographic region (e.g. Foucault mode, see

67

Ref 1:128). These error dynamics are also influenced by the mission

geometry--primarily the radius magnitude. The mission velocity

translates the gravitational disturbance quantities from the spatial to

temporal domain. In this manner the design mission can be used as

an analysis tool.

To realize this goal we must account for the variation of gravi-

tation within the geographic region of interest. The gravitational

disturbance information for this region can be statistically summar-

ized in terms of reference surface covariance functions of anomalous

gravitation quantities. We want to include the effect of gravitation

over this entire region since the gravitational disturbance along a

design mission trajectory may not be truly representative of the entire

region. So, we shall seek the performance cost estimate for a given

region as a statistical estimate over all possible gravitational disturb-

ances in the region and structure the analysis for those reference

surface covariance functions we expect to be available from survey

data (see Appendix C).

The variations of the INS error propagation model with geography

is predictable; therefore, we can partition the mission space in such a

manner that the design mission INS error propagation model repre-

sents well the entire mission region. A similar partition argument

can be made for the geometrical variations of the mission space.

Therefore, we shall assume the mission space is partitioned such that

the INS error propagation along the design mission is acceptable over

the entire range of missions within the mission region. This assumption is essential to define a manageable analysis problem. The variations of INS error dynamics with geography are smooth enough that the mission space partitions on this account might be widely spaced.

The system cost function must, also, be understood before practical analyses can be planned. The gravitational modeling errors excite the INS error state vectors through well-known (Ref 1) differential equation models. The specific disturbance time function depends on the particular trajectory (position-time history). The INS errors which result from the disturbance input will cause the overall system to miss some system target. A _miss vector space_ is defined in terms of these component deviations from the coordinated system objectives. While spatial objectives are familiar (e.g. downrange and crossrange), we can have non-spatial objectives as well. An error in time-on-target or attitude errors during antenna pointing operation are example non-spatial system miss quantities. For our analysis, we shall consider the mapping from INS error state vector space to system miss vector space to be linear by use of well known linear perturbation methods. That is,

$$\underline{y}(t) = H(t)\underline{X}(t) \qquad (50)$$

where $\underline{y}$ is the system miss vector corresponding to an INS error state vector $\underline{X}$. The techniques developed can be generalized to a broader class of mappings (i.e. convex) but the linear model should

69

apply to most problems of interest.

We assume the miss vector components are each important to system effectiveness such that an increase in the magnitude of any component implies, by itself, an increase in the system cost function. The system cost function is assumed to be a positive definite, convex functional over the system miss vector space. This assumption should certainly characterize the performance for a region near the origin of the miss vector space. The motivation for such assumptions is to describe those problems for which the analysis can concentrate on the INS error state statistics. To reach this goal, we must have the capability of reflecting a system cost criteria back onto the miss vector space and then onto the INS error state space. The effect of large scale miss on system effectiveness is not necessarily well-modeled by such convex functionals. The probability of kill envelopes for nuclear weapons, for example, define markedly non-convex sets due to the various effects of the weapon. In such cases a convex cost functional can be derived by forming a performance index from the maximum or minimum level within a radial distance from the aim point. The alternative is to generate the statistical performance index by Monte Carlo analysis techniques.

With the convex functional assumptions, we can formalize the relationship between system cost criteria and the gravitational modeling errors. This relationship is normally established through a system error budget.

The system error budget is a design tool used to distribute the performance cost criteria, through analysis and assumption, to various system error sources. Once established the error budget forms the subsystem design goals for a design iteration. The cost is assumed to be stated as a level on the expected cost (e.g. circular-error-probable less than 1 n.mi). This level criteria yields an interval on the positive half of the real number line which corresponds to acceptable expected system performance cost. The inverse image of this acceptable interval onto the miss vector space defines a convex, compact set with symmetry in each of the miss vector component directions. The miss vector set so established can be related to the statistical expectation of the various system error sources. The INS allocation of this acceptable expected error set can be reflected onto the INS error state vector coordinates. Since all INS error state coordinates may not contribute directly to system miss, the INS error state set so defined may not be bounded. With our previous linear assumption it will be convex and symmetric with respect to all component directions. Thus, we have a set which we can view as a restriction on the INS error state covariance matrix.

We shall not treat system cost functions or miss vector coordinates in further analyses since, under our assumptions, these concerns can be stated as constraints on the INS error state covariance matrix. The INS error state covariance restrictions so derived are, in turn, distributed across the INS component error sources--the gravitational

71

model being one such element. In this manner, we view the design criteria for the gravitational model to be stated in terms of bounds on the INS error state covariance matrix resulting from gravitational modeling errors acting alone. An inherent assumption in this process is the independence of gravitational modeling errors from other INS error sources (e.g. accelerometer noise) and from other system error sources (e.g. errors in the estimate of ballistic coefficient).

With this manner of specifying the system level performance of the gravitational model, we need to develop analytical means of estimating the INS error covariance matrix which results from gravitational modeling errors acting alone. The necessary elements of this analysis have been discussed previously. We need the mission type description to fix the INS error propagation model. The geographic region defined by the mission type can be used along with gravity survey data to estimate the covariance of anomalous gravitation. We must devise a means of altering this anomaly covariance or anomalous potential covariance to include the effects of our additional modeling of the gravitational disturbance. That is, we need to derive the covariance of the residual field qu ititty.

Then, an analytical means must be derived to propagate this expected gravitational modeling residual noise through the INS taking into account the design mission effects on both the residual gravitation field statistics and on the INS error propagation. The means for accomplishing this task must be statistical. If we knew the gravitational

field exactly along all mission trajectories, we could form the ensemble statistics through well-known statistical techniques. Lacking such extensive information, we can form the outer product of the INS error vector and apply our expectation operation over the mission region. As discussed in Appendix C, the INS error covariance from gravitational modeling errors has been studied by simulation methods for some rather benign INS missions. Since we want a method which is generally applicable, we need analytical methods which are not restricted to simple mission geometries.

This generalized design mission analysis technique will provide the answer to whether a proposed model concept and complexity level provide acceptable system level performance. The system resource costs can then be compared for various model concepts or the system level performance can be compared for fixed system resource investment. The design mission context allows us to address the overall system mission performance by analyzing a finite, but representative, subset of missions. The information on system performance and system resource costs can thus be made available to answer the design trade-off questions which will arise in selecting an extended gravitational model.

B. Specific Objective

The goal of this research is to provide analytical methods for selecting a computationally efficient, INS gravitational model which is

73

accurate in terms of expected INS accuracy. The research will focus

on providing a means of estimating INS errors due to gravitational

model errors acting alone. The system resource cost will be approx-

imated as a linear function of the number of gravitational model

parameters.

C. Implementation Study

The method discussed above will vary with the model concept.

The reason is that the residual field depends entirely on the manner

in which the anomalous field is modeled. The Poisson Integral (36)

will be analyzed as an example to demonstrate the application of the

method. The hypothetical design study will be to determine the

Poisson Integral approximation grid which meets an INS accuracy

criteria with the minimum number of grid elements (i. e. number of

parameters). The Poisson Integral was selected as an example

because (1) it has not received much attention in previous works; (2)

current satellite altimetry will provide the necessary data base over

large regions of the Earth; (3) this integral may prove amenable to

solution by transform techniques; and (4) the relationship between

gravitation and potential is more straightforward than the relationship

to gravitational anomaly which is the data basis for Stokes Integral.

D. Assumptions

The following assumptions will be made in this research. The

assumptions fall into one of two categories:

1. Those assumptions which provide details outside the direct path of the proposed research (e.g. on survey errors), and,

2. Those assumptions which clarify the objective and ensure mathematically tractable results.

The proposed research will not deal directly with either survey errors or total gravitational model algorithm computational requirements. These quantities are needed to complete the analysis and we shall assume

1. That system resource cost will be reflected in the number of model parameters (i.e. number of grid elements for Poisson Integral example),

2. That gravity survey and subsequent data processing will supply anomalous potential estimates on an arbitrary, computationally convenient grid, and

3. That survey errors are independent of the data and are a white, Gaussian, two-dimensional sequence.

The assumptions which will be made to yield tractable mathematics have, for the most part, been discussed previously. The additional assumptions on the anomalous and residual fields seem reasonable and yield significant simplifications in the covariance functions (see Appendix C). These assumptions are

1. That system performance cost will be stated as a restriction on the INS error state covariance matrix due to gravitational model errors acting alone,

75

2. That the design mission represents the entire mission region for INS error propagation modeling,

3. That the statistics of the anomalous gravitational field are known or can be approximated over the reference surface in the geographic area of the mission region, and

4. That the statistics of the anomalous or residual field are well-approximated by assuming either field is a homogeneous and isotropic process over the reference surface.

E. Proposed Approach

A major portion of the approach to this problem is contained in the Problem Context section. For a general class of INS applications, the overall model selection process is based on the performance results from a finite set of design missions. The basic problem remaining is to develop an analytical procedure for determining the expected system performance, on any specific design mission. To us system performance is synonymous with the INS error state covariance matrix, given (1) the model concept, (2) the model complexity level, (3) the regional anomalous field statistics, (4) the design mission, and (5) the survey error statistics.

This problem will be broken into two distinct parts (see Figure 5). In the first phase, we shall characterize the residual gravitational field statistically. For our Poisson Integral problem this summary will be in the form of the residual potential covariance function over the reference surface. This residual field statistic will contain all

76

necessary information on the gravitational model, the mission region and the survey errors. The second phase of this analysis is generally applicable for all model concepts. Given the residual field statistic from the first phase, we shall form a statistical estimate of the system cost function based on the design mission and our INS error propagation model (Refs 1 or 2).

Along with this system performance cost our implementation study will use the model complexity as the system resource cost. We shall investigate the solution to the design trade-off question: Find the least complex Poisson Integral approximation which meets an INS accuracy level specification.

The start of this overall analysis is to form the residual field statistics. For our Poisson Integral problem, we assume that the anomalous potential covariance function $K(\underline{R}, \underline{R}')$ is known (see Appendix C for a general discussion of such covariance functions). The radius vectors $\underline{R}$ and $\underline{R}'$ are on the reference surface of radius R. The covariance argument will usually be simply the central angle, ψ, separating $\underline{R}$ and $\underline{R}'$; the form $K(\underline{R}, \underline{R}')$ will be used, however, to allow a more general class of arguments. We shall use $K(\underline{R}, \underline{R}')$ for the worldwide covariance function. The symbol Θ will signify the mission region being considered and $K(\underline{R}, \underline{R}'; \Theta)$ will be the anomalous potential covariance formed from data in the geographic region associated with Θ.

The modeling of anomalous gravitation results in a residual field with statistics dependent on the anomalous field statistics and the model approximation performance. The residual potential covariance function will be called $K^*(\underline{R}, \underline{R}')$ and this quantity will be formed for our Poisson Integral example.

We are using this example to provide concrete terms for what would otherwise be an abstract analysis. The nature of how we approximate the Poisson Integral will influence the results. Recall (36)

$$\widehat{T}(\underline{r}) = \frac{R(r^2-R^2)}{4\pi} \int_\sigma \frac{\widehat{T}(\underline{R}')}{|\underline{R}'-\underline{r}|^3} \, d\sigma \qquad (51)$$

where T is shown in Figure 4 on page 56. We shall approximate (36) directly rather than use the Equation (44). This choice was made for example simplicity since otherwise we would need to analyze the three integrals of (44) in addition to (36). The spatial derivative will be approximated by a discrete number of evaluations of (51) in the vicinity of the navigation position estimate, $\hat{\underline{r}}$. We shall approximate (51) with a finite sum replacing the integral. The sum will be formed from a uniform grid of square surface elements. We shall neglect any problems these square elements encounter in covering the spherical reference surface because the grid extent will be limited. From our previous Stokes Integral discussion, we expect the integral approximation to converge slowly as the grid extent increase past ten degrees

78

of central angle from the evaluation point. Depending on the stringency

of our INS accuracy requirement, we can anticipate a relatively small

grid will suffice for many applications. The approximation to (51)

will be

$$\widehat{\widehat{T}}(\underline{r}) = \frac{R(r^2 - R^2)}{4\pi} \sum_{j=1}^{m} \frac{A_j \widehat{T}(\underline{R}_j)}{|\underline{R}_j - \underline{r}|^3} \tag{52}$$

where A_j is the area of the jth surface element and m is the number

of grid elements. With our uniform grid we get

$$\widehat{\widehat{T}}(\underline{r}) = \frac{R(r^2 - R^2)}{4\pi} A \sum_{j=1}^{m} \frac{\widehat{T}(\underline{R}_j)}{|\underline{R}_j - \underline{r}|^3} \tag{53}$$

The Poisson Integral approximation model concept has com-

plexity level indicated by m in (53)--the number of grid elements.

Since the radius of the reference surface is fixed at R, we need two

parameters to specify the grid point $\underline{R}_j$ which applies to the survey

data $\widehat{T}(R_j)$. Thus, three computer memory storage locations might

be required to identify the required information. We can use the uni-

form grid structure to reduce this storage to just the anomalous

potential data with a grid center point, for example.

The kernel of (51) is well behaved for all $\underline{r}$ such that $r > R$. So

if our data $\left\{ \widehat{T}(\underline{R}_j) \right\}_{j=1}^{m}$ is without survey error, we expect (52) or (53)

to converge to the true value in the limit as $m \to \infty$ and each $A_j \to 0$.

This quality is the prime motivation for choosing such integrals as

79

the basis for a model concept. Another way of specifying the grid is by the spherical cap size and the grid element dimension.

The spherical cap is the reference surface area within a central angle ψ_0 (discussed previously) of the evaluation point $\underline{r}$. The element, being square, is specified by the length of the side, h. We expect convergence as $\psi_0 \rightarrow \pi$ and as $h \rightarrow 0$. The choice of this pair is motivated by the symmetry of the (51) kernel radially from $\underline{r}$ and by the connection of h with the Shannon Sampling Theorem--here applied to representation rather than sampling.

Clearly for a fixed m, there exists a family of (ψ_0, h) pairs which satisfy the equation

$$m = \frac{\text{total cap area}}{\text{grid element area}} = \frac{2 R^2(1-\cos \psi_0)}{h^2} \qquad (54)$$

We envision the INS specification as a partition on the ψ_0-h plane dividing the possible grid designs into acceptable and not acceptable grid specifications. Our task in the implementation study will be to select from the "acceptable" set the grid specifications which minimize m.

We shall discuss this problem later, our task now is to form the K^* function and this grid design data is needed. Recall that in forming K^* we assume the grid design (i.e. ψ_0 and h) is given as part of the model definition. Clearly the statistic K^* is a key to our predicting INS error performance with our compensated gravitational model.

80

The method of determining $K^*(\underline{R}, \underline{R}'; \Theta)$ from $K(\underline{R}, \underline{R}'; \Theta)$ and the grid specifications is a major problem to be undertaken. We know, by Shannon's Sampling Theorem, that the grid spacing affects the frequency content of the residual field. So, expanding $K(\underline{R}, \underline{R}'; \Theta)$ in spherical harmonics may provide the insight for accounting for grid size effects. The cap size study should follow the previously discussed methods of Hirvonen and Moritz (Ref 64 and Ref 14:242-243).

Since the survey errors are independent from the data (potential in our Poisson Integral example), we can treat their contribution at the covariance matrix level and write K^* as

$$K^*(\underline{R}, \underline{R}'; \Theta) = K_m(\underline{R}, \underline{R}'; \Theta) + K_s(\underline{R}, \underline{R}') \qquad (55)$$

where K_m is the covariance of the residual field assuming perfect data and $K_s(\underline{R}, \underline{R}')$ is the extended survey error covariance function which results from the Poisson Integral acting on $K_s(\underline{R}_i, \underline{R}_j)$.

We want K_s and K_m to be symmetric with respect to the central angle argument for later computational ease. We can study K_s by considering the Poisson Integral as merely performing an interpolation between grid points. The details for this development have not been completed. A simple one dimensional example will illustrate the intended approach. Suppose our grid points are R_1 and R_2 and we want an evaluation at $R \epsilon [R_1, R_2]$. Then we may express R as

$$R = \alpha R_1 + (1 - \alpha) R_2 \qquad (56)$$

for $0 \leq \alpha \leq 1$. Using the parameter α and the grid data we form our interpolation as

$$\widehat{T}(R) = \alpha \widehat{T}(R_1) + (1 - \alpha)\widehat{T}(R_2) \qquad (57)$$

Let

$$\widehat{T}(R_i) = T(R_i) + q_i \qquad (58)$$

for $i = 1$ and 2 where q_i is the uncorrelated error associated with the ith survey data point. We have then

$$\mathcal{E}[q_i q_j] = \begin{cases} \sigma_s^2 & \text{for } i = j \\ 0 & \text{else} \end{cases} \qquad (59)$$

Using our definition for error again, let

$$\widehat{T}(R) = T(R) + q_T(R) \qquad (60)$$

where q_T represents the total error at R. Combining (57), (58) and (60) we get $q_T(R) = q_m(R) + q_s(R)$ $\qquad (61)$

where $q_m(R)$ is the error due to our interpolative model given by

$$q_m(R) = \alpha T(R_1) + (1 - \alpha) T(R_2) - T(R) \qquad (62)$$

and where $q_s(R)$ is the error at R due to survey errors at R_1 and R_2 given by

$$q_s(R) = \alpha q_1 + (1 - \alpha) q_2. \qquad (63)$$

82

By our assumed independence of the survey errors with the true field
we get

$$\mathcal{E}[q_T^2(R)] = \mathcal{E}[q_m^2(R)] + \mathcal{E}[q_s^2(R)]. \tag{64}$$

Now the survey error contribution to this covariance can be calcu-
lated using the property expressed in (59):

$$\mathcal{E}[q_s^2(R)] = (1 - 2\alpha + 2\alpha^2)\, \sigma_s^2. \tag{65}$$

With σ_s^2 a constant statistic across the grid, we would find this form
repeated between each successive pair of grid points. The Poisson
Integral approximation can be viewed as a two dimensional interpola-
tion using all grid data points. While the analysis for $K_s(\underline{R}, \underline{R}')$ of (55)
will be more complicated, the example above demonstrates the intended
approach.

The statistics for $q_m(R)$ above would be $\mathcal{E}[q_m^2(R)]$. This quantity
corresponds to $K_m(\underline{R}, \underline{R}'; \Theta)$ of (55). We shall approach this quantity
in an entirely different man.~r. The grid direction will be such that
the downrange groundtrack lies along a partition boundary. The
distance between data points will be h so we can apply sampling and
approximation theory to form $K_m(\underline{R}, \underline{R}'; \Theta)$ from $K(\underline{R}, \underline{R}'; \Theta)$. This
analysis is incomplete at this time, but the approach will be to assume
$K_m(\underline{R}_j, \underline{R}_j; \Theta) = 0$ since the infinite kernel of (52) or (53) implies the
weighting of the true field at that point will be such that the remainder
of the data points can be ignored (recall K_m deals with perfect data

83

since K_s incorporates the survey errors). A means of formulating the error at points on the reference surface between the gridded data points is required. Given this error function, the covariance will be given by taking an expectation over all gravitational fields we expect to encounter. This expectation can be construed to be over Θ and $K(\underline{R}, \underline{R}'; \Theta)$ should provide all the required information.

Assuming K_s and K_m can be calculated or approximated, we have K^* by (55) which summarizes the statistics of the residual potential field throughout Θ. Let θ signify a mission trajectory; then our analysis must consider all $\theta \in \Theta$. Let θ_o signify the design mission which represents the mission region Θ. We can now form an estimate of the INS error state covariance matrix.

Using Reference 1 methods, we can model the INS error propagation for our gravitational residual as

$$\underline{\dot{X}}(t; \theta) = F(t; \theta) \underline{X}(t; \theta) + \underline{G}(t; \theta) \underline{u}(t; \theta) \qquad (66)$$

where $\underline{X}$ is the INS error state vector including position, velocity, and attitude errors; F is the error propagation matrix dependent on the time in to trajectory θ by the associated geography and geometry; G is the driving noise distribution matrix; and $\underline{u}$ is the particular residual field errors along θ. The driving noise $\underline{u}$ will contain the residual acceleration $\underline{\delta}$ and possibly the residual potential δT for a barometric altimeter aided INS. For completeness we assume

84

$$\underline{u} = \left\{ \frac{\delta}{\delta T} \right\}. \qquad (67)$$

Since our analysis is for gravitational modeling errors only, we assume initial conditions for (66) of $\underline{X}(0;\theta) = 0.$ $\qquad (68)$

We can form a solution to (66) using a state transition matrix which satisfies

$$\dot{\Phi}(t, t_1; \theta) = F(t; \theta) \Phi(t, t_1; \theta), \qquad (69)$$

and

$$\Phi(t, t; \theta) = I \qquad (70)$$

where I is the identity matrix. Such a matrix also satisfies a semi-group property

$$\Phi(t_3, t_1; \theta) = \Phi(t_3, t_2; \theta) \Phi(t_2, t_1; \theta) \qquad (71)$$

Using $\Phi(t, t_1; \theta)$ with (66) and (68) we get,

$$X(t;\theta) = \int_0^t \Phi(t, p; \theta) G(p; \theta) \underline{u}(p; \theta) dp \qquad (72)$$

Forming the outer product of this error vector yields

$$\underline{X}(t;\theta)\underline{X}^T(t;\theta) = \int_0^t \int_0^t \Phi(t, p;\theta) G(p;\theta)\underline{u}(p;\theta)\underline{u}^T(q;\theta) G^T(q;\theta)\Phi^T(t, q;\theta) dp dq \qquad (73)$$

Now, we define the INS error state covariance function, $P_{xx}(t)$, as the expectation $\mathcal{E}$, over all missions θ within the mission region Θ.

85

That is,

$$P_{xx}(t) = \underset{\theta \in \Theta}{\mathcal{E}} [\underline{X}(t;\theta)\underline{X}^T(t;\theta)]. \tag{74}$$

Equations (74) and (73) give a truly general definition of P_{xx} due to gravitational model errors. For cases with a small set of trajectories and with a well known gravitational field, these equations provide the total analysis. For most cases of interest the mission region Θ contains a continuum of trajectories and we know very little about the field for any particular θ. We seek then a less general form of (74) which is better aligned with the information we expect to have available.

One mission space partition requirement was that each mission region, such as Θ being discussed here, is well represented by a single design mission θ_0 as far as INS error dynamics are concerned. With this stipulation applied to (73) we get

$$\underline{X}(t;\theta)\underline{X}^T(t;\theta) = \int_0^t\int_0^t \Phi(t,p)G(p)\underline{u}(p;\theta)\underline{u}^T(q;\theta)G^T(q)\Phi^T(t,q)dpdq \tag{75}$$

where Φ and G are defined for θ_0. Now applying (74) to (75) we can take the expectation operation inside the integral to yield

$$P_{xx}(t) = \int_0^t\int_0^t \Phi(t,p)G(p)Q[\underline{r}(p),\underline{r}(q),K^*(\underline{R},\underline{R}';\theta)] G^T(q)\Phi^T(t,q) dpdq \tag{76}$$

where

86

$$Q[\underline{r}(p), \underline{r}(q), K^*(\underline{R}, \underline{R}'; \Theta)] = \underset{\theta \in \Theta}{\mathcal{E}} \left\{ \underline{u}(p; \theta) u^T(p; \theta) \right\} \qquad (77)$$

and $\underline{r}(p)$ and $\underline{r}(q)$ are on θ_0 since θ_0 also represents the geometry associated with the $\theta \in \Theta$. The Q-matrix is discussed in Appendix E. The covariance function $K^*(\underline{R}, \underline{R}'; \Theta)$ characterizes the residual field statistics as a function of the geometry inherent in the $\underline{R}$ and $\underline{R}'$ arguments. This function can be continued upward (see Appendix C) to form $K(\underline{r}, \underline{r}'; \Theta)$. Now given $\underline{r}(p; \theta)$ and $\underline{r}(q, \theta)$ as geometric arguments associated with the trajectory θ, we can form $K^*[\underline{r}(p, \theta), \underline{r}(q, \theta); \Theta]$. From this function we can form a Q-matrix for each θ. Since the K^* function is a function of the geometry of $\underline{r}(p, \theta)$ and $\underline{r}(q, \theta)$ we can use the evaluation along the design mission θ_0 to approximate the expectation over all $\theta \in \Theta$.

In (76) we have the analysis method we have been seeking. The covariance P_{xx} provides the data for either computing system-level performance cost (see Appendix D) or for comparison to an INS-level accuracy criteria for the gravitational model. The gravitational modeling errors over Θ are summarized in the Q-matrix and their expected effect on INS estimates are propagated through the G and Φ functions. Equation (76) appears to be a useful form for other analyses, as well. For example, suppose our original question were "Do we need to consider more than the reference field model to meet our INS gravitational model error budget?" To answer this question we apply (76) to each design mission using $K(\underline{R}, \underline{R}'; \Theta)$ rather than K^*

since our hypothesis is only the reference field. We can estimate the ultimate accuracy attainable by forming an equivalent continuum version of K_S and applying (76) with this covariance under an assumed perfect Poisson Integral approximation. These analyses form a worst case, with $K(\underline{R}, \underline{R}'; \theta)$, and a best case, with $K_S(\underline{R}, \underline{R}')$, set of numbers which will be useful in judging the relative effectiveness of our model.

Also, if one were designing a Kalman filter for an INS application, (76) allows for explicit consideration of this system noise source. Another possible use, along this line, is to let (76) provide the statistics for a truth model gravitational noise model at the INS estimate level.

Equations of the form of (76) appear in Kalman filter development and are typically put in differential equation form for computer solution. The appearance of $\underline{r}(p)$ and $\underline{r}(q)$ in the Q-matrix argument list will complicate this approach. The first step is to differentiate (76) with respect to the mission time t:

$$\dot{P}_{xx}(t) = G(t) \int_0^t Q[\underline{r}(t), \underline{r}(q); K^*] G^T(q) \Phi^T(t, q) dq$$

$$+ \left\{ \int_0^t \Phi(t, p) G(p) Q[\underline{r}(p), \underline{r}(t); K^*] dp \right\} G^T(t)$$

$$+ F(t) P_{xx}(t) + P_{xx}(t) F^T(t) \tag{78}$$

subject to

$$P_{xx}(0) = [0]. \tag{79}$$

88

Q is a covariance matrix hence symmetric so

$$Q[\underline{r}(t), \underline{r}(q); K^*] = Q[\underline{r}(q), \underline{r}(t); K^*] \qquad (80)$$

We can rewrite (78) as

$$\dot{P}_{xx}(t) = G(t)D(t) + D^T(t)G^T(t) + P_{xx}(t)F^T(t) + F(t)P_{xx}(t) \qquad (81)$$

where

$$D(t) = \int_0^t Q[\underline{r}(t), \underline{r}(q); K^*]G^T(q)\Phi^T(t, q)dq \qquad (82)$$

The $\underline{r}(t)$ in the Q argument of (82) makes it undesirable to continue with a $\dot{D}(t)$ equation for computational purposes. The set (81), (82) and (69) subject to initial conditions of (70) and (79) form a complete set for computational analysis. The approach will be to write computer programs to solve the differential-integral equation set so defined as a means of estimating the INS-level performance of the gravitational model.

While the differential form of (82) is computationally unwieldy, this equation is important for the insights it affords.

$$\dot{D}(t) = Q[\underline{r}(t), \underline{r}(t); K^*]G^T(t) + D(t)F^T(t)$$

$$+ \int_0^t \left\{ \frac{\partial}{\partial \underline{r}} Q[\underline{r}, \underline{r}(q); K^*] \right\}_{\underline{r}=\underline{r}(t)} \underline{v}(t)G^T(q)\Phi^T(t, q)dq. \qquad (83)$$

The first term on the right hand side of (83) represents the new

gravitational disturbance entering at point $\underline{r}(t)$. The second term is just the propagation of previous errors. The third term represents a "missing link" between the analysis leading to (76) and our previous intuitive examples. The partial of Q--with respect to a spatial variable can be shown to be related to the gravitational tensor Γ of the residual field. The v(t) term is the mission velocity which in conjunction with Γ forms the time varying gravitational disturbance derivative.

In summary, the system-level performance cost estimation occurs in three distinct steps. This process is shown in flow chart form in Figure 5. The model concept, mission region, and survey characteristics are used to form a residual field covariance function. This function along with the INS error dynamics and the design mission are used to form the INS error state covariance matrix as a function of time into the mission. This covariance function, $P_{xx}(t)$, contains all the information needed to calculate the expected system cost (see Appendix D); recall that we do not plan to use J(t) in our example but shall assume the requirements placed on $\mathcal{E}[J(t)]$ be interpreted as restrictions on $P_{xx}(t)$.

With this presentation of the approach for performance cost evaluation, let us turn to the implementation study. We have (76) and (54) to represent the opposing performance and resource costs. Our example application is to find the minimal grid (least m) which meets an INS accuracy requirement. This performance requirement might be to arrive at terminal time t_f with an rms position uncertainty due
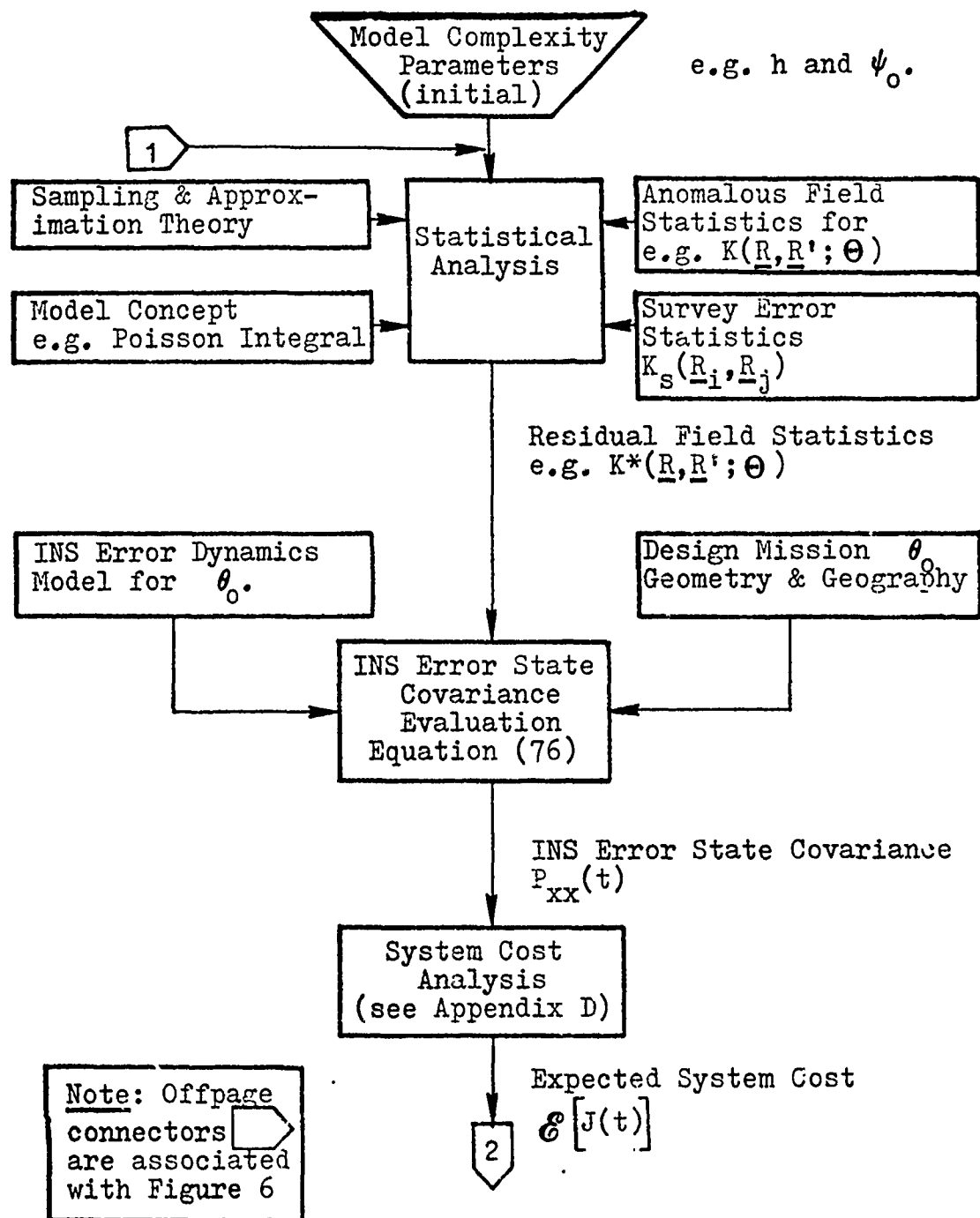
Figure 5. Gravitational Modeling Accuracy Cost

to the gravitational model of no more than Z feet.

The control parameters for grid specification are ψ_o and h. Our task is to select ψ_o and h to minimize m from (54) such that the performance cost from (76) meets specification. This problem falls into the category of constrained optimization. We know performance will improve as ψ_o is increased since more information is available. We expect performance to improve as h decreases, however the interplay between h, the mission velocity profile, and the Schuler loop may cause a surprise. With either decreasing h or increasing ψ_o we get an increase in m-system resource cost. Therefore, we can expect the minimal grid solution to lie on the boundary of the hypothetical performance cost partition on the ψ_o-h plane.

The example search logic is shown in Figure 6. This figure is designed to form an overall flow chart with Figure 5. The actual search logic will be defined after some characterization studies; e.g. constant performance cost and constant resource cost studies. These studies should provide information on the smoothness of constant performance curves on the ψ_o-h plane. We can also gain some insight by studying the variations in performance cost along a constant m line.

This concludes the description of the Proposed Approach. Any analysis must face a test to prove its worth. With this in mind, we direct the discussion to the methods which will demonstrate the effectiveness of these analyses.
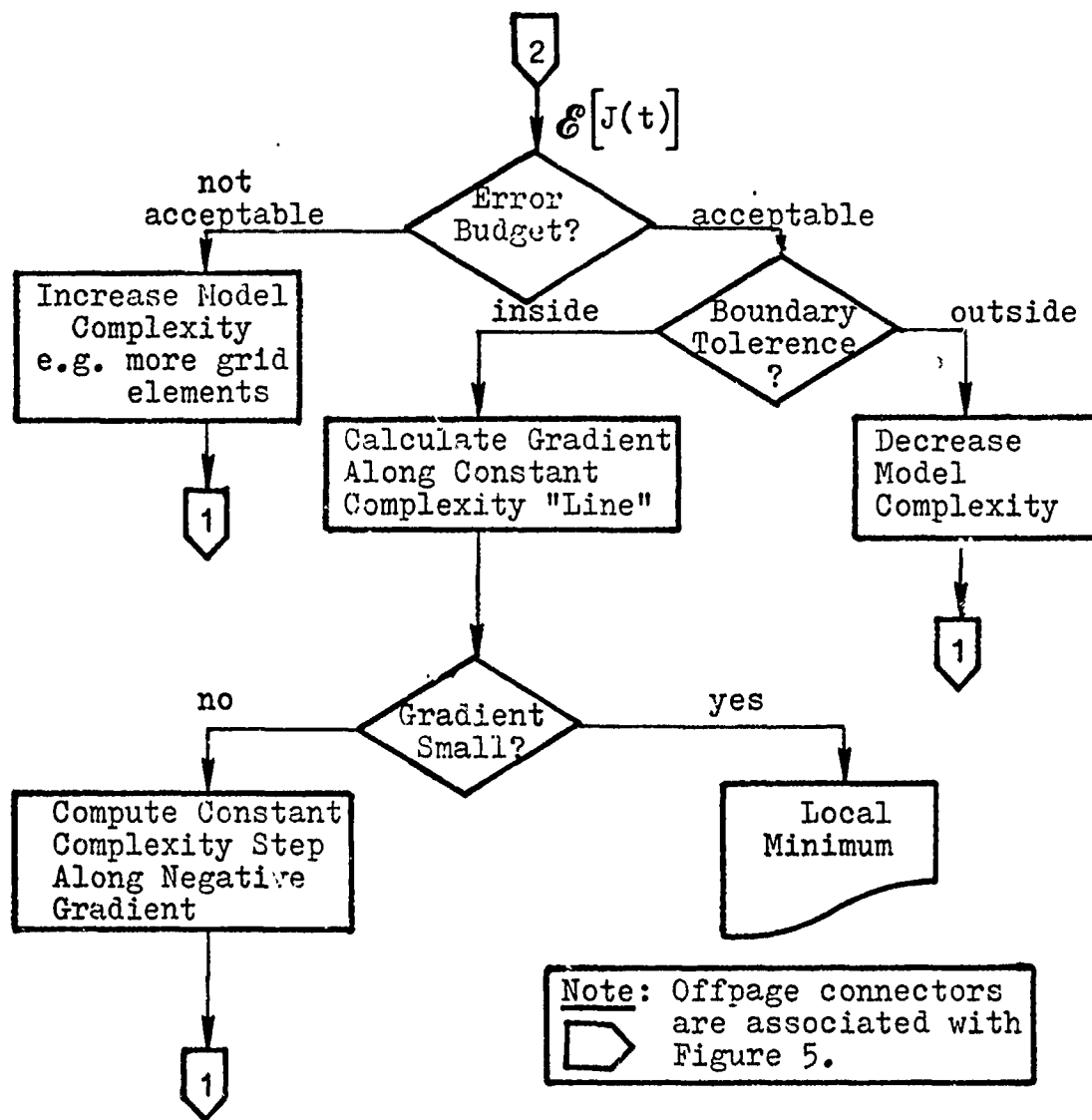
Figure 6. Minimal Grid Search Logic

F. Confirmation Method

The manner of evaluating the developed theory will be by simu-
lating true gravitational fields, by applying the theory to these fields
for a predefined mission, and by studying the errors in a simulated
INS using the derived compensation model. Two types of simulated
gravitational fields come to mind. One type is pure simulation. An
analytical field is constructed to reflect or approximate the statistics
of the observed field--say by producing the same $K(\underline{R}, R'; \Theta)$ as an
empirically derived function. Another simulation approach is to
attempt to reproduce the field in a general area by closed form approx-
imations (e.g. point masses as in Ref 24). Both methods have advant-
ages. The pure simulation allows us to control the field to the (nearly)
identical statistics upon which our analysis will be based. The real
field approximation will allow a more convincing test of our hypothesis.

To use the analytical fields the survey specifications will be
solved for a predetermined mission type. Grid sampling will be accom-
plished by direct computation of the analytical field equations. Survey
errors can be added to these data for Monte Carlo simulations. Since
the gravitational modeling errors are the issue, the simulated INS will
be initialized with perfect knowledge of the initial state vector and with
perfect alignment. Simulated mission position and velocity along with
the simulated true gravitational field will be used to derive INS sensor
inputs. The INS algorithm, not just the error propagation model, will
be programmed with the INS reference gravitation field compensated

94

with the Poisson Integral approximation of gravitational disturbance.

The resulting INS errors can be subducted from the simulated true and the INS estimated states. These error time histories can be compared with our specification. A Monte Carlo study with variations on the true field and the trajectory fixed or variations on the trajectory with the field fixed is necessary to demonstrate the required ensemble performance.

G. Ancillary Questions

The confirmation methods will measure our ability to construct grids which deliver the advertised INS accuracy. The Poisson Integral will require a major investment of our computer resources, and it is reasonable to ask what we are getting in return. For example, can less sophisticated, but perhaps less flexible, compensations be compared. To put the Poisson Integral in perspective this question and others will be addressed:

1. How effective is a pre-mission initial condition offset based on the nominal trajectory and a possible more complex model for ground-based evaluation?

2. What is the sensitivity of our performance to the choice of nominal trajectory?

3. How sensitive are our results to errors in covariance function $K(\underline{R}, \underline{R}')$?

4. Can the integral be implemented by transform techniques?

95

5. Can the grid spacing be varied in the crossrange direction to lower the number of elements required?

IV. Outline of the Final Report

The dissertation will be based on this prospectus. The background provided herein will, with some modification, be repeated in the introductory discussion. The completion of the theoretical analysis with the necessary basis from the proposed approach herein will be recorded. The numerical confirmation tests and ancillary questions will be provided in the results section. The major subdivisions and their general content should be as follows.

1. Introduction: The background discussion necessary to put the theoretical work in context. The reference gravity model will be more thoroughly discussed--perhaps as an appendix.

2. Theory of System-Level Performance Cost Estimation for Gravitational Models: Completion of the development leading to (76).

3. Theory of Poisson Integral Approximation (for INS application): The fundamental theory will be cited and summarized for the Poisson Integral and for the approximation of such integrals by finite element summation. The developments of the Proposed Approach will be repeated and completed.

4. Implementation: Those considerations necessary to bridge from theoretical development to computer code.

5. Example Application Problem: Discussion of the minimal

grid problem.

6. <u>Numerical Results</u>: The confirmation studies and replies to the ancillary questions.

7. <u>Summary and Conclusions</u>: Self-explanatory.

8. <u>Suggestions for Future Research</u>: Self-explanatory.

9. <u>Appendices</u>: As required to package lengthy developments not directly in line with the theoretical development.

V. <u>Air Force Applicability</u>

The applicability of the proposed research to the Air Force has been touched on in several sections (e.g. pages 24-25). The precise and unaided INS is an obvious flexible asset in employing strategic weapons. The techniques proposed herein, once developed, could also be applied to the test flight problem. The regression analyses for identifying INS component error model parameters would employ the gravitational compensation model to remove the corruption of the results due to the spectral spillover of gravitational disturbances.

The potential for this theory being directly applied cannot truly be estimated. If the upward continuation integrals can be cast in a form compatible with Fast Fourier Transform (FFT), the potential application increases. The onboard memory space in most operational systems will make the expensive fine model unacceptable. With FFT formulation we can consider an off-line, separate gravitation computer (see Figure 7) which is an input-output device on the data bus. Hardware is presently available to perform the FFT "butterfly" operations. This concept would be an asset for strategic bomber and missile application. Even in tactical situations we might find a highly accurate, all-inertial capability useful in many ways.
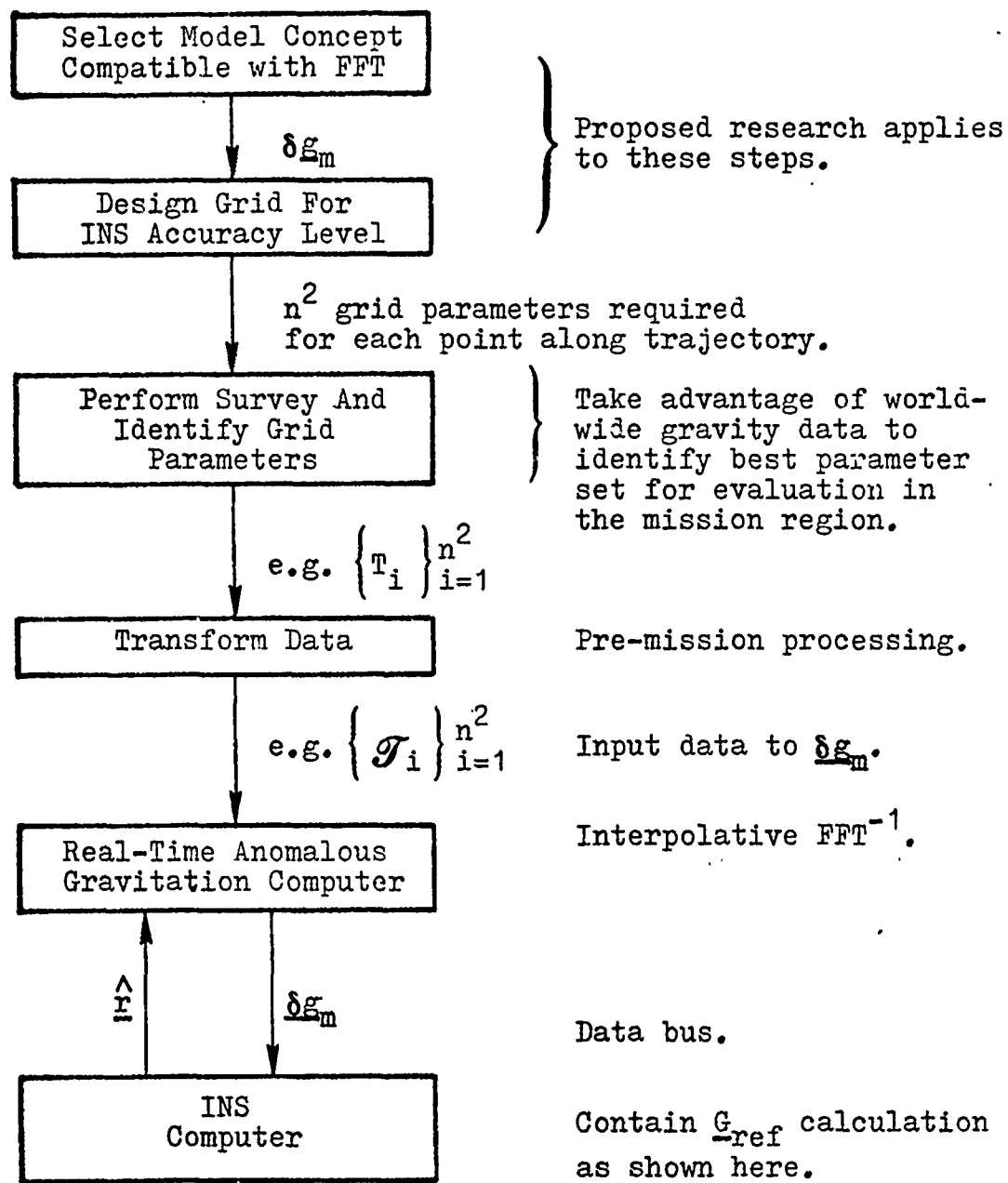
Figure 7. Future Application Possibility

VI. Originality

The proposed approach is original in the concept of focusing on the INS results rather than anomalous gravitation per se. The idea of using an INS error budget as a criteria or design constraint is common practice, but the application to this problem of gravitational modeling is new. Equation (76) and the rationale leading up to it are also original. The general applicability of (81), (82) and (69) mean they can be employed in many ways whenever the rationale fits and the covariance function is known or approximated. Applying these concepts to the grid specification problem is an uncompleted task. The end result will be a definite extension of grid specification which might have application in survey design tasks as well. The remaining task of deriving the residual potential covariance, $K^*(\underline{R}, \underline{R}'; \Theta)$ from the anomalous potential covariance, $K(\underline{R}, \underline{R}'; \Theta)$, and the grid specifications should also provide an original contribution.

Appendix A

The Gravity Tensor

The gravity tensor plays an important role in the INS error propagation model, and it has received much attention recently with the development of inertial instruments, gradiometers, which measure elements of the matrix. The following discussion covers certain interesting mathematical properties and addresses the problem of expressing the tensor in arbitrary coordinate frame

The representative gravitation function, $\underline{G}(\underline{r}^e)$, is only defined for an Earth-relative argument which we indicate by the generic e-frame notation. Now, define

$$\Gamma_e(\underline{r}^e) = d\ \underline{G}(\underline{r}^e)/d\ \underline{r}^e \qquad (A-1)$$

This quantity will be referred to as the "e-frame gravity tensor."

To explore some of the mathematical properties of this e-frame gravity tensor consider its original form. The tensor is the spatial derivative of the gravitation function which is in turn the spatial derivative, or gradient, of the gravitational potential function, $V(\underline{r}^e)$. So,

$$\underline{G}^e(\underline{r}^e) = dV(\underline{r}^e)/d\ \underline{r}^e \qquad (A-2)$$

and

102

$$\Gamma_e(\underline{r}^e) = d^2V(\underline{r}^e)/(d\ \underline{r}^e)^2. \qquad \text{(A-3)}$$

Consider now a Cartesian e-frame with orthorgonal axes and

$$\underline{r}^e = \begin{Bmatrix} x \\ y \\ x \end{Bmatrix}. \qquad \text{(A-4)}$$

Then,

$$\underline{G}^e(\underline{r}^e) = \begin{Bmatrix} V_x \\ V_y \\ V_z \end{Bmatrix} \qquad \text{(A-5)}$$

where the subscript on V indicates the appropriate partial derivative. We shall now assume that the mass of the air above the Earth's surface can be neglected. In practice, gravity data is reduced taking this assumption into account. Then, in the region of interest $V(\underline{r}^e)$ is harmonic (Ref 14:126-145). This property allows us to state that $V(\underline{r}^e)$ and $\underline{G}(\underline{r}^e)$ are continuous. Then, the second partial derivatives commute. For example,

$$V_{xy} = \partial^2V/\partial x\partial y = \partial^2V/\partial y\partial x = V_{yx}. \qquad \text{(A-6)}$$

Since,

$$\Gamma_e(\underline{r}^e) = \begin{bmatrix} V_{xx} & V_{xy} & V_{xz} \\ V_{yx} & V_{yy} & V_{yz} \\ V_{zx} & V_{zy} & V_{zz} \end{bmatrix} \qquad \text{(A-7)}$$

From (A-6) we see that (A-7) is symmetric. Again, since the potential function is harmonic, it satisfies LaPlace's equation:

$$\nabla^2V = V_{xx} + V_{yy} + V_{zz} = 0. \qquad \text{(A-8)}$$

103

So,

$$\text{Trace} \left\{ \Gamma_e(\underline{r}^e) \right\} = 0. \tag{A-9}$$

With symmetry and (A-8) we conclude that of the nine elements of the gravity tensor only five are independent.

These mathematical properties of $\Gamma_e(\underline{r}^e)$ are tied to the e-frame. Since we encounter other frames of reference in measurements and calculations, we need a means of expressing the gravity tensor in these frames. This problem is similar to transforming an inertia tensor from one frame to another, and, not unsurprisingly, the answer is a transformation of the same form. Consider some arbitrary orthogonal k-frame. We can express

$$\underline{G}^k(\underline{r}^e) = C_e^k \, \underline{G}^e(\underline{r}^e) = C_e^k \, \underline{G}^e(C_k^e \underline{r}^k) \tag{A-10}$$

So,

$$d \, \underline{G}^k(\underline{r}^e)/d \, \underline{r}^k = C_e^k \, [d \, \underline{G}^e(\underline{r}^e)/d \, \underline{r}^e] \, [d \underline{r}^e/d \underline{r}^k] \tag{A-11}$$

And we get,

$$\Gamma_k(\underline{r}^e) = C_e^k \, \Gamma_e(\underline{r}^e) \, C_k^e \tag{A-12}$$

With these derivations and explanations the use of the gravity tensor should be clearer.

Appendix B

Fundamental INS Properties

The propagation of INS errors is modeled by first-order perturbation techniques. References 1 and 2 present a detailed development along this line. Some of the more basic modes of inertial navigation can be discerned from even simpler models. The vertical channel of an inertial system is unstable, and the horizontal channels display an oscillation known as the Schuler mode. These fundamental characteristics appear, in some form, in all INSs. The following development shows these underlying relationships between the position estimates and the gravity model in extremely simple terms.

We have from previous developments:

$$\delta \ddot{\underline{r}} = \delta \underline{g}(\underline{r}^e) + \Gamma(\underline{r}^e) \, \delta \underline{r} \tag{9}$$

where

$$\Gamma(\underline{r}^e) = \partial \underline{G}(\underline{r}^e)/\partial \underline{r}$$

For convenience, suppose at $t = 0$ the Cartesian z-axis goes through the true position. The gravitation function can be viewed as an expansion about the centroidal point mass function,

$$\underline{G}(\underline{r}) = - \frac{\mu}{r^3} \, \underline{r}. \tag{B-1}$$

The remainder of the gravity field will be included in $\delta \underline{g}(\underline{r}^e)$ and will be ignored for this development in order to concentrate on the $\delta \underline{r}$ effects. We can now write much simplified error equations for the vertical and horizontal channels.

For the vertical channel, we get from (9):

$$\delta \ddot{z} = \delta g_z + [\partial G_z / \partial x]_P \delta x + [\partial G_z / \partial y]_P \delta y + [\partial G_z / \partial z]_P \delta z \quad (B-2)$$

where point P for this case will be $(0, 0, r_o)$ for (x, y, z). In this vertical channel case, we will assume δg_z, δx, and δy are zero. From (B-1) we get

$$G_z = - \mu / z^2 \quad (B-3)$$

So,

$$[\partial G_z / \partial z]_{z = r_o} = 2 \mu / r_o^3 \quad (B-4)$$

Identifying μ / r_o^2 as g, equation (B-2) becomes

$$\delta \ddot{z} = (2g / r_o) \, \delta z \quad (B-5)$$

This homogeneous error differential equation indicates solutions of the form

$$\delta z = A \, e^{\alpha t} + B \, e^{-\alpha t} \quad (B-6)$$

where

$$\alpha = \sqrt{2g / r_o} \text{ and A and B are constants.}$$

The positive exponential term demonstrates the underlying instability of the vertical channel. We should note here that altimeter aiding of

106

the vertical loop is the standard remedy for this INS problem.

Now, turning our attention to the horizontal channel, we may write an equation in x analagous to (B-2). This time we will assume δx is the only active term and get

$$\delta \ddot{x} = [\partial G_x / \partial x]_{x = 0} \delta x \qquad (B-7)$$

The term $\partial G_x / \partial x$ can be obtained from the following vector diagram if we assume δx is approximately equal to the chord in both magnitude and direction.

$\underline{r}, \hat{\underline{r}}$ are true, estimated position.

$\underline{G}, \hat{\underline{G}}$ are true, estimated gravitation.

θ is central angle in the plane of estimation error.

Earth Center of Mass
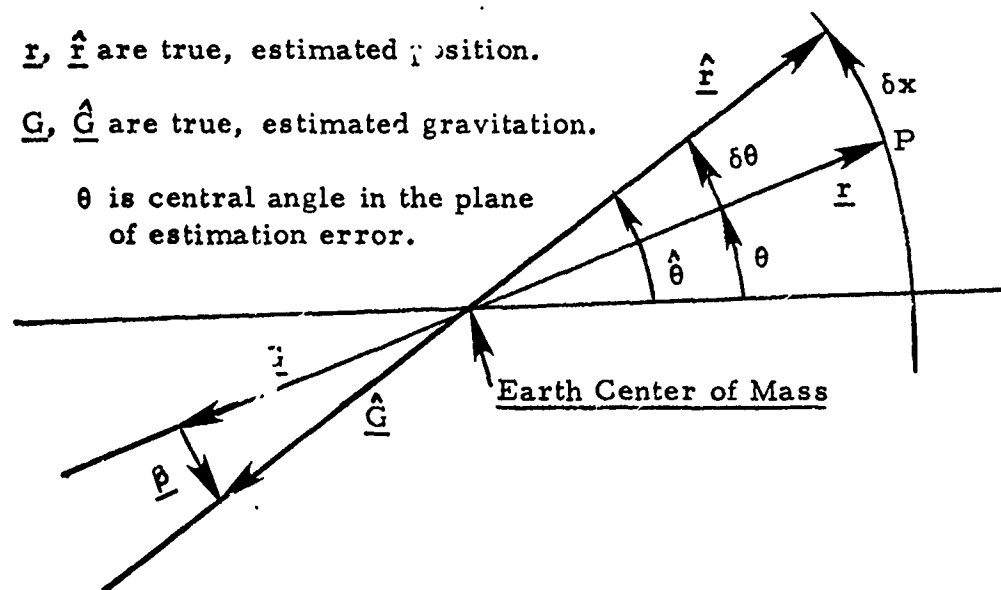
By using a first order approximation we get,

$$\hat{\underline{G}} = \underline{G} + [\partial \underline{G} / \partial x]_P \, \delta x \qquad (B-8)$$

From the diagram we get, $\hat{\underline{G}} = \underline{G} + \underline{\beta}$. $\qquad (B-9)$

107

So,

$$\underline{\beta} = [\partial \underline{G}/\partial x]_P \, \delta x. \tag{B-10}$$

Using small angle approximation we get,

$$|\underline{\beta}| = |\underline{G}| \cdot |\delta \theta| \tag{B-11}$$

and

$$r \, \delta \theta = \delta x. \tag{B-12}$$

Combining (B-10), (B-11), and (B-12) yields

$$\frac{|\underline{G}| \cdot |\delta x|}{r} = \left| (\partial \underline{G}/\partial x)_P \, \delta x \right| \quad \text{which reduces to}$$

$$(1/r) \, |\underline{G}| = g/r = \left| (\partial \underline{G}/\partial x)_P \right| \tag{B-13}$$

Since $\underline{\beta}$ is parallel and opposite in direction to the δx line segment, we conclude that $(\partial G_x/\partial x)_P = -g/r.$ (B-14)

Then, (B-7) becomes

$$\delta \ddot{x} = (-g/r) \, \delta x \tag{B-15}$$

From this homogeneous error differential equation, we expect solutions of the form

$$x = A \sin \omega_s t + B \cos \omega_s t \tag{B-16}$$

where ω_s is the Schuler rate $\sqrt{g/r}$ which is characterized by an 84 min. period and where A and B are constants.

108

·This mode was first postulated in a gyrocompass design application (Ref 3:15-16), however it appears in all terrestrial INS applications (Ref 1). These characteristic oscillations of the estimate, $\hat{\underline{r}}$, about the true position, $\underline{r}$, result because horizontal position errors create an opposite error in gravitational acceleration.

Appendix C

Anomalous Gravity Statistical Methods

We know the gravity function through a relatively sparse sampling using measurements subject to errors. Our sketchy and imperfect knowledge of this field is insufficient for many analyses in Physical Geodesy (e.g. Ref 65) and Inertial Navigation (e.g. Ref 21). A statistical approach to these problems can provide predictions or error assessments. We need a statistical description of the deterministic gravity, or anomalous gravity, field to perform these tasks. The anomalous field is completely specified by boundary conditions of either anomalous potential or gravity magnitude over a reference closed surface. The statistics are also completely specified by the statistics of either of these quantities on the reference surface. We require at least second-order statistics for such an analysis. The mean of either of these basis quantities should be zero since the zeroth term of our model totally accounted for Earth's mass. The following discussion summarizes some methods used to approximate or simulate the required second-order statistic: the covariance function.

The basic "signal" of the anomalous field is represented by either the gravity anomaly or anomalous potential. The quantity required in an analysis may be a related term such as deflection of the vertical or geoidal height (Ref 66:67). Figure C-1 graphically portrays these
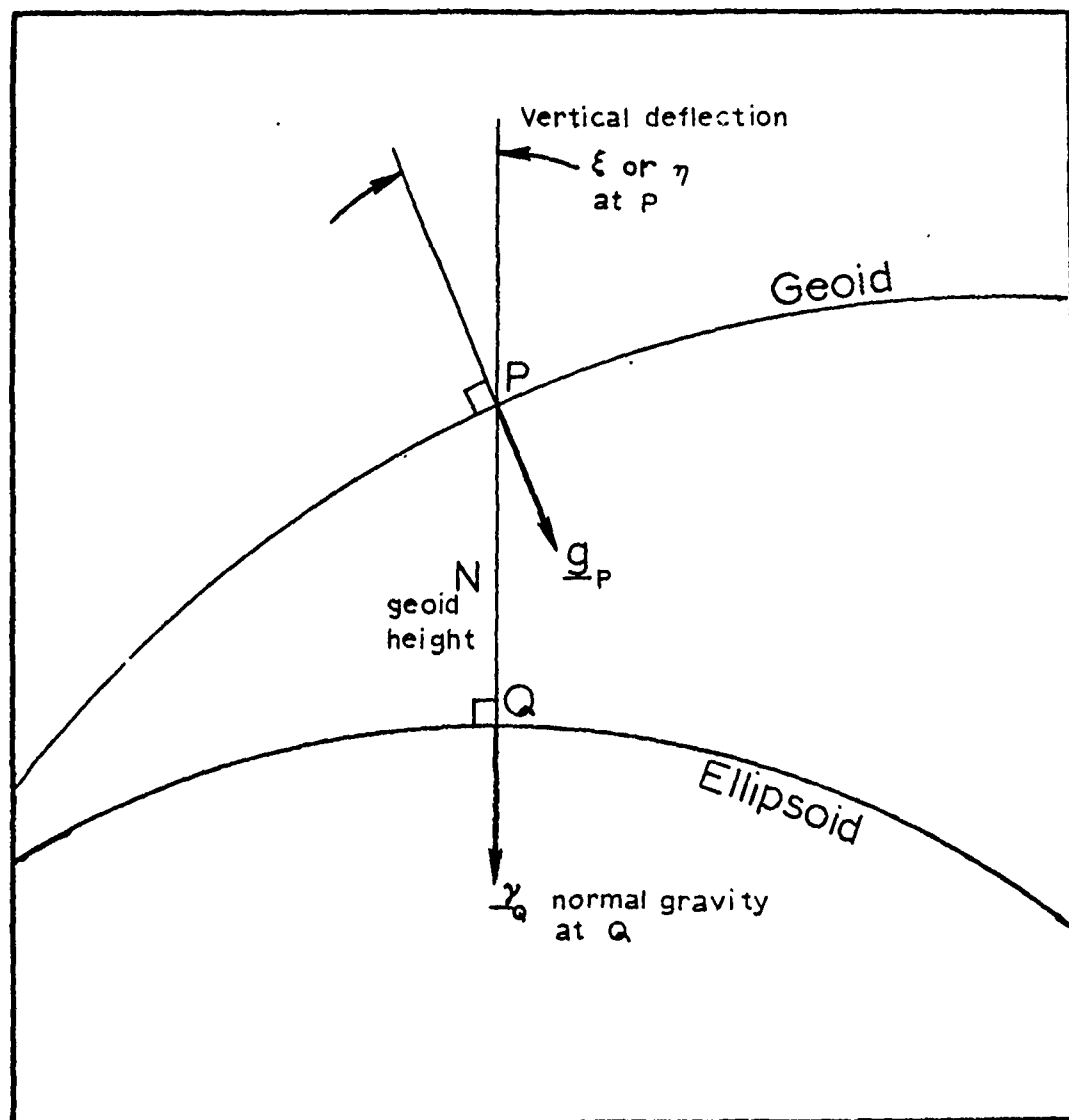
Figure C-1. Anomalous Gravity Quantities[*]
(Ref 14:83)

quantities; References 14 and 67 give detailed definitions for these and

other anomalous gravity manifestations. Some of the interrelationships

are

Gravity anomaly vector: $\Delta \underline{g} = \underline{g}_p - \underline{\gamma}_Q$ (C-1)

Gravity anomaly: $\Delta g = g_p - \gamma_Q$ (C-2)

---

[*]$\underline{\gamma}$ is used here for the reference or normal field. This field may
or may not coincide with the model field $\underline{g}_m$.

111

Geoid height or undulation: N, as shown.

Anomalous potential: $T = \gamma_Q N$ (C-3)

Also relating Δg and T: $\Delta g = -\dfrac{\partial T}{\partial r} - \dfrac{2T}{r}$ (C-4)

Radial gravity disturbance is sometimes used with deflection angles as a complete definition for the anomaly vector. The radial disturbance is simply $\delta g = -\dfrac{\partial T}{\partial r}$ (C-5)

Through these interrelationships, the statistics of all these anomalous gravity manifestations are coupled. It has been shown (Ref 66:94-98) that the individual covariance functions for all these quantities can be derived from either the anomalous potential or the gravity anomaly covariance function. The anomalous potential covariance function is mathematically easier to manipulate, however the gravity anomaly covariance function empirical approximations are more directly accessible since gravity measures are the prime data. Once we select the basis quantity, say gravity anomaly, we need to clearly define the covariance relationships of these quantities.

A covariance function must, in general, be defined for a two-position-vector argument. This generality should be kept in mind, but we do not have data to empirically calculate such a function. We do have data on the Earth's surface and we can estimate this function over this closed surface. The problem is simplified by reducing these Earth surface measurements to a surface which is more mathematically

convenient: the Bjerhammar sphere (Ref 68:25-26) which approximates the reference ellipsoid. This function can be continued upward, if necessary, to yield the function at another level or to show the correlation between anomalies at two different levels. The upward continuation follows from the harmonic nature of the anomalous potential. With this general background, we shall discuss more fully the reference surface covariance function for gravity anomaly before introducing the approximation techniques.

The definition of gravity anomaly covariance function is couched in deterministic (mean) rather than stochastic (expectation) terms. Since the mean of the gravity anomaly over the Bjerhammar sphere is zero (Ref 14:252), the covariance function is the autocorrelation function (ACF). By restricting to the reference sphere, we can specify any two points with four arguments. That is $C(\underline{r}_1, \underline{r}_2)$ can become $(\lambda_1, \phi_1; \lambda_2, \phi_2)$, where λ is the longitude and ϕ is the latitude. This function can be approximated for those points with gravity measurements, but a more representative form is needed to approximate the relationship between unmeasured points. Two forms of these average or representative functions appear in the literature most often.

The first form, $C(\psi, \alpha)$, is defined in terms of a shift (arc) distance $s = R\psi$ and an arc azimuth argument α. Here, ψ represents the central angle between the two points on the sphere. Figure C-2 portrays this relationship. The defining equation is

$$C(\psi, \alpha) = M_K \left[\Delta g_P \, \Delta g_{P'} \right] \qquad (C-6)$$
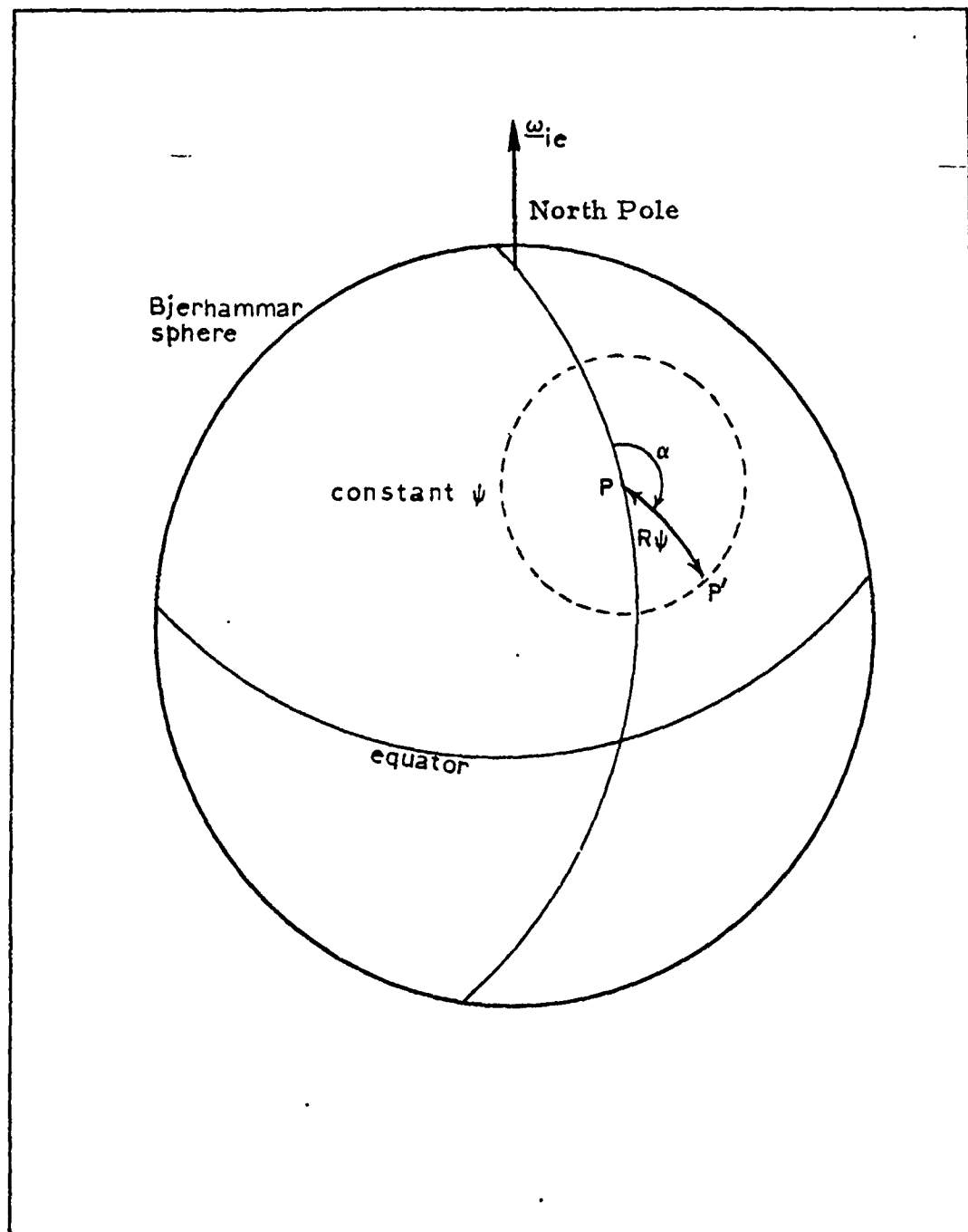
113

Figure C-2. Covariance Function Geometry
(Ref 14:257)

where M_K is the mean over the set K which is defined by

114

$$K = \left\{ (P, P') \middle| \begin{array}{l} \text{(1) P and P' are on the sphere;} \\ \text{(2) Central angle } \angle POP' \text{ is } \psi; \\ \quad \text{ and} \\ \text{(3) Arc } \overparen{PP'} \text{ has azimuth } \alpha. \end{array} \right\}$$

$C(\psi, \alpha)$ is then the average, or mean, pair product over all point pairs
on the sphere which subtend a central angle of ψ and which have a join-
ing arc of azimuth α. This average covariance function is consistent
with the assumption of homogeneity (Refs 66:85 and 69:1).

The other common form of the covariance function is generated
in a manner that is consistent with symmetry in the argument ψ. This
radial (in the horizontal distance sense) symmetry is a characteristic
of an isotropic field over the sphere (Refs 66:85 and 69:1). The function
$C(\psi)$ is easily defined in terms of $C(\psi, \alpha)$ by

$$C(\psi) = \underset{\alpha \in (0, 2\pi)}{M} [C(\psi, \alpha)]. \tag{C-7}$$

The assumption of an isotropic field may not be valid for a particular
section (see Ref 49:37-39 and Ref 70:26 for example real data), but this
assumption is attractive for its mathematical simplifications (Ref 71:39).

Equation (C-7) can be approximated with available gravity measure-
ment data which results in a tabular form of $C(\psi)$. Examples of such
tabulations abound--each generated under different rules or data base
(e.g.s Ref 14:254 and Ref 69:80-83). Such a table is our only true
measure of the covariance function, however this form is cumbersome

115

for mathematical manipulations. A closed form mathematical approximation is useful in many applications, and many such approximations have been suggested (Ref 72:10-13 and Ref 73:10-14). The Hirvonen covariance function model (Ref 14:255) is one example

$$C(\psi) = \frac{C_o}{1 + (R\psi/d)^2} \tag{C-8}$$

where R is spherical radius and C_o and d are parameters. In the cited example, a value of 337 $mgal^2$ was provided for C_o, and d was specified as 40 km. These parameters were selected for a specific geographic area (southern Ohio).

The selection of such model parameters is critical for the uses of these closed form approximation. These expressions are primarily used for statistical weightings in the region of small shift distance (within the half-variance range, see Figure C-3), so the behavior of these closed form approximations in this region receives special
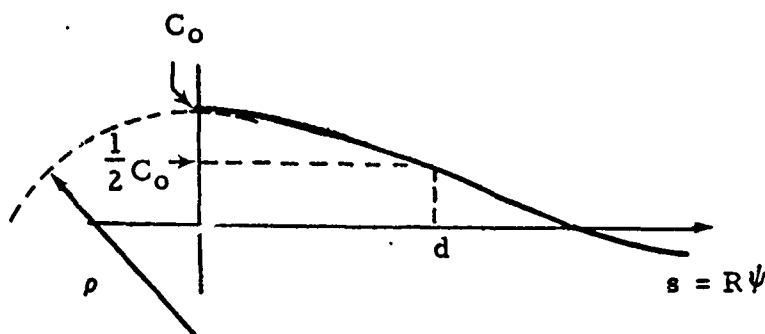

Figure C-3. Covariance Shaping Factors
(Ref 72:22)

attention. The three shaping factors which are used to judge the good-
ness of fit of these approximations are (1) the variance, C_o, (2) the
radius of curvature, ρ, at zero shift, and (3) a representative distance,
d, quantity defined by the shift distance to the half-variance level.
Figure C-3 portrays these parameters; Reference 72 has a thorough
discussion of these issues in Section 3.

Another modeling approach is to develop a closed form approxi-
mation for the spherical harmonic coefficients of the covariance func-
tion spherical harmonic decomposition. These coefficients are referred
to as degree variances since they represent the variance of the particu-
lar wavelength components. This technique is developed in Reference
69. This modeling technique is sometimes combined with the previous
technique: the closed form model is used for the near zero shift region
and the degree variance model for the remainder of required covariance
evaluations.

Our discussion, thus far, has been confined to the reference
surface form of the covariance function. The more general form which
allows points P and P' to be at different levels is needed for some
analyses. An example of this need to span altitude differences is in the
least-squares combination of satellite data with surface data (Ref 74).
If we construct the covariance function with arguments $\underline{r}_1$ and $\underline{r}_2$, we
can theoretically continue the function upward in one argument, say $\underline{r}_2$,
while fixing the other, $\underline{r}_1$, to the reference surface (e. g. Ref 68:32).
Heller and Thomas (Ref 50:Appendix B) have recently demonstrated

117

·some concise analytical techniques to handle such upward continuations in a more general, spherical rather than planar, manner.

These, then, are some of the statistical modeling approaches in Physical Geodesy. Inertial Navigation analyses are interesting in comparison. The Physical Geodesy task is based on sample measurements of anomalous gravity and a statistical model used in conjunction to adjust data, predict gravity, or estimate the associated errors. The inertial analyses attempt to characterize INS errors based on a statistical model of gravity modeling errors and a dynamic error propagation model. The tasks while quite different share the covariance statistics.

A covariance function or autocorrelation function (ACF) for gravity anomaly is useful in these INS statistical error analyses. An INS is expected to operate globally--or at least anywhere within some large region. We wish to characterize INS performance throughout this region. If the anomalous gravity field were known exactly throughout this area, we would need data from the ensemble of possible trajectories to calculate average INS error statistics. Fortunately, given an ACF, · · we can estimate these INS performance indices by simulating the anomalous field with stochastic processes. These processes can be cast in a form compatible with the linear time-invariant INS error propagation models (Refs 1 and 2). The subject ACF is the key to this modeling process.

The deterministic anomalous gravity field for some area is characterized by second order statistics--means and covariances--of

118

the gravity anomaly. The INS error performance is, then, simulated

by the performance of an INS driven by the outputs of a shaping filter

driven in turn by white Gaussian noises (Ref 75:217-218). The ensemble

of trajectories is simulated by the ensemble of noise functions in that

sample space. The shaping filter design and the strength of the associ-

ated noises are selected such that the filter output covariance approxi-

mates well the empirically determined (estimated) anomaly ACF. The

mission velocity, as we have previously seen, translates these spatial

ACFs to temporal ACFs.

This concept of approximation has several years of development

history. The conflicting requirements of mathematical tractability and

physical reasonableness have channeled this effort. We shall identify

some major areas of interest in this evolutionary process before pro-

ceeding with a chronological account of the milestones in the develop-

ment of this modeling concept.

Most gravity data is reduced to either the reference ellipsoid or

the geoid, so we can only readily calculate an ACF for trajectories

bound to these surfaces. These data are in the form of gravity anomaly

or geoid undulation (anomalous potential is linearly related to geoidal

undulation by Brun's formula). The practical problem is to statistically

produce the INS error inputs at mission altitude and velocity based on

these available statistics. The physical interrelationships between

these simulated inputs--vertical deflections, gravity disturbance, and

geoid undulation--must be consistently reflected in the joint statistics

119

of these inputs. A concise method for upward continuing these data to mission altitude is desired, and as mentioned, the model must blend with INS models for maximum usefulness.

The fundamental modeling choices are (1) which anomalous gravity variable to use as a basis for deriving other ACFs and (2) which variables to use for INS error inputs. Early studies were quasi-static parametric analyses of the horizontal channels of a local-level INS mechanization. The vertical deflection angles were natural choices for this task. Later studies generalized the deflection angles to "along-track" and "cross-track" coordinates to fully exploit the isotropic assumption. Barometric altimeter aiding of the vertical channel introduces an additional disturbance error driving source due to geoidal undulation. Since all these sources can be related through surface integrals to either anomaly or undulation, it is physically unreasonable to assume them all to be statistically uncorrelated. Answers to these modeling questions have evolved over the years. A chronological account of this development is a suitable context for further discussion.

Levine and Gelb (Ref 21) developed models to approximate ACFs of the prime and meridional vertical deflections. The physical processes were simulated as independent outputs of first-order spatial stochastic differential equations of the form

$$\frac{d\xi(x)}{dx} = -\frac{1}{d_\xi} \xi(x) + q_\xi(x) \tag{16}$$

120

where x is shift distance, d_ξ is correlation distance, and q_ξ is a white Gaussian noise process with power spectral density of $2\sigma_\xi^2/d$. σ_ξ^2 is then the process output, hence vertical deflection, variance. The parameters σ_ξ^2 and d_ξ (Ref 76:86-88) can be varied to produce the best overall fit between the empirically derived ACF and the exponential ACF resulting from (16):

$$\phi_{\xi\xi}(x) = \sigma_\xi^2 \, e^{-\frac{|x|}{d_\xi}} . \tag{14}$$

This simple model was criticized on two counts. First, the ACF is non-negative and empirically derived ACFs have evinced negative regions. We shall see later that a positive-only covariance function is physically unreasonable; in fact it must be zero mean over the sphere. Also, the ACF is expected to be rounded (zero slope) at zero shift. The surface integral relationships of anomaly to Earth mass distribution implies at least first-derivative continuity at zero shift. This notion is also observed in empirically generated anomaly ACFs, but is lacking in the first-order, exponential model.

These physical reasonableness objections can be overcome at the cost of additional model mathematical complexity. Shaw et al (Ref 77) led the way by forming more complete models. They developed the relationships between deflection ACFs which we want and anomaly ACF which we have--at least empirically. Since vertical deflections can be calculated from anomaly data by the Vening Meinesz formula (Ref 14: 114), this relationship provides the link between anomaly ACF and

121

deflection ACFs and deflection cross-correlation function (CCF). Flat

Earth approximations are used along with the assumptions that the

gravity anomaly is homogeneous and isotropic on the geoid. The anom-

aly ACF can then be expressed in terms of a horizontal radial shift

distance. The Bessel function which follows quite naturally is not com-

patible with our linear filter goal. The exponential ACF of Reference

21 (Levine and Gelb) is further developed in Reference 77 by the intro-

duction of deflection CCF. An improvement was identified in the CCF.

It was shown that a change of coordinates from the traditional east-west

and north-south for deflection definition could result in a zero CCF. If

generic "along-track" and "cross-track" coordinates are used for

expressing deflection components, the isotropic assumption then implies

zero deflection CCF. Since the partial derivatives used in defining the

deflection angles are not tied to a particular azimuth, the statistical

representation is an average over all azimuths which yields this desir-

able modeling result.

Kasper (Ref 78) added another step with second-order Gauss-

Markov process models. He achieved the zero-slope-at-zero-shift

goal, but continued with a positive-only ACF. Simulation results com-

paring this second-order model to the previous first-order one show

almost identical rms position error per unit of input standard deviation.

The rms velocity errors were apart by a factor of two, however. The

lower errors associated with the second-order Markov covariance

model compare favorably with results obtained with measured gravity

disturbances as INS input. This result demonstrates the importance of the rounded correlation feature. This should come as no surprise since the importance of the near-zero-shift region received so much attention in the discussion of Physical Geodesy applications.

Bellaire (Ref 79) developed methods for continuing these geoid or ellipsoid based ACFs up to mission altitude. By employing harmonic function analysis, the upward continuation is cast in the form of surface integrals. The anomaly ACF is shown to be non-stationary in altitude due to attenuation. The anomaly field is stationary in the horizontal arguments at all levels if it is so on the geoid. The ACF between anomalies at two different altitudes is shown to be equal to the ACF at the average altitude. This new analytical tool allows a much more general trajectory study than the constant-altitude, constant-velocity previous approach.

The models and methods of Kasper (Ref 78) and Bellaire (Ref 79) support a statistically coordinated simulation of anomalous gravity driving all three INS axes over a range of variable altitude and velocity trajectories. The only important unmodeled effect at this point is the geoidal undulation disturbance of the barometric altimeter used to aid the vertical channel. Jordan (Ref 80) provided the theoretical development to include this term. More importantly, however, Reference 80 introduces a set of mathematical consistency "necessary conditions" with which we can judge these proposed models.

These consistency criteria are based on our understanding of anomalous potential and its relationships to gravity anomaly and to vertical deflections. The method consists of starting with the ACF which our statistical simulation produces, say the anomaly ACF. The undulation, or anomalous potential, ACF is derived from this anomaly ACF using the relationship

$$\left(\frac{\partial^2}{\partial x^2} + \frac{\partial^2}{\partial y^2}\right)\phi_{NN}(x, y) = -\frac{1}{\gamma_o^2}\phi_{gg}(x, y) \qquad (C-9)$$

where ϕ_{NN} is undulation ACF, ϕ_{gg} is anomaly ACF, x and y are horizontal plane shift distances, and γ_o is reference gravity. We can relate the second partials above to the negatives of the vertical deflection ACFs. Since these deflection ACFs at zero shift represent variances they must be positive there. Hence, a derived undulation ACF which is not concave at zero shift indicates the original anomaly ACF is physically unreasonable. Since the kernel associated with (C-9) is singular, another specific condition must be met by the anomaly ACF for the associated undulation ACF to be bounded everywhere on the plane. The constraint is that the anomaly ACF must be zero mean over the plane. In summary, if our statistical model generates an anomaly ACF which yields an associated undulation ACF which is either unbounded or is not concave down at the origin, that statistical model is physically inconsistent.

The previous models were each found lacking in some way. New

124

second- and third-order[*] Gauss-Markov process models were proposed. Even this second-order model fails to meet all criteria. Both new models accommodate a negative ACF at some shift distance, but only the third-order model has the rounded zero-shift profile. This third-order model represents the apex of this evolution.

What more could we ask for? The models discussed above all assume a flat Earth using the justification that correlation distance is much smaller than the Earth's radius. Statistical studies of long-range missions, such as ICBM trajectories, require a more global setting. Heller and Thomas (Ref 50) have begun work on such modeling techniques. They propose modeling the global free-air anomaly field as the result of buried spherical white noise processes which are continued up to and summed on the reference surface. This technique has successfully modeled some empirical anomaly ACFs. The present approach, however, yields an all-positive ACF. So, research on the global modeling problem is likely to continue.

In summary, we have seen the development and use of the gravity anomaly ACF or covariance function from two different points of view. The Physical Geodesy problems require the covariance function as an interpolation or prediction tool. The Inertial Navigation studies require

---

[*]The term "Third-order Markov" means that either the anomaly or undulation can be modeled as a Third order linear system driven by White Gaussian noise. To form a complete system to statistically produce ξ, η, N, and Δg requires eight integration levels (Ref 81:3-29 to 3-31).

the anomaly ACF to supply the input parameters to stochastic models which allow simulation of INS errors we expect the anomalous field to produce.

Appendix D

INS Gravitational Model Performance
Cost Function

Gravitational modeling errors should be studied in terms of
their effect on mission performance. For example, we might require
the overall system to meet some circular-error-probable (CEP) cri-
teria. The performance cost of each system component would then be
stated in terms of the effect on CEP. In such statistics, it is custom-
ary--and justifiable in most cases--to consider the overall system
performance estimate to be the root-sum-square (rss) of the individual
(supposedly independent) contributions. The effects of gravitational
modeling errors can be statistically characterized in terms of the INS
error state covariance matrix, $P_{xx}(t)$. This error covariance matrix
can be processed to yield the CEP cost due to the gravitational model-
ing errors alone. With this example as justification, the following
presentation describes how $P_{xx}(t)$ can be processed to form such a
system cost.

We begin by discussing a _terminal_ cost strategem. In many
instances of payload or weapon release, the total delivery accuracy
can be related to the terminal state estimation accuracy by a linear
propagation of errors using linear perturbation techniques. Let $\underline{y}$ be
the system "miss" coordinates; let $\underline{X}(t)$ be the INS error state vector

127

(e.g. downrange and crossrange); and assume terminal error is given by

$$\underline{y} = H\underline{X}(t_f) \qquad\qquad \text{(D-1)}$$

where t_f is terminal time.

We can form a terminal cost by

$$J = \underline{y}^T\underline{y} = \text{Trace}\left\{\underline{y}\,\underline{y}^T\right\}. \qquad\qquad \text{(D-2)}$$

To be more general we can weigh the "miss" vector with a matrix W which can be considered symmetric without loss of generality. Such a W matrix should be either positive semi-definite or positive definite. For terminal cost we get

$$J = \underline{y}^T(t_f)W\underline{y}(t_f) = \underline{X}^T(t_f)H^TWH\underline{X}(t_f)$$

$$= \text{Trace}\left\{\underline{X}(t_f)\underline{X}^T(t_f)H^TWH\right\} \qquad\qquad \text{(D-3)}$$

Since our error state $X(\cdot)$ is being treated statistically, we are interested in the expectation, $\mathscr{E}$, of J over the ensemble in our sample space:

$$\mathscr{E}[J] = \mathscr{E}\left\{\text{Trace}\ [\underline{X}(t_f)\underline{X}^T(t_f)H^TWH]\right\}$$

$$= \text{Trace}\left\{\mathscr{E}[\underline{X}(t_f)\underline{X}^T(t_f)]H^TWH\right\}$$

$$= \text{Trace}\left\{P_{xx}(t_f)H^TWH\right\} \qquad\qquad \text{(D-4)}$$

128

assuming H and W are invariant over our sample space. An analagous running cost function can be defined for those missions which require INS accuracy over all mission time. Again, we can conceive of a transformation to those coordinates on which system performance is judged.

$$\underline{y}(t) = H(t)\underline{X}(t) \qquad (D-5)$$

Then

$$\dot{J}(t) = \underline{y}^T(t)W(t)\underline{y}(t)$$

$$= \text{Trace}\left\{\underline{X}(t)\underline{X}^T(t) H^T(t)W(t)H(t)\right\} \qquad (D-6)$$

Then,

$$J(t) = \int_0^t \text{Trace}\left\{\underline{X}(p)\underline{X}^T(p)H^T(p)W(p)H(p)\right\}dp \qquad (D-7)$$

And

$$\mathcal{E}[J(t)] = \int_0^t \text{Trace}\left\{P_{xx}(p)H^T(p)W(p)H(p)\right\}dp \qquad (D-8)$$

assuming H(t) and W(t) are invariant over our sample space. The cost functions given by (D-4) and (D-8) are reminiscent of stochastic terminal controller and stochastic regulator cost functions (Ref 82:415). Indeed the model parameters involved in the optimization process may be viewed as control variables we use to minimize these costs. As with stochastic control problems, there may be missions where a

129

combination of terminal and running costs are appropriate. The

fundamental quantity needed for these cost evaluations is the INS

error state covariance matrix, $P_{xx}(t)$.

Appendix E

The Q-Matrix

The Q-matrix statistically summarizes the anomalous gravitational information. As mentioned in Appendix C, the covariance functions of various anomalous gravitation quantities can be derived from either the anomaly covariance, C, or the anomalous potential covariance, K. This result holds, as well, for the residual field after inclusion of the disturbance model δgm since this model is based on a harmonic potential field. So, while the following discussion uses the gravitation disturbance, δg, and the anomalous potential, T, the same relationships hold for residual disturbance, $\underline{\delta}$, and residual potential, δT. By our previous definition we have

$$Q[\underline{r}_1, \underline{r}_2; K(\underline{R}, \underline{R}'; \theta)] = \underset{\theta \epsilon \Theta}{\mathcal{E}} \begin{bmatrix} \delta g(\underline{r}_1)\delta g^T(\underline{r}_2) & \delta g(\underline{r}_1)T(\underline{r}_2) \\ T(\underline{r}_1)\delta g^T(\underline{r}_2) & T(\underline{r}_1)T(\underline{r}_2) \end{bmatrix} \qquad (E-1)$$

where $\underline{r}_1$ and $\underline{r}_2$ are in the design mission trajectory $\theta_o \epsilon \Theta$. Let x, y and z be our generic Cartesian coordinates; then,

$$\delta g(\underline{r}_1) = \begin{Bmatrix} \delta g_x(\underline{r}_1) \\ \delta g_y(\underline{r}_1) \\ \delta g_z(\underline{r}_1) \end{Bmatrix} \qquad (E-2)$$

and $\delta g_x(\underline{r}_1) = \left. \dfrac{\partial T}{\partial x} \right|_{\underline{r}_1} = \dfrac{\partial T}{\partial x_1}.$ \qquad (E-3)

With the understanding from (E-3) notation (E-1) can be rewritten as

$$Q[\underline{r}_1,\underline{r}_2;K(\underline{R},\underline{R}';\theta)] = \underset{\theta \epsilon \Theta}{\mathcal{E}} \left\{ \begin{bmatrix} \dfrac{\partial^2}{\partial x_1 \partial x_2} & \dfrac{\partial^2}{\partial x_1 \partial y_2} & \dfrac{\partial^2}{\partial x_1 \partial z_2} & \dfrac{\partial}{\partial x_1} \\[2ex] \dfrac{\partial^2}{\partial y_1 \partial x_2} & \dfrac{\partial^2}{\partial y_1 \partial y_2} & \dfrac{\partial^2}{\partial y_1 \partial z_2} & \dfrac{\partial}{\partial y_1} \\[2ex] \dfrac{\partial^2}{\partial z_1 \partial x_2} & \dfrac{\partial^2}{\partial z_1 \partial y_2} & \dfrac{\partial^2}{\partial z_1 \partial z_2} & \dfrac{\partial}{\partial z_1} \\[2ex] \dfrac{\partial}{\partial x_2} & \dfrac{\partial}{\partial y_2} & \dfrac{\partial}{\partial z_2} & 1 \end{bmatrix} \right.$$

$$\left. \cdot\ T(\underline{r}_1)T(\underline{r}_2) \right\} \qquad\qquad\qquad\qquad (E\text{-}4)$$

For practical reasons, we expect the partial derivatives to be uniformly bounded. Hence, these operations are bounded and linear. So, we may interchange the partial derivatives with the linear expectation operator. Then, (E-4) becomes

$$Q[\underline{r}_1,\underline{r}_2;\ K(\underline{R},\underline{R}';\theta)] = \begin{bmatrix} \dfrac{\partial^2}{\partial x_1 \partial x_2} & \dfrac{\partial^2}{\partial x_1 \partial y_2} & \dfrac{\partial^2}{\partial x_1 \partial z_1} & \dfrac{\partial}{\partial x_1} \\[2ex] \dfrac{\partial^2}{y_1\ x_2} & \dfrac{\partial^2}{y_1\ y_2} & \dfrac{\partial^2}{y_1\ z_2} & \dfrac{\partial}{y_1} \\[2ex] \dfrac{\partial^2}{\partial z_1 \partial x_2} & \dfrac{\partial^2}{\partial z_1 \partial y_2} & \dfrac{\partial^2}{\partial z_1\ z_2} & \dfrac{\partial}{\partial z_1} \\[2ex] \dfrac{\partial}{\partial x_2} & \dfrac{\partial}{\partial y_2} & \dfrac{\partial}{\partial z_2} & 1 \end{bmatrix} K(\underline{r}_1,\underline{r}_2;\theta)$$

$$(E\text{-}5)$$

Since $K(\underline{r}_1,\underline{r}_2;\theta)$ can be derived from $K(\underline{R},\underline{R}';\theta)$, this equation demonstrates that all necessary statistics are embodied in the single reference

132

surface covariance function. With this point made, we shall not implement (E-5) directly. Rather, the elements of the Q-matrix can be derived (Ref 50) from the (E-5) relationship with proper coordinate choice.

The usual form of the covariance functions (Appendix C) is in terms of a central angle, ψ, argument. That is,

$$K(\underline{R}, \underline{R}') = K(\psi) \tag{E-6}$$

where

$$\psi = \cos^{-1}[R^{-2}\underline{R} \cdot \underline{R}'] . \tag{E-7}$$

We have dropped the sample space argument, here, since the development is generally applicable. It has been shown (Ref 50) that potential covariances of the form (E-6) can be continued upward with arguments r_1, r_2 and ψ. That is,

$$K(\underline{r}_1, \underline{r}_2) = K(r_1, r_2, \psi) \tag{E-8}$$

A particularly useful coordinate choice in this case is Inplane-Transverse-Radial (ITR) coordinates shown in Figure E-1.

If we use the autocorrelation notation of Appendix C we can summarize (E-5) as

$Q[r_1, r_2, \psi ; K(\psi; \Theta)] =$

$$\begin{bmatrix} \phi_{xx}(r_1, r_2, \psi) & \phi_{xy}(\ ) & \phi_{xz}(\ ) & \phi_{xT}(\ ) \\ \\ \phi_{yx}(r_1, r_2, \psi) & \phi_{yy}(\ ) & \phi_{yz}(\ ) & \phi_{yT}(\ ) \\ \\ \phi_{zx}(r_1, r_2, \psi) & \phi_{zy}(\ ) & \phi_{zz}(\ ) & \phi_{zT}(\ ) \\ \\ \phi_{Tx}(r_1, r_2, \psi) & \phi_{Ty}(\ ) & \phi_{Tz}(\ ) & \phi_{TT}(\ ) \end{bmatrix} \qquad \text{(E-9)}$$

The tasks remaining are to provide the various auto-and cross-correlation functions based on the reference surface version of the lower right-hand element of (E-9): $\phi_{TT}(R, R', \psi)$.

Note: View is in the

$r_1 \, r_2$ plane

z-axis radial

x-axis inplane (downrange)
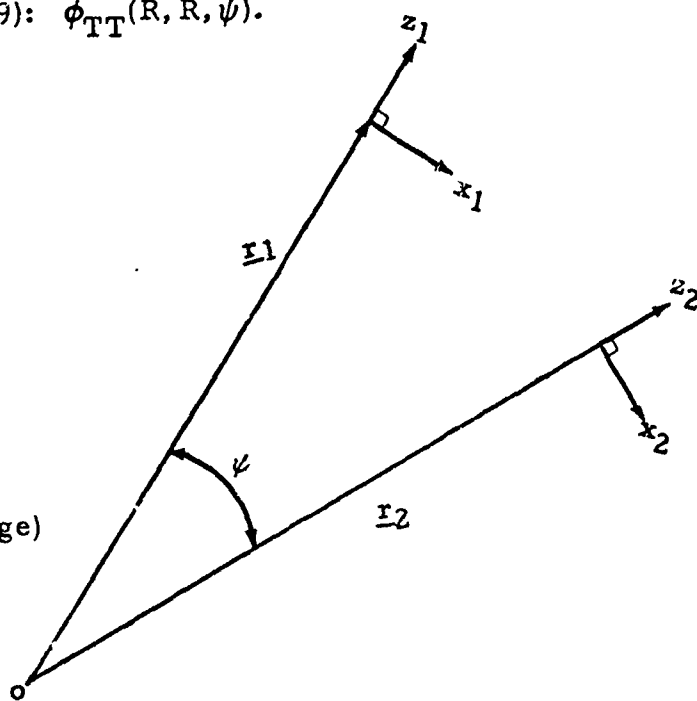
y-axis transverse (crossrange)

Figure E-1. Inplane-Transverse-Radial Coordinates

134

References

1. Britting, K. R. Inertial Navigation Systems Analysis. Wiley-Interscience, division of John Wiley & Sons, Inc., 1971.

2. Widnall, W. S. and P. A. Grundy. Inertial Navigation System Error Models. Intermetrics Report TR-03-73, 11 May 1973. Also, AFSWC-TR-73-26 (AD 912 489L).

3. Wrigley, W., et al. Gyroscopic Theory, Design and Instrumentation. Cambridge, MA. The M.I.T. Press, 1969.

4. Sciegienny, J., et al. Inertial Navigation System Standardized Software, Final Technical Report, Volume II, INS Survey and Analytical Development. The Charles Stark Draper Laboratory Inc. Report R-977, June 1976.

5. Kayton, M. Coordinate Frames in Inertial Navigation (PhD dissertation). M.I.T. Instrumentation Laboratory Report T-260, Vol. I & II, August 1960.

6. Britting, K. R. Unified Error Analysis of Terrestrial Inertial Navigation Systems (PhD dissertation). M.I.T. Measurement System Laboratory Report TE-42, 1970.

7. Kayton, M. "Fundamental Limitations on Inertial Measurements," presented at the ARS Guidance, Control, and Navigation Conference, Stanford, Ca., August 1961. Also, under "Guidance and Control," pp 367-389, Progress in Astronautics and Rocketry, Vol. 8, Academic Press, 1962.

8. King, Hele, D. "The Shape of the Earth." Science, Vol. 192, No. 4246, 25 June 1976.

9. Burkard, R. K. Geodesy for the Layman. Aeronautical Chart and Information Center, St. Louis, February 1968 (AD 670 156).

10. Pitman, G. R., et al. Inertial Guidance. John Wiley & Sons, Inc., 1962.

11. Fernandez, M. and G. R. Macomber. Inertial Guidance Engineering. Prentice-Hall, Inc., 1962.

12. Broxmeyer, C. _Inertial Navigation Systems_. McGraw-Hill Book Company, 1964.

13. Heiskanen, W. A. and F. A. Vening Meinesz. _The Earth and Its Gravity Field_. The McGraw-Hill Book Company, Inc., 1958.

14. Heiskanen, W. A. and H. Moritz. _Physical Geodesy_, W. H. Freeman and Company, 1967.

15. Kellog, O. D. _Foundations of Potential Theory_. The Murry Printing Company, Frederic Ungar Publishing Company, 1929.

16. Bate, R. R., et al. _Fundamentals of Astrodynamics_. Dover Publications, Inc., 1971.

17. Seppelin, T. O. _The Department of Defense World Geodetic System 1972_. Defense Mapping Agency, Washington, D.C., May 1974.

18. Nettleton, L. L. _Gravity and Magnetics in Oil Prospecting_. McGraw-Hill Book Company, 1976.

19. Heller, W. G. _Free-Inertial and Damped-Inertial Navigation Mechanization and Error Equations_. The Analytic Sciences Corporation Report TR-312-1-1, 18 April 1975 (AD A014 356).

20. Rice, D. A. "A Geoidal Section in the United States." The XII General Assembly of the International Union in Geodesy and Geophysics, Helsinki, July-August 1960.

21. Levine, S. A. and A. Geib. "Geodetic and Geophysical Uncertainties - Fundamental Limitations on Terrestrial Inertial Navigation." AIAA Paper No. 68-847 presented at the AIAA Guidance, Control, and Flight Dynamics Conference, Pasadena, Ca., 12-14 August 1968. Also, "Effects of Deflections of the Vertical on the Performance of a Terrestrial Navigation System." _AIAA Journal of Spacecraft_, Vol. 6, No. 9, pp 678-684, September 1969.

22. Bernstein, U. and R. I. Hess. "The Effects of Vertical Deflections on Aircraft Inertial Navigation Systems." _AIAA Journal_, Vol. 14, No. 10, October 1976.

23. Nash, R. A. et al. "Error Analysis of Hybrid Aircraft Inertial Navigation." AIAA Paper No. 72-848 presented at the AIAA Guidance and Control Conference, Stanford, California, 14-16 August 1972.

24. Chatfield, A. B. et al. "Effects of Gravity Model Inaccuracy on Navigation Performance." AIAA Journal, Vol. 13, No. 11, pp 1494-1501, November 1975.

25. Chatfield, A. B. and M. M. Bennett. "Geodynamics Navigation Error Analysis Software." Geodynamics Corporation briefing charts presented at the Air Force Avionics Laboratory, 24 February 1977.

26. Tsipis, K. "The Calculus of Nuclear Counterforce." Technology Review, October/November 1974.

27. Hepfer, J. W. "M-X and the Land-Based ICBM." Astronautics and Aeronautics, Vol. 13, No. 2, February 1975.

28. Hall, A. C. "The Case for an Improved ICBM." Astronautics and Aeronautics, Vol. 15, No. 2, February 1977.

29. McKinley, H. L. "Geokinetics and Geophysical Influences on 1980's ICBM Guidance." AIAA Paper No. 75-1064 presented at the AIAA Guidance and Control Conference, Boston, August 1975.

30. Bennett, M. M. and P. W. Davis. "MINUTEMAN Gravity Modeling." AIAA Paper No. 76-1960 presented at AIAA Guidance and Control Conference, San Diego, August 1976.

31. Tsipis, K. "Cruise Missile." Scientific American, Vol. 236, No. 2, February 1977.

32. Trageser, M. B. A Gradiometer System for Gravity Anomaly Surveying. Charles Stack Draper Laboratory Report R-588, June 1970.

33. Rose, R. C. and R. A. Nash. "Direct Recovery of Deflections of the Vertical Using an Inertial Navigator." IEEE Trans. on Geoscience Electronics, Vol. GE-10, No. 2, pp 85-92, April 1972.

34. Rapp, R. H. "The Geoid: Definition and Determination." Proceedings of the Geodesy/Solid Earth and Ocean Physics (GEOP) Research Conferences. Ohio State Univ. Dept. of

Geodetic Science Report No. 231, September 1975. Also, NASA-CR-146540. Reprinted from E⊕S, Vol. 55, No. 3, March 1974.

35.   Koch, D. W. GRAVSAT/GEOPAUSE Covariance Analysis Including Geopotential Aliasing. NASA-TM-X-71057, Goddard Space Flight Center, October 1975.

36.   Morrison, F. "Algorithms for Computing the Geopotential Using a Simple Density Layer." Journal of Geophysical Research, Vol. 81, No. 26, pp 4933-4936, 10 September 1976.

37.   Grant, F. S. and C. F. West. Interpretation Theory in Applied Geophysics. McGraw-Hill Book Company, 1965.

38.   McLaughlin, W. I. Representation of a Gravitational Potential with Fixed Mass Points. Bellcom, Inc., 23 December 1968. Also, NASA-CR-116806.

39.   Hopkins, J. "Point Mass Models from Various Data Sources Singly and in Combination." Presented at the Fall Annual Meeting of the Americal Geophysical Union, San Francisco, CA, 12-17 December 1974.

40.   Lavrentiev, M. M. Some Improperly Posed Problems of Mathematical Physics. Springer-Verlag New York, Inc., 1967.

41.   Junkins, J. L. "Investigations of Finite-Element Representation of the Geopotential." AIAA Journal, Vol. 14, No. 6, pp 803-808, June 1976.

42.   _____. Development of Finite Element Models for the Earth's Gravity Field. Phase I. Macro Gravity Field for Satellite Orbit Integration. University of Virginia Research Laboratories for the Engineering Sciences Report No. UVA/525023/ESS77/103, March 1977. Also, U.S. Army Topographic Laboratories Report ETL-0096 (AD A-unknown).

43.   _____. Development of Finite Element Models for the Earth's Gravity Field. Phase II. Fine Structure Disturbance Gravity Representations. Univ. of Virginia Research Laboratories for the Engineering Sciences Report No. UVA/525023/ESS77/104, March 1977. Also, U.S. Army Topographic Laboratories Report ETL-0097 (AD A-unknown).

44. Bhattacharyya, B. K. "Bicubic Spline Interpolation as a Method for Treatment of Potential Field Data." Geophysics, Vol. 34, No. 3, pp 402-423, June 1969.

45. Hardy, R. L. Geodetic Application on Multiquadric Equations. Iowa State Univ. Engineering Research Institute Final Report ISU-ERI-Ames-76245, May 1976 (PB-255-296 from NTIS).

46. Brown, R. D. Geopotential Modeling by Binary Sampling Functions. PhD Dissertation, Catholic Univ. Computer Sciences Corporation Report No. CSC/TR-75/6006, April 1975.

47. Davis, T. M. et al. Analysis of Deflection-of-the-Vertical Inner-Zone Methods. Naval Oceanographic Office Special Publication 260 (NOO SP 260), February 1974 (AD 776225).

48. _____. Theory and Practice of Geophysical Survey Design (PhD dissertation at Pennsylvania State Univ.). Naval Oceanographic Office Reference Publication 13 (NOO RP 13), October 1974 (AD A003 078).

49. Long, L. T. Determination and Statistical Studies of Gravimetric Deflections. Georgia Institute of Technology School of Geophysical Sciences, 31 August 1975. Also, Army Engineer Topographic Laboratories Report ETL-0017 (AD A022 293).

50. Thomas, S. and W. G. Heller. Efficient Estimation Techniques for Integrated Gravity Data Processing. The Analytic Sciences Corp. Report TR-680-1, 30 September 1976. Also, AFGL-TR-76-0232 (AD A 034 055).

51. Prado, G. "The Role of the Hilbert Transform on Potential Theory Problems." AGS Memo No. 4300-77-01, The Charles Stark Draper Laboratory, Inc., 10 January 1977.

52. _____. "Calculating the External Gravity Field, A Signal Processing Approach." Preprint of paper presented at the National Aerospace & Electronics Conference (NAECON 77), 19 May 1977.

53. Oppenheim, A. V. and R. W. Schafer. Digital Signal Processing. Prentice-Hall, Inc., 1975.

54. Comfort, G. C. A Study of Airborne Gravimetry Using Repeated Flight Paths. Frank J. Seiler Laboratory Report SRL-TR-74-0014, August 1974 (AD A003 498).

55. Meissl, P. _Probabilistic Error Analysis of Airborne Gravimetry._ Ohio State Univ. Dept. of Geodetic Science Report No. 138, June 1970. Also, AFCRL-70-0396 (AD 715 268).

56. Moritz, H. _Kinematical Geodesy._ Ohio State Univ. Dept. of Geodetic Science Report No. 92, November 1967. Also, AFCRL-67-0626 (AD 666 052).

57. Heller, W. G. _Gradiometer-Aided Inertial Navigation._ The Analytical Sciences Corp. Report No. TR-312-5, 7 April 1975 (AD A013 274).

58. Heller, W. G. and S. K. Jordan. "Mechanization and Error Equations for Two New Gradiometer-Aided Inertial Navigation System Configurations." AIAA Paper No. 75-1091 presented at AIAA Guidance and Control Conference, Boston, August 1975.

59. Hildebrandt, R. R. et al. "The Effects of Gravitational Uncertainties on the Errors of Inertial Navigation Systems." _Navigation,_ Journal of Institute of Navigation, Vol. 21, No. 4, Winter 1974-75.

60. Gerber, M. A. "Propagation of Gravity Gradiometer Errors in an Airborne INS." AIAA Paper No. 75-1089 presented at AIAA Guidance and Control Conference, Boston, August 1975.

61. Grubin, C. "Accuracy Improvement in a Gravity Gradiometer-Aided Cruise Inertial Navigator Subjected to Deflections of the Vertical." AIAA Paper No. 75-1090 presented at AIAA Guidance and Control Conference, Boston, August 1975.

62. Pogorzelski, W.A. _Integral Equations and Their Applications,_ Vol. I. Pergamon Press, 1966.

63. Lee, D. A. "Objective-Oriented Identification." _Proceedings_ of the Pittsburg Conference on Modeling and Simulation, Vol. VI, pp 163-167, 1975.

64. Hirvonen, R. A. and H. Moritz. _Practical Computation of Gravity at High Altitudes._ Ohio State Univ. Institute of Geodesy, Photogrammetry and Cartography Report No. 27, May 1963. Also, AFCRL-63-702 (AD 420541).

65. Moritz, H. A. _A General Theory of Gravity Processing._ Ohio State University Dept. of Geodetic Science Report No. 122, May 1969. Also, AFCRL-69-0258 (AD 694 112).

66. Moritz, H. *Advanced Least Squares Method*. Ohio State University Dept. of Geodetic Science Report No. 175, June 1972. Also, AFCRL-72-0363 (AD 749 873).

67. Hotine, M. *Mathematical Geodesy*. ESSA Monograph 2. U.S. Government Printing Office, 1969.

68. Moritz, H. *Least-Squares Estimation in Physical Geodesy*. Ohio State Univ. Dept. of Geodetic Science Report No. 130, March 1970. Also, AFCRL-70-0202 (AD 707 508).

69. Tscherning, C. C. and R. H. Rapp. *Closed Covariance Expressions for Gravity Anomalies, Geoid Undulation*, and Deflections of the Vertical by Anomaly Degree Variance Models. Ohio State Univ. Dept. of Geodetic Science Report No. 208, May 1974. Also, AFCRL-TR-74-0231 (AD 786 417).

70. Long, L. T. *Determination and Statistical Studies of Gravimetric Deflections*. Georgia Institute of Technology School of Geophysical Sciences, 30 November 1973. Also, Army Engineer Topographic Laboratories Report ETL-CR-74-8 (AD A003 271).

71. Hirschorn, R. M. *Rotational Invariant Probability Distributions in Geodesy*. (PhD Dissertation). M. I. T. Measurement Systems Laboratory Report TE-41, June 1970.

72. Moritz, H. *Covariance Functions in Least-Squares Collocation*. Ohio State Univ. Dept. of Geodetic Science Report No. 240, June 1976. Also, AFGL-TR-76-0165 (AD A 030 302).

73. Schwarz, K. P. *Geodetic Accuracies Obtainable from Measurements of First and Second Order Gravity Gradients*. Ohio State Univ. Dept. of Geodetic Science Report No. 242, August 1976. Also, AFGL-TR-76-0189 (AD A 031 331).

74. Rapp, R. H. *Gravity Anomaly Recovery from Satellite Altimetry Data Using Least Squares Collocation Techniques*. Ohio State Univ. Dept. of Geodetic Science Report No. 220, December 1974. Also, AFCRL-TR-74-0642 (AD A009 629)..

75. Laning, J. H. and R. H. Battin. *Random Processes in Automatic Control*. McGraw-Hill Book Company, Inc., 1956.

76. Gelb, A. editor. *Applied Optimal Estimation*. The M. I. T. Press, 1974.